Cell Biology of the ICA69 Protein Family in Neurosecretory Cells

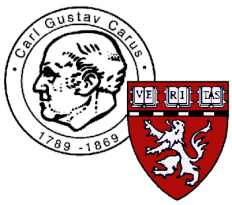

Laura Buffa

Faculty of Medicine

Dresden University of Technology / International Max Planck Research School

A thesis submitted for the degree of

Doctor rerum medicinalium

December 2006

To Nicoletta, my sister

Acknowledgements

First, I would like to thank my supervisor, Michele Solimena, for having given me the possibility of doing my PhD in his laboratory and for the enthusiasm and positive attitude he always had in regard of my project, even in front of the most puzzling data.

I would also like to thank the other members of my thesis advisory committee Marino Zerial, Wolfgang Zachariae and Bianca Habermann, for helpful discussions during our meetings and for critical comments on my project.

Thanks to all the present and former members of the Solimena lab, including our secretary Katia Pfriem, for the nice working atmosphere. In particular I would like to thank Barbara Borgonovo for many constructive discussions and advice as well as Anke Altkrüger and Carolin Wegbrot for excellent technical assistance.

I am grateful to Massimo Pietropaolo for purifying and providing the α-ICA69 antibody used in this thesis, to Francis Barr for sharing reagents with us as well as the results of a two-hybrid screening performed in his lab. I thank Marino Zerial for providing most of the GST constructs and antibodies, as well as Carsten Schnatwinkel for advice on the GST pull down assay.

I am indebted to all the students of the PhD program, for the unique atmosphere in the institute: I really think this is an extraordinary place where to do a PhD. Special thanks to my friends for keeping me up, and especially, here in Dresden, to Alessio Attardo and Gaspare Benenati, for being "my family abroad", as I always referred to them, and for all the laughs we had together.

I would like to manifest my indebtedness to my parents, for the unconditional and endless moral support, and for letting me go my way, even when this meant away from them. Last, but certainly not least, I want to express my deepest gratitude to Andreas Hilfinger for proof reading this thesis, but above all for being there to listen

to “my complaints” and for his constant and crucial support and encouragement, especially in the most difficult moments.

Abstract

In type 1 diabetes (T1D), an autoimmune disease, autoantibodies are preferentially directed against proteins associated with Golgi and post-Golgi secretory vesicles, including insulin secretory granules and synaptic-like microvesicles. Thus, the study of β-cell autoantigens with yet unknown function may provide novel insight into the secretory machinery of β-cells and lead to the discovery of novel pathways.

Islet cell autoantigen of 69 kDa (ICA69) is a T1D autoantigen. It is a cytosolic protein of still unknown function. An impairment in neurotransmitter release upon mutation of its homologue in *C. elegans* suggests, however, an involvement of ICA69 in neurosecretion. Interestingly, ICA69 contains a BAR domain, present in several proteins involved in intracellular transport. The BAR domain functions as a dimerization motif, provides a general binding interface for different types of GTPases, and is a membrane binding/bending module. Its presence in ICA69 is a further hint supporting the putative involvement of ICA69 in intracellular membrane trafficking.

The first part of this thesis was concerned with the characterization of ICA69, and the elucidation of its role in membrane traffic in pancreatic β-cells. ICA69 was shown to be enriched in the perinuclear region, where also markers of the Golgi region are found. ICA69 was shown to interact with several membrane lipids, preferentially with PI(4)P, enriched on the Golgi complex. During the course of this thesis a combination of biochemical and imaging techniques were applied to investigate the interaction between ICA69 and Rab2, a small GTPase associated with the intermediate compartment and involved in the trafficking between the ER and the Golgi complex. ICA69 was shown to co-immunoprecipitate with Rab2 from INS-1 cells extracts. GST-pull down assays demonstrated that this interaction is GTP-dependent. Furthermore, confocal microscopy indicated that ICA69 and Rab2 extensively colocalize in particulate structures throughout the cytoplasm. Immunocytochemistry

and subcellular fractionation experiments suggested that Rab2 recruits ICA69 to membranes. Functional studies indicated that ICA69 over-expression in INS-1 cells has effects that resemble, and in some cases amplify those observed upon Rab2 over-expression. Specifically, it impairs the trafficking between ER and Golgi, measured through the appearance and the conversion of the pro-form of ICA512 in the mature form of the protein. Moreover, it correlates with a redistribution of the β-COP subunit of the coatomer, participating in the early secretory pathway, between membrane-bound compartments and the cytosol and it reduces stimulated insulin secretion. The data reported in this thesis conclusively point to ICA69 as a novel Rab2 effector, and may therefore contribute to the elucidation the yet poorly understood mechanism of action of Rab2 in the secretory pathway.

The second part of the thesis was devoted to the study of an ICA69 paralogue gene, called ICA69-RP. Similarly to ICA69, ICA69-RP mRNA was shown to be primarily present in tissues such as brain and pancreatic islets, showing the expression pattern of a gene preferentially expressed in neuroendocrine cells. Unlike ICA69, however, and similar to other genes associated with the secretory machinery of β-cells, ICA69-RP appeared to be glucose regulated, as shown by a 1.55 fold increase in mRNA levels upon stimulation of the cells with 25 mM glucose for two hours. Glucose stimulation of β-cells prompts the activation of post-transcripional mechanisms which quickly up-regulate the expression of secretory granule genes and consequently renew granule stores. The increased expression of ICA69-RP upon glucose stimulation of cells may be part of this process. Unfortunately, all attempts to elucidate the intracellular localization of endogenous ICA69-RP failed, and it was not possible to obtain significant insights about its localization by over-expressing a fusion protein between ICA69-RP and GFP. Unlike other paralogues containing the BAR domain, such as amphiphysin 1 and 2 or Rvs167p and Rvs161p, ICA69 and ICA69-RP were shown not to form heterodimers. Furthermore, ICA69-RP did not show any interaction with Rab2 or Rab1, involved in the anterograde transport between ER and Golgi. Thus, its physiological role remains to be investigated.

Nomenclature

AP ... amino acid

AP ... adaptor protein complex

APPL ... adaptor protein containing PH domain, PTB domain and Leucine zipper motif

ARL ... ARF-like protein

ARF ... ADP-ribosylation factor

bp ... base pairs

BAR ... bin, amphiphysin and Rvs161/167

BFA ... brefeldin A

BRAP1/Bin2 ... breast cancer associated protein1/bridging integrator 2

btail-GFP ... citocrome b-tail in fusion with GFP

CAPS ... Ca^{2+} dependent activator protein for secretion

CC ... coiled-coil

CCVs ... clathrin-coated vesicles

Cg ... chromogranin

COS-7 ... Transformed African Green Monkey Kidney Fibroblast Cells

CPE/H ... carboxypeptidase E/H

DAG ... diacylglycerol

DMEM ... Dulbecco's modified Eagle's minimal essential medium

DTT ... dithiothroitol

EBI ... European Bioinformatic institute

ENTH ... epsin amino terminal homology

ER ... endoplasmic reticulum

ERGIC ... ER-Golgi intermediate compartmen

ERES ... ER exit sites

FBS ... fetal bovine serum

FCH ... Fes/CIP4 homology

FFA ... free fatty acid

FYVE ... Fab1-YOTP-Vac1-EEA1

GAD 65/67 ... glutamic acid decarboxylase 65/67

GAP ... GTPase-activating protein

GDP ... guanosine-5'-diphosphate

GDI ... GDP dissociation inhibitor

GEF ... guanine nucleotide exchange factor

GFP ... green fluorescent protein

GGAs ... Golgi-localized, γ-ear-containing, ARF-binding proteins

GK ... glucokinase

GLUT-2 ... glucose transporter-type 2

GPI ... glycosylphoshatidylinositol

GTP ... guanosine-5'-triphosphate

HEK ... Human Epidermal Keratinocytes

HNF1 ... hepatocyte nuclear factor 1

HRP ... horseradish-peroxidase-coniugated

KRPs or KIFs ... kinesin related proteins

HS ... high salt

HSP ... high speed pellets

HSS ... high speed supernatants

IC ... intermediate compartment

ICA ... islet cell autoantigen

ICA69-RP ... ICA69 Related Protein

IDDM ... insulin-dependent diabetes mellitus

IDM ... immune mediated diabetes

IP ... immunoprecipitations

IP3 ... inositolpolyphosphate 3

IPTG ... isopropyl-β-D-thiogalactopyranoside

IRS-1 ... insulin receptor substrate 1

IR ... insulin receptor

ISGs ... immature secretory granules

LB medium ... Luria-Bertani broth

LDCVs ... large dense core vesicles

LPCs ... large pleiomorphic carriers

LS ... low salt

min ... minutes

MODY ... maturity-onset diabetes of the young

MPR ... mannose-6-phosfate receptor

MSGs ... mature secretory granules

MWCO ... molecular weight cut off

NE ... nucleotide exchange

nm ... nanometer

NOD ... nonobese diabetic

NS ... nucleotide stabilization

NSF ... N-ethylmaleimide-Sensitive-Factor

NRK ... Normal Rat Kidney

PBS ... phosphate buffer saline

PBST ... 0.1%Triton in PBS

PC ... pro-hormone convertase

PFA ... paraformaldehyde

PFK ... phosphofruttokinase

PGCs ... post-Golgi carriers

PH ... pleckstrin homology

PHD ... plant homeodomain

PIs ... phosphatidylinositides

PI3K ... phosphoinositide 3-kinase

PKA ... protein kinase A

PKC ... protein kinase C

PKD ... protein kinase D

PMSF ... phenylmethylsulfonyl fluoride

PNS ... post nuclear supernatants

POMC ... pro-opiomelanocortin

PTB ... polypirimidine tract-binding protein

PX ... phox homology

Rab ... Ras-related proteins in brain

RB6K ... Rabkinesin-6

REP ... Rab escort protein

RER ... rough endoplasmic reticulum

RIA ... radioimmunoassay

RRP ... readily releasable pool

RSP ... regulated secretory protein

RT ... room temperature

SD ... standard deviation

SDS-PAGE ... SDS-Polyacrylamide Gel Electrophoresis

SE ... standard error of the mean

sec ... seconds

SER ... smooth endoplasmic reticulum

SGs ... secretory granules

SH3 ... Src homology 3

S.I. ... Stimulation Index

SLMVs ... synaptic-like microvesicles

SM ... Sec1/Munc18-like

SNAP ... soluble NSF association factor

SNARE ... SNAP receptor

SRP ... Signal Recognition Particle

SVs ... synaptic vesicles

TGN ... *trans*-Golgi network

TGR ... *trans*-Golgi reticulum

TRAPP ... transport protein particle

T1D ... type 1 diabetes

T2D ... type 2 diabetes

TBS ... Tris buffer saline

TBST ... 0.1%Triton in TBS

UTR ... untranslated region

VAMP ... vesicle-associated membrane protein

V ... Volt

VSV ... vesicular stomatitis virus (VSV)

VTCs ... vesicular-tubular clusters

Contents

List of Figures

Chapter 1

Introduction

1.1 The intracellular traffic

Eukaryotic cells have, if compared with prokaryotic cells, an elaborate compartmentalization of their cytoplasm reached through the evolution of distinct membrane-enclosed compartments, or organelles. Each organelle contains a characteristic set of enzymes and other specialized molecules which define the organelle's structural and functional properties. Thirty years ago, the work of G. Palade (1) and C. de Duve (2) on protein secretion established that newly synthesized secretory proteins pass through a series of organelles, including the endoplasmic reticulum (ER), the Golgi complex and the secretory granules, on their way to the extracellular space, where they are released (Fig. 1.1). It was found that proteins destined for residence at the plasma membrane, within endosomes or lysosomes, share the early stations with the secretory proteins. Also carbohydrates and lipids follow similar routes. The molecular mechanism that underlies vesicular transport was subsequently investigated by R. Schekman through the isolation in yeast of secretion mutants (3) and by J. Rothman through a cell-free biochemical approach (4).

The transport between organelles involves the dynamic exchange of lipids and proteins. This membrane traffic occurs along highly organized directional routes and preserves membrane composition, protein topology and the biochemical and morphologic features of the different organelles.

1.1.1 Vesicular carriers

The observation that secretory proteins are often found within small (60-100 nm), membrane-enclosed vesicles, interspersed among the major organelles of the pathway inspired the "vesicular

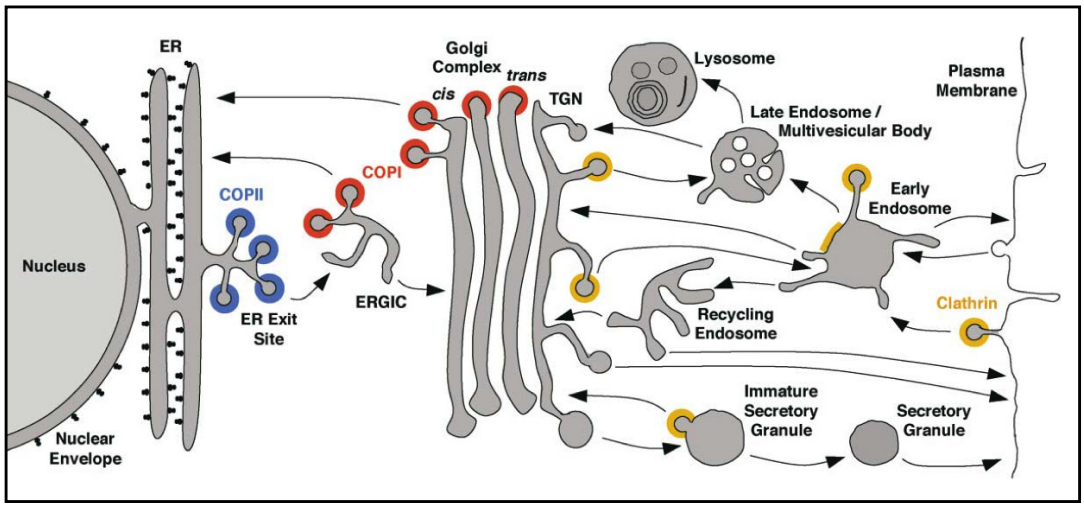

Figure 1.1: **Intracellular pathways**
Schematical representation of the organelles taking part in the secretory, endocytic and lysosomal pathways. Arrows indicate the transport steps; the yellow indicates clathrin coats, the red and the blue indicate COPI and COPII coats, respectively. Other coats exist, though not represented in the figure. Reproduced from (5).

transport hypothesis", schematically illustrated in Fig. 1.2 A. This hypothesis states that the transfer of cargo between different compartments of the secretory pathway is mediated by vesicles (5).Traffic proceeds through several steps, collectively referred to as anterograde transport, and includes the formation of vesicles at a donor compartment (budding) and their targeting and subsequent fusion to a specific acceptor compartment. As soon as the carrier reaches the final destination, it fuses with the acceptor compartment and lumenal proteins (cargo) are released. At this step, the carrier returns to the donor compartment to be recycled for a new cycle of transport, allowing the retrieval of escaped resident proteins back to the corresponding compartment (retrograde transport)(6). This process has in addition been suggested to play a role in quality control and concentration of secretory cargo (7). Retrograde transport is also hypothesized to occur mainly by vesicular transport (8; 9).

1.1.2 Tubular carriers

Until a decade ago vesicles were believed to be the only carriers mediating intracellular transport. However, recent evidence suggest the existence of carriers that are larger and more

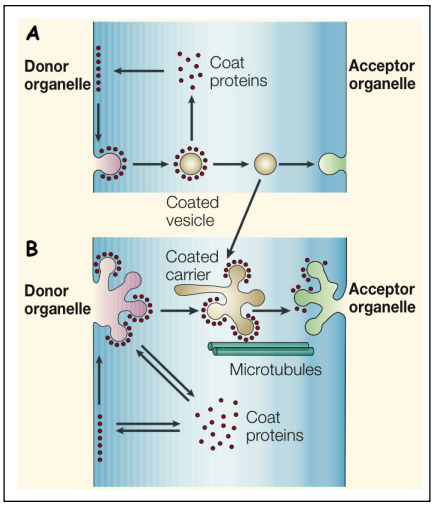

Figure 1.2: **Vesicular and tubular carriers**
In addition to vesicles (A), large and pleiomorphic carriers (PCGs) moving along microtubule tracks (B). PCGs appear to be responsible the bulk of the secretory transport between distant compartments. Reproduced from (10).

pleiomorphic than conventional vesicles (10; 11). The formation of these large pleiomorphic carriers (LPCs) is illustrated in Fig. 1.2 B. Ultrastructural studies have shown the existence of a network of tubules in the *cis*-Golgi area (12). Imaging of the transport of cargo proteins tagged with the green fluorescent protein (GFP) has indicated a tubule-mediated export from the ER to the Golgi and from the Golgi to the plasma membrane (13). In the endocytic pathway, tubules emerge from the early endosomes and participate in recycling to the plasma membrane (14). LPCs have interconnected tubular and saccular components, varying in size and shape from 100-200 nm containers to several microns long tubules or saccules with diameter of $\sim 1\mu$m.

1.2 Components of the secretory pathway

1.2.1 Endoplasmic Reticulum

The endoplasmic reticulum (ER) is the starting point of the secretory pathway. It is the largest intracellular compartment, with an extensive array of interconnecting tubules and *cisternae* that extend throughout the cell including the nuclear envelope. ER membranes are differentiated into smooth and rough regions (SER and RER, respectively) depending on whether

ribosomes are associated with their cytoplasmic surfaces. The SER is the site of lipid biosynthesis, detoxification and storage of calcium, whereas the RER is the entry site of proteins in the secretory pathway.

Nascent polypeptide chains are recognized by a protein complex called Signal Recognition Particle (SRP) that delays transcripts translation and docks protein synthesizing ribosomes to ER membranes (15). Following the docking step, polypeptides translation on membrane bound ribosomes is continued, accompanied by translocation into the ER lumen by the Sec61 complex (16). In rare cases the translocation into the ER lumens occurs post-translationally. This is the case, for example, for C-tail anchored proteins, such as the SNARE proteins, which do not contain a signal peptide and are probably integrated in the membrane by a different mechanism (17).

Upon insertion into the ER, newly synthesized proteins encounter lumenal chaperones whose role is to facilitate folding reactions necessary for protein maturation and oligomerization. Because only properly folded and assembled proteins are exported towards the Golgi, the ER plays an important quality control role in protein transport (18). Additionally, in in the ER lumen, most of the proteins are N-glycosilated by addition of a precursor oligosaccharide containing 14 sugars (19) and some of them acquire a covalently attached glycosylphoshatidylinositol (GPI) anchor.

Protein export from the ER takes place in specialized regions of the ER, devoid of ribosomes, called ER exit sites (ERES) (20). These are highly organized membrane domains (1-2 μm in diameter) adjacent to the pre-Golgi intermediates.

1.2.2 ER-Golgi intermediate compartment

The ER-Golgi intermediate compartment (ERGIC or IC)[1] is a complex membrane system between the ER and the Golgi complex (21). It is also sometimes referred to as vesicular-tubular clusters (VTCs) (22) or pre-Golgi intermediates (23) and consists of a large convoluted mass of tubules and vesicles individually 50 nm in diameter with an average diameter for the cluster of 0.4 microns (24). The ERGIC is enriched in the 53 kDa membrane protein ERGIC53 and the protein composition of its membranes differs from that of ER and Golgi membranes (25). Since its identification it has been matter of debate whether the ERGIC is a specialized domain of the ER (26), or of the Golgi complex (27), or a transient structure composed of transport

[1]The ERGIC is absent in *S. cerevisiae*. Despite yeast and mammals sharing the same secretory pathway, mammalian cells show a greater morphological complexity of the secretory pathway compared with yeast.

vehicles for protein delivery to the Golgi complex (28), or a distinct organelle separated from the ER and the Golgi complex (29).

The ERGIC is the first sorting station for anterograde and retrograde protein traffic, and it also contributes to the concentration, folding and quality control of the secretory cargo (30).

1.2.3 Golgi complex

In animal cells the Golgi complex (or Golgi apparatus) consists of a collection of flattened, membrane-enclosed *cisternae*, that are interconnected by tubules, and are clustered near the nucleus and close to the centrosome at the minus ends of microtubules. It is morphologically and functionally polarized, with a *cis* entry face and a *trans* exit face. The Golgi complex is the site where cargo proteins "mature". Modifications such as oligosaccharide remodeling, proteolytic cleavage, phosphorylation, or sulfation take place, while proteins transit through the *cisternae* before vesicle packaging and transport to the final destination (31).

Although the Golgi complex has been known for over a century, key issues regarding this organelle have remained controversial. Regarding its biogenesis two different theories have been proposed: the Golgi complex could originate by the self-organization of components as they are exported from the ER (32), or it could be an autonomous organelle that forms using a persistent matrix (33). Another open issue is the modality of cargo movement through the Golgi. In the past it has been postulated that forward transport of cargo through *cisternae* may occur following two possible models: cisternal anterograde vesicle transport or maturation, respectively. Evidence in favour of the first model go back to the identification, through the Golgi stacks, of membrane vesicles containing the cargo vesicular stomatitis virus (VSV)-encoded G protein (34). However, studies on large molecules progression through the Golgi, such as procollagen (35; 36), favored the now more credited maturation model. Nowadays most of the investigators believe that both mechanisms play an important role in directing traffic through the Golgi (37).

Yet, the understanding of the Golgi apparatus remains largely incomplete. There is not a definite model that explains how *cisternae* are connected, how many types of vesicles are present and how the shape and the function of the *cisternae* are maintained.

1.2.4 *Trans*-Golgi network

The compartment sorting cargo for exiting from the Golgi was defined as *trans*-Golgi network (TGN) by G. Griffiths and K. Simons (38). It has also been referred to as the *trans*-Golgi reticulum (TGR) (39). The TGN is a collection of the last *trans-cisterna* of the Golgi and

a network of large, pleiomorphic, tubular formations and vesicles that extends from it (the network of these carriers is called post-Golgi carriers - PGCs). In the TGN, the proteins and lipids destined for distinct subcellular compartments are sorted and packaged into specific transport carriers (40). At least three transport pathways originate from the TGN: pathway to the lysosomal compartment and two (constitutive and regulated) directed towards the cell surface.

After detaching from the Golgi complex, PGCs undergo dramatic shape changes, including extension, retraction and bifurcation (41).

1.3 Vesicle budding and fusion

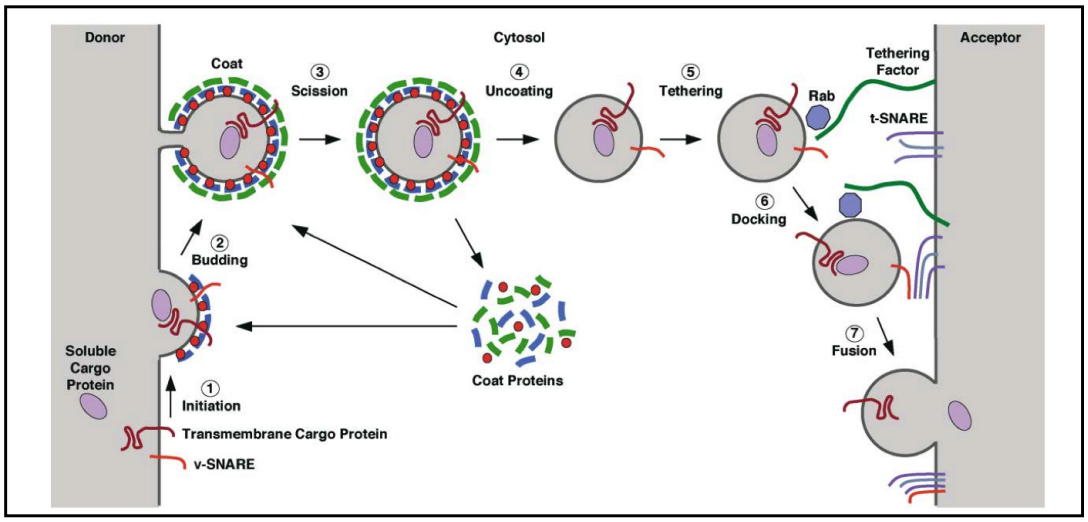

Figure 1.3: **The vesicular transport hypothesis**
The formation of a coated vesicle involves the recruitment of coat proteins from the cytosol, the budding of the vesicle from the "donor" compartment and the scission of the vesicle. Follow by the uncoating of the vesicle (and consequent recycling of coat components), the tethering, the docking and the fusion of the vesicle with the specific "acceptor" compartment. Reproduced from (10).

According to the "vesicular transport hypothesis" discussed above and illustrated schematically in Fig. 1.3, the formation of a vesicle follows a prescribed course of events. Coat components are recruited from the cytosol to the "donor" compartments. These initiate and propagate the assembly of a coat, determine the invagination of the underlying membrane (budding) and

at the same time the sorting of the cargo molecules and their inclusion in the budding vesicles. When the formation of the coat ends, the vesicle bud separates from the "donor" compartment by scission of the neck connecting the invaginated membrane to the donor surface. Afterwards, by a process of uncoating, the coat components are released (and recycled). The vesicle moves then to the "acceptor" compartment, probably on cytoskeletal tracks. Follow the tethering, docking, priming and fusion of the vesicle to the "acceptor" compartment. These final steps are directed by Rab proteins, tethering factors and SNARE proteins. Finally the cargo is released to its final destination (5).

1.3.1 Formation of coated vesicles

Although several kind of of carriers have been identified, some of which have a coat seen by electron microscopy, vesicles clearly identifiable by their coat components (clathrin-coated, COPI-coated and COPII-coated vesicles) are the best studied. The attention here is focused on those coats which have a recognized role in the secretory pathway.

1.3.1.1 Clathrin-coated vesicles

Clathrin-coated vesicles (CCV) were the first coated vesicles to be discovered (42) and are considerably more complex than the other coated vesicles regarding the network of proteins involved in their formation. Initially they were assumed to participate in most, if not all, vesicular transport steps within the cell. However, as demonstrated in later studies, the function of these coats is restricted to the receptor-mediated endocytosis, the trafficking from the TGN to the late endosomes and the remodeling of immature secretory granules.

Clathrin is the main constituent of the clathrin-coated vesicles. It is composed of three heavy chains and three light chains that together form a structure called triskelion (42). Clathrin triskelions assemble into a basket-like framework of hexagons and pentagons to form coated pits, which constitute the scaffold of the budding vesicle.

A second major component of the clathrin-coated vesicles is an adaptor protein complex (AP), described in section 1.3.2 on page 14. Focusing on the most characterized adaptors AP-1 and AP-2, the formation of the coated vesicle, as outlined in Fig. 1.4, is initiated by the recruitment of the AP to the membrane. Synaptotagmin, a calcium sensor, and phosphatidylinositol-4,5-bisphosphate ($PI(4,5)P_2$) are probably involved in the binding of AP-2 to the plasma membrane. ADP-ribosylation factors (ARFs) (see section 1.3.3 on page 15), ARF1 and ARF3, in particular, are involved in the recruitment of AP-1 to Golgi membranes (43; 44). APs have

many functions, such as the recruitment of clathrin, the selection of specific cargo to be incorporated in the nascent vesicle, and the binding of accessory factors involved in the formation of the vesicle. Specific transmembrane proteins and their lumenal cargo molecules become concentrated in the budding vesicle. Some receptors, such as the low density lipoprotein receptor are constitutively included in the pits (45), while some others, like the insulin receptor, are included in the pits only in response to ligand (46). Also Rab and SNARE proteins, involved in the later steps of targeting and fusion of the vesicle to the acceptor compartment, are recruited into the vesicle.

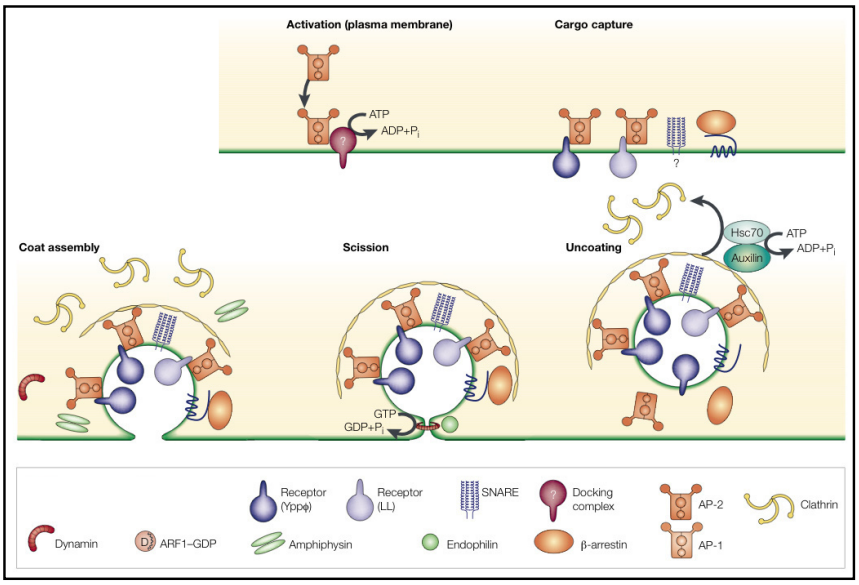

Figure 1.4: **Formation of clathrin-coated vesicles**
Coat assembly is initiated by recruitment of AP complexes on the membrane which subsequently recruit other components, including clathrin. The polymerization of clathrin leads to membrane deformation. The pinching off of the vesicle is caused by dynamin. Modified from (44).

Several accessory proteins play a role in facilitating and regulating vesicle formation. For example amphiphysin, which binds clathrin, AP-2 and dynamin (regulating its GTPase activity), and can contribute to membrane bending with its BAR domain (as described in section 1.3.8 on page 23) (47; 48). Epsin contributes to membrane bending by inserting its ENTH (epsin amino terminal homology) domain into the membrane (49). Endophillin, which induces membrane bending via its BAR domain (50). Synaptojanin, with its phosphoinositide phosphatase activity plays a role, through removal of a phosphate from $PI(4,5)P_2$, in the disassembly of the

clathrin coat by decreasing the affinity of AP-2 for the vesicle (51).

The final fission of the vesicles is mediated by the GTPase dynamin, which can self assemble in spirals at the vesicle neck (52). Its precise mechanism of action remains unclear. Several hypotheses regarding the role of dynamin have been proposed. Following GTP hydrolysis the dynamin ring could contract leading to the fission of the vesicle ("pinchase" model). Alternatively, dynamin could, in its GTP-bound state, recruit effectors (not yet identified) which are the actual "pinchases" (53). Or, according to recent reports, dynamin could act as a mechanoenzyme causing fission of the vesicle if membrane tension is generated by other factors, maybe by the actin cytoskeleton (54) . After the fission the clathrin coat is removed. The heat shock protein Hsc70 and auxillin cause the uncoating of the vesicle, through an ATP-dependent reaction.

Some experiments indicate the presence of clathrin and the adaptors GGA1 and AP-1 in highly pleiomorphic (vesiculo-tubulo)-intermediates in the TGN (55). This would constitute a coat partially different from the classical clathrin coats.

Recently a new type of clathrin coats has been observed in association with pre-melanosomes and with early endosomes, and whose understanding requires further investigations. They contain 2 layers of clathrin, and instead of adaptors contain the protein Hrs, which binds to clathrin and to ubiquitinylated membrane proteins (10).

1.3.1.2 COPI vesicles

COPI-coated vesicles (also referred to as coatomer-coated vesicles) were originally identified through the use of a cell-free assay to study the transport between the ER and Golgi as vesicles with a diameter of 75 nm derived from the Golgi complex (56). The function of COPI-coated vesicles is still a matter of ongoing debate. What is known is that they have a clear function in the retrograde transport from the ERGIC and from the Golgi complex to the ER. Additionally, they could play a role in anterograde transport from the ERGIC to the Golgi complex and within the *cisternae* of the Golgi (Fig. 1.5). Microinjection of antibodies against COPI components, indeed, also blocks anterograde ER to Golgi transport (57). This inhibition of the anterograde transport could be indirect. Because given that the anterograde and retrograde pathway are tightly coupled, continued anterograde transport requires a functional recycling of cargo receptor and other factors back to the ER.

However an increasing number of studies have pointed to a role of COPI-coated vesicles in anterograde transport. COPI-coated vesicles, for example, mediate the transport of proteins

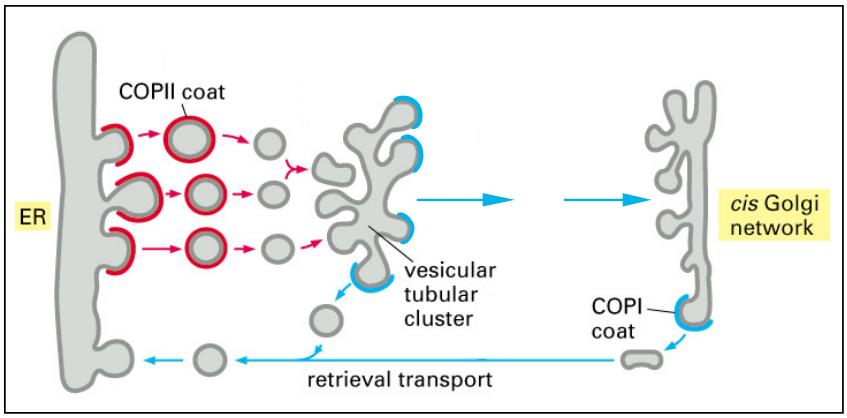

Figure 1.5: **Involvement of COPI vesicles both in anterograde and retrograde ER-to-Golgi transport**
Anterograde transport from ER to the Intermediate compartment occurs through COPII-coated vesicles. As described in the text, recent results suggest an involvement of COPI-coated vesicles in both the retrograde transport (back to the ER) as well as the anterograde transport, from the Intermediate compartment to the Golgi. Modified from (58).

through the Golgi stacks. Two distinct populations of COPI vesicles which contain either anterograde or retrograde cargo have been identified. Furthermore, live-imaging has revealed the existence of COPI coated carriers moving the cargo protein VSV-G to the Golgi (30; 41; 59; 60). Several mechanisms have been proposed to explain the distinction between anterograde and retrograde traffic mediated from COPI vesicles budding from ERGIC. Differential and ARF-dependent sorting of proteins by COPI, or alternatively involvement of different ARF isoforms, or molecular variations of the COPI coat. Also, differential Rab-dependent sorting through different effectors that the two Rabs associated with the ERGIC (Rab1 and Rab2)[1] might activate effectors, which in turn could involve different tethering complexes (30).

The COPI coatomer (700 kDa) is a cytoplasmic complex of seven protein subunits: α, β, β', γ, δ, ϵ and ζ. COPI vesicles efficiently incorporate specific proteins to be transported. γ-COP seems to be the component responsible for cargo recognition, done on the basis of the presence, on cargo proteins, of di-lysin motifs KKXX or KXKXX (K is lysine, X is any amino acid) in their cytosolic domain (or in the cytosolic domain of the receptor that mediate

[1] Rab1 is involved in the anterograde transport between the ER and the Golgi complex, whereas Rab2 is involved in the retrograde transport (61). Evidence point also to the involvement of Rab2 in the anterograde transport from the intermediate compartment to the Golgi (30; 62; 63).

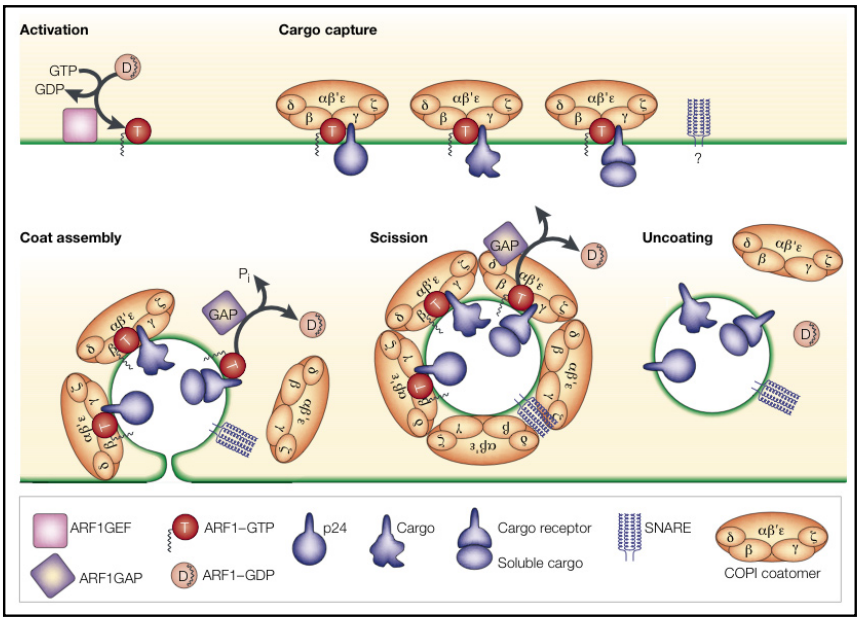

Figure 1.6: **Formation of COPI-coated vesicles**
Coat assembly is initiated by ARF1-GTP which recruits the COPI coatomer. Membrane deformation occurs during coat recruiting. When the coat is complete the vesicle buds. Reproduced from (44).

their transport). The initial event in the formation of a COPI-coated vesicle, as outlined in Fig. 1.6, is the activation and subsequent binding to the membrane of ARF1 (ARF proteins are described below in section 1.3.3 on page 15) . ARNO3, the GEF implied in this activation, promotes the GDP-GTP exchange in ARF1, which changes its conformation and, by exposing its myristoyl group, binds to the membrane. Activated ARF1 recruits the coatomer *en bloc*. The polymerization of the coat and the membrane deformation into buds first and vesicles follow afterwards (44; 64). Additional, though not essential proteins such as p24, might be involved in the recruitment of COPI coatomers to membrane (65). The energy for the fission reaction of the vesicle comes from the hydrolysis of GTP to GDP and from the mechanical curvature of the membrane induced by the coatomer, and does not involve any "pinchase", contrary to the fission of clathrin coated vesicles.

Afterwards ARF-GAP1, and possibly other members of the same family, induce GTP hydrolysis in ARF1-GTP and an uncoating of the vesicle. Some evidence suggest that ARF-GAPs might be involved in the sorting of some cargo, namely the KDEL receptor, and the v-SNAREs (involved in the targeting and fusion steps of the vesicle with the acceptor membrane) (66).

1.3.1.3 COPII vesicles

COPII-coated vesicles were originally identified in *S. cerevisiae* through the analysis of *sec*-mutants with a defective secretion (67) and the use of a cell-free assay to study the transport between the ER and Golgi (68). They are approximately 60-65 nm in diameter and mediate the export of newly synthesized proteins from the ER to the ERGIC.

The formation of COPII-coated vesicles is outlined in Fig. 1.7. Vesicle budding occurs at the ER exit sites and is initiated by Sec12p, a GEF for Sar1p of the ARF family (see section 1.3.3 on page 15). Sec12p may act in conjunction with Sec16p, a putative scaffold protein. The active form of Sar1p binds to the ER membranes and recruits first the Sec23p/Sec24p complex and then afterwards the Sec13p/Sec31p complex, which induces coat polymerization and membrane deformation into buds and then vesicles (10; 69).

The Sec24p subunit is involved in the recruitment of the cargo in the vesicles (70). The sorting signals recognized by the COPII coat are found in the cytosolic domain of transmembrane cargo proteins. Some of them are di-hydrophobic motifs, such as di-phenylalanine (found in ERGIC53) whereas others are di-acidic motifs, such as Asp-X-Glu (found in the VSV-G protein and in the potassium channel proteins, with X standing for an arbitrary aminoacid) (60). Certain soluble cargo molecules depend on receptor-like proteins for efficient ER export,

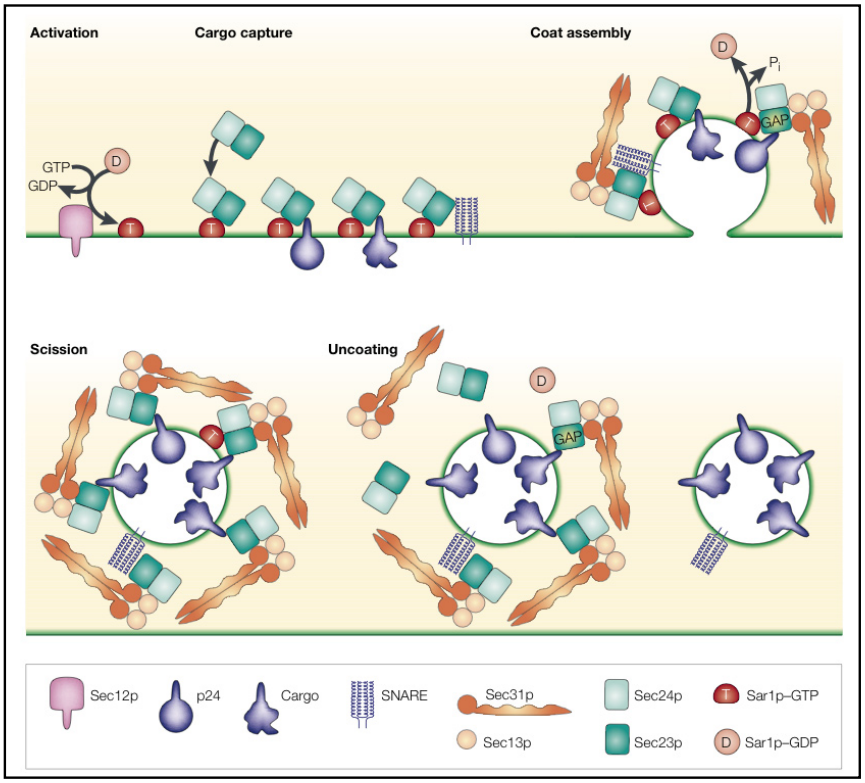

Figure 1.7: **Formation of COPII-coated vesicles**
Coat assembly is initiated by Sar1p-GTP which recruit sequentially the Sar23p/Sec24p and the Sec13p/Sec31p complexes. Membrane deformation occurs during coat recruiting. Upon completion of the coat the vesicle buds. Reproduced from (44).

although signals that direct soluble cargo into ER-derived vesicles are not well understood. The Sec23p subunits binds specific SNAREs involved in the docking and fusion steps of the vesicle with the acceptor membrane. It also acts as a GAP for Sar1p. Sar1p in the GDP-bound form is released, leading to uncoating of the vesicle.

As for the COPI vesicles, the energy for the fission reaction of the vesicle comes from the hydrolysis of GTP to GDP and from the mechanical curvature of the membrane induced by the coat.

1.3.2 Adaptor complexes

At least four major classes of AP complexes (APs) exist (71): AP-1, which is involved in the constitutive secretory pathway and in the TGN-endosomal-lysosomal pathway; AP2, which is required in clathrin-mediated endocytosis; AP-3, which binds clathrin but does not require it for function and plays a key role in melanosome sorting in melanocytes, in synaptic vesicle biogenesis in neurons, and in granule biogenesis in platelets (72); and AP-4, which does not bind to clathrin, but is associated to non-clathrin coated vesicles in the TGN area (73). The Golgi-localized, γ-ear-containing, ARF-binding proteins (GGAs) belongs to the same family, moves along the same AP-1 route, and may share some of its functions (74). A different type of adaptor proteins are the arrestins, which recruit G protein-coupled receptors to clathrin coated vesicles at the plasma membrane (75).

APs are heterotetrameric complexes formed by two large subunits (β associated to μ in AP-1, to α in AP-2, to γ in AP-3, and to ϵ in AP-4), a medium μ ($\mu 1 - \mu 4$) subunit, and a small σ ($\sigma 1 - \sigma 4$) subunit. The core region, the "head", is flanked by two "ears", mainly composed by the large subunits (76). The GGAs are monomers that contain all the previously described functional domains in the same protein.

The function of adaptors has already been addressed in the section regarding the formation of clathrin-coated vesicles (section 1.3.1.1 on page 7).

1.3.3 ARF proteins

The ARF family of proteins belong to the Ras superfamily of small GTPases. Like the other members of the superfamily, they cycle between an active GTP-bound form and an inactive GDP-bound form. ARF proteins function depends on several classes of proteins: guanine nucleotide exchange factors (GEFs) which promote the formation of ARF-GTP, and GTPase-activating proteins (GAPs) which induce GTP hydrolysis. All ARF proteins are myristoilated,

and this is important for their binding to membranes (77). ARF proteins have many effectors. The involvement of different ARFs in specific processes is achieved in an effector- and compartment-specific fashion (78).

Six different ARF proteins (ARF1-ARF6) have been isolated in mammals. They regulate the assembly of coats on budding vesicles along the secretory and the endocytic pathway, activate lipid-modifying enzymes and are involved in actin polymerization as well as in phagocytosis (79). Sar1p belongs to the ARF family of proteins and is involved in the formation of COPII vesicles (80). Contrary to the ARFs, Sar1p is not myristoilated. Also the so-called ARF-like (ARL) proteins belong to the same family. They do however appear to have distinct roles compared to the other ARFs (e.g. Arl1 is involved in the tethering of endosomes derived vesicles to the TGN and Arl2 is involved in the folding of β-tubulin) (81).

1.3.4 Vesicle transport and the cytoskeleton

The cytoskeleton plays a clear role in the transport and the positioning of membrane-enclosed organelles (82). In non-polarized cells the minus ends of microtubules are located near the center of the cell, at the centrosomes, with the plus ends extending to the cell periphery. In polarized cells such as epithelial cells and neurons, which have more than one distinct plasma membrane domain, to which different types of vesicles must be directed, the organization of microtubules is more complex. For example, in epithelial cells the minus ends of the microtubules are localized at the apical surface, whereas the plus ends are at the basolateral surface (24). In neurons, in the axons the plus ends of the microtubules are pointed towards the nerve termini, and the minus ends towards the cell body, whereas in the dendrites the microtubules are found in both orientations (82). Actin microfilaments are concentrated in a cortex, just beneath the plasma membrane, but are also found dispersed throughout the cell.

As pointed out in Fig. 1.8, in non-polarized cells, ER elements (and endosomes, though not indicated in the figure) are dispersed along microtubules towards the plus ends pointed at the cell periphery, with the Golgi complex (plus late endosomes and lysosomes) clustered at the minus ends of the microtubule, at the center of the cell (84). The microtubule-dependent localization of organelles within the cytoplasm is confirmed by experiments in which the treatment of cells with colchicine or nocodazole, which depolimerize microtubules, causes ER collapse to the center of the cell as well as Golgi fragmentation and dispersion throughout the cytoplasm (85).

It has been proposed that the long-range vesicle transport takes place along microtubules using the plus-end directed motor kinesin (83) (or a member of the superfamily of kinesin related

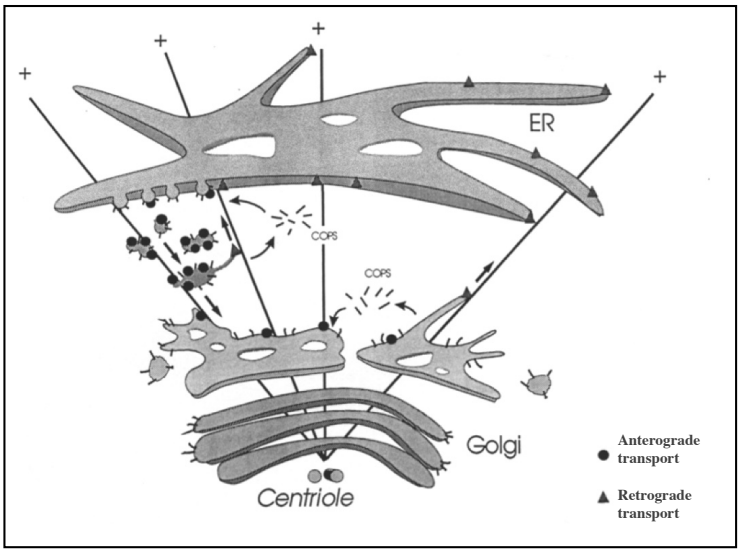

Figure 1.8: **Vesicle transport and cytoskeleton**
The microtubule-dependent distribution of ER, intermediate compartment and Golgi complex within the cell. Microtubules provide a scaffold for the plus-end directed extensions of the ER and the minus-end anchored Golgi *cisternae*. Anterograde transport (circles), dynein-directed and retrograde transport (triangles), kinesin-directed are also indicated. Modified from (83).

proteins (KRPs or KIFs)) and the minus-end directed motor dynein (cytoplasmic dynein, in particular). The short range vesicle transport takes place on actin filaments by myosin motors (82). The molecular mechanism by which kinesin is recruited to membranes is not clear. It is known that several kinesins directly interact with specific cargoes (86). Some evidence, however, point to an involvement of Rab proteins in this process (with no clear consensus emerging) (30; 87), an aspect that is investigated further in section 1.3.5 on page 17). The mechanism by which dynein binds to membranes is better understood. It is known that dynein attaches to the membrane indirectly by interacting with dynactin, which is a multi-subunit complex that binds to integral membrane proteins in the vesicle through its spectrin/ankyrin skeleton (24).

1.3.5 Rab proteins and membrane tethering

The final steps in vesicle-mediated transport between organelles are: the targeting of the vesicles to the appropriate acceptor compartment; the initial and reversible interaction between the membranes of the vesicle and the acceptor compartment (tethering); the docking of the vesicle to the acceptor compartment, which leads to a more tight interaction between their membranes; the priming of the vesicle, which activate membranes for the subsequent fision; and finally the fusion of the vesicle with the acceptor compartment.

The Rab (Ras-related proteins in brain) family of proteins belongs to the Ras superfamily of small GTPases and plays a key role in (but not only) the tethering of the vesicles to the acceptor compartment, providing the necessary specificity to this process. Rab proteins are initially synthesized as soluble proteins in the cytosol, and post-translationally modified by prenilation, meaning the addition of usually two but in some cases one geranyl-geranyl group. To be more detailed, the newly synthesized Rab proteins are first recognized by a Rab escort protein (REP), which presents them to a Rab geranyl-geranyl transferase and escorts the already prenilated Rab proteins to their target membrane. As previously described for the small GTPases ARFs (see section 1.3.3 on page 15), Rab proteins cycle between an active GTP-bound form and an inactive GDP-bound form, the switch between the two forms being controlled by guanine nucleotide exchange factors (GEFs) and GTPase-activating proteins (GAPs). After performing their function, Rab proteins are extracted from membranes by a Rab GDP dissociation inhibitor (GDI), and remain in the cytosol until the next cycle (77). More than 60 mammalian Rab proteins have been identified, each one with a specific intracellular localization, as illustrated in Fig. 1.9.

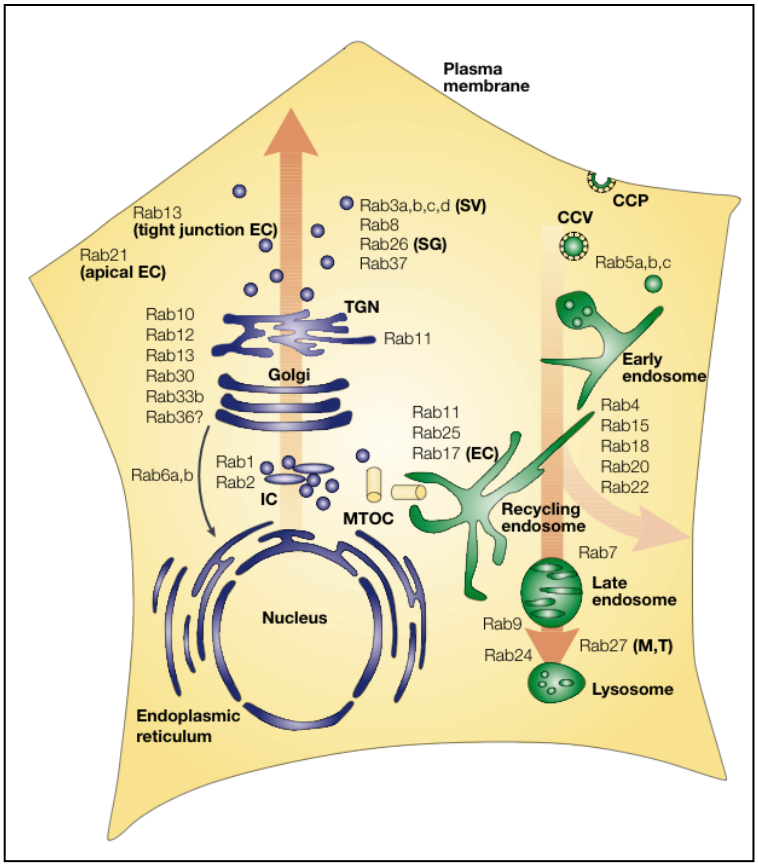

Figure 1.9: **Subcellular localization of Rab proteins**
Rab proteins show a precise distribution within the cell: some of them are present in all cell types, while others (e.g. Rab3, Rab27 and Rab17) are cell specific. EC: epithelial cell; M: melanosomes, T: T-cell granules; SG: secretory granule; SV: synaptic vesicle; MTOC: centrosome; CCP and CCV: clathrin-coated pits and vesicles, respectively. Reproduced from (88).

Rab effectors are defined as proteins that interact with a GTP-bound Rab, but not with a GDP-bound Rab, and transduce the signal of the Rab protein in the transport mechanism (88). Many Rab effectors have been identified and new ones are continuing to be discovered, providing the basis of the understanding of how Rab proteins regulate and coordinate diverse processes like vesicle budding, transport along the cytoskeleton, docking and fusion of vesicles to the acceptor compartment (89), and interact with signaling pathways to regulate membrane traffic spatially and temporally (77).

Focusing on the docking and fusion of vesicles to the acceptor compartment, Rab proteins facilitate and regulate the rate of vesicle docking and the matching of cognate SNAREs: this is accomplished through the recruitment, by the GTP-bound Rab, of specific docking factors from the cytosol, which remove putative inhibitor factors (SNARE protectors, that block SNARE pairing at all times) and facilitate the SNAREs pairing, conferring also additional specificity to the identification between the vesicle and the appropriate acceptor compartment (90). Several macromolecular complexes have been identified that function as docking factors: the Exocyst, originally identified in yeast (91), and present also in mammals (92), required for docking of vesicles to the plasma membrane; the Rabaptin-5 complex (93), important for Rab5-dependent early endosome fusion; the TRAPP (transport protein particle) complex, required for ER-to-Golgi transport in yeast (94).

1.3.6 Other Rab functions

Rab proteins are also required for vesicle budding. It has been hypothesized that vesicle formation is regulated such that budding only occurs if the vesicle contains both Rab and SNARE proteins necessary for docking and fusion (90). However, recent results suggest that Rab proteins play an active role in vesicle budding as detailed in the following. Expression of a dominant negative form Rab1 ($Rab1_{S25N}$, with a lower affinity for GTP than normal and almost uniquely present in its GDP-bound form) inhibits export from the ER to the Golgi (95). In the intermediate compartment Rab2, through the protein kinase C PKCι/λ, promotes the recruitment of COPI to generate retrograde transport of vesicles (63). A dominant negative form of Rab9, $Rab9_{S21N}$, strongly inhibits mannose-6-phosfate receptor (MPR) recycling from endosomes to the trans-Golgi network (96). On the plasma membrane, Rab5 seems to be involved in ligand sequestration in the clathrin-coated pits (97).

As discussed in section 1.3.4 on page 15, Rab proteins are also involved in controlling the recruitment of motor proteins on defined compartments. The first description of a Rab protein

directly coupling to a motor protein was for the Golgi-associated Rab6, which binds Rabkinesin-6 (RB6K), a kinesin-like protein (98). Since then, a growing number of similar examples have been reported in the literature. For example, BicD1 and BicD2, can bind Rab6 and dynactin (which in turn binds dynein) (99); Rab4, in the GTP bound form, binds KIF3B, a kinesin-2 family member (100); and Rab5 interacts with the dynactin/dynein complex (101), as well as with KIF16B, a kinesin-like protein (102; 103).

1.3.7 SNARE protein and vesicle fusion

The SNARE proteins (SNAREs or SNAP receptors) play a central role in the docking and especially in the fusion processes of the vesicle with the acceptor compartment (104). SNAREs are a superfamily of small proteins originally identified as plasma membrane receptors for α-SNAP (soluble NSF association factor), which binds NSF (N-ethylmaleimide-Sensitive-Factor), required for membrane fusion, to membranes. These proteins had previously been implied in the binding of synaptic vesicles to the plasma membrane (105; 106). SNAREs are small C-tail anchored proteins (C-terminally anchored transmembrane proteins, with their N-terminal domain facing the cytosol, as described in section 1.2.1 on page 3) of around 100-300 aminoacids in length. They share a common homologous sequence of 60 residues, known as SNARE motif, involved in the formation of a complex with a coiled-coil structure between SNAREs on opposite membranes (three SNAREs, SNAP-23, SNAP-25 and SNAP-29, contain two tandem SNARE motifs) (107). SNAREs are structurally classified as Q-SNAREs and R-SNAREs, depending on the presence of a glutamine (Q) or an arginine (R) at a characteristic position within the SNARE motif (108). In the early '90s the SNARE hypothesis for membrane fusion, outlined in Fig. 1.10, was proposed. According to this hypothesis every vesicle has its own v-SNARE, and every target membrane has its own t-SNAREs. Fusion of membranes occurs when the cognate v- and t-SNAREs engage[1], in a parallel fashion (109). The complex so generated is a very stable four-helix bundle, with one α-helix contributed by the monomeric v-SNARE and three α- helices contributed by the oligomeric t-SNARE (107). Assembly of SNAREs in the opposing membranes pulls the membrane close to each other, generating the energy needed to bring the two negatively charged opposing membranes close enough, and cause the formation of a stalk hemifusion intermediate and then the opening of a fusion pore, with fusion of the vesicle to the acceptor compartment. Upon fusion, the SNARE complex is disassembled. NSF is an ATPase

[1] Despite the distinction between v- and t-SNAREs is not meaningful during the homotypic fusion of organelles, this classification remains useful. Moreover there is a rough correspondence between R- and v-SNAREs and between Q- and t-SNAREs.

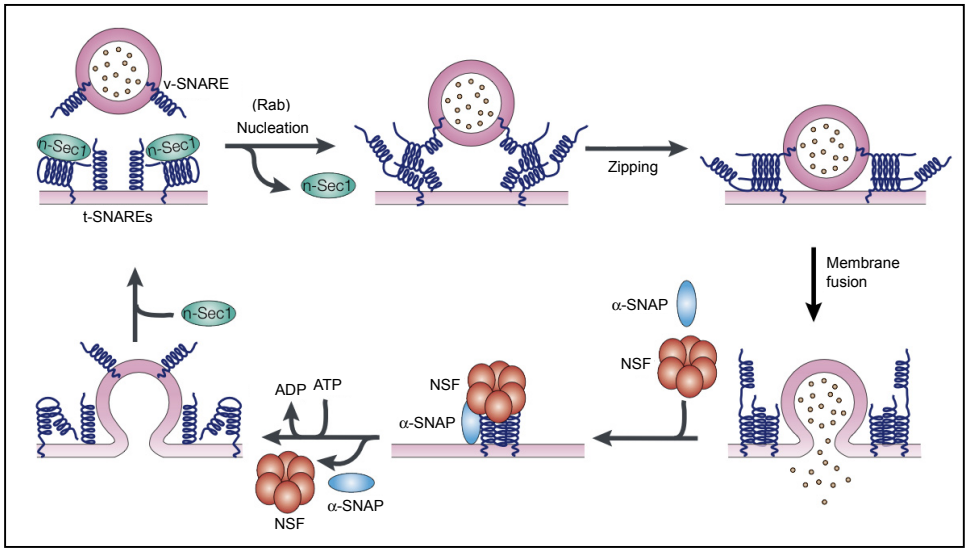

Figure 1.10: **SNAREs in membrane fusion**
After the tethering and docking steps, directed from Rab proteins and their effectors, appropriate SNAREs pair. The SNARE complex is formed by a monomeric v-SNARE on the vesicle and an oligomeric t-SNARE on the "acceptor compartment". The pairing, first loose, becomes tight following the priming, and this results in membrane fusion and release of vesicle content. After fusion, the SNARE complex is disassembled by NSF (recruited through α-SNAP). Modified from (104).

that binds the SNARE complex via an adaptor called SNAP (α-SNAP described above belongs to this class of proteins), and generates the energy necessary to dissociate the SNARE complex (110).

Besides NSF and SNAPs, many additional factors, which facilitate and regulate the fusion reaction, have been identified. An important group of SNARE-interacting proteins is the SM family (Sec1/Munc18-like proteins). These proteins play a prominent role in vesicle trafficking, and each membrane fusion step requires a specific SM protein. Despite this, their function remains enigmatic. Depending on the specific SM protein, they can stimulate or inhibit SNARE complex assembly (this seems to be the case for Munc13 and Munc18 respectively), they may confer additional specificity in the pairing of cognate SNAREs or couple the assembly of the SNARE complex to membrane attachment, or act as chaperones for the SNAREs (110; 111). Moreover, some evidence point to the existence of an inhibitory class of SNAREs, the i-SNAREs, which prevent incorrect fusions from occurring. They could act by competing with either the v-SNARE or the t-SNARE during the formation of the SNARE complex, or by binding to the SNARE complex and prevent it from driving membrane fusion (112).

The role of Ca^{2+} in SNAREs-dependent membrane fusion (in exocytosis, in particular) will be addressed later, in section 1.4.2.2 on page 32.

1.3.8 Proteins with BAR domain

Proteins carrying a BAR (bin, amphiphysin and Rvs161/167) domain are a class of cytosolic proteins with membrane-binding and/or membrane-deforming properties, mostly involved in intracellular transport and especially in endocytosis. The BAR domain, first solved by Peter and coll. (48; 113), and illustrated in Fig. 1.11, is an elongated banana-shaped dimer which can fit a curved membrane with an outer diameter of 22 nanometers (nm): each monomer (200 amino acids long) is a coiled-coil of three kinked α-helices, which give rise to a six-helix bundle upon dimerization. Both ends and the concave surface of the dimer are positively charged, suggesting their interaction with the negatively charged phospholipids of membranes. The BAR domain can either bind and deform membranes ("strong" BAR domain) (114; 115) or act only as a curvature-sensing module, sensing rather than imposing membrane curvature ("weak" BAR domain) (116).

Some of the proteins with a BAR domain have, in addition, an N-terminal amphipatic helix which folds upon membrane binding, causing the displacement of lipids in one leaflet. This helix enhances the ability of these proteins to deform membranes. The combination of the N-terminal

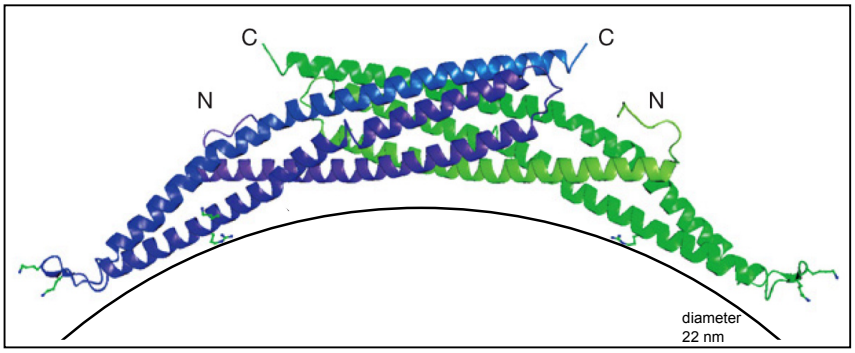

Figure 1.11: **Structure of the BAR domain**
Ribbon representation of the antiparallel homodimer of the *Drosophila* BAR domain: the two monomers are indicated in purple and green. The banana shape is generated upon dimerization and can fit a curved membrane with an outer diameter of 22 nanometers. Modified from (117)

helix and the BAR domain is referred to as N-BAR domain. Examples of proteins carrying a N-BAR domain are amphiphysins, BRAP1/Bin2 (breast cancer associated protein1/bridging integrator 2), endophillins and nadrins (48). Recently it has been reported the presence, in a family of proteins implied in the regulation of actin cytoskeleton (e.g. Toca-1 and syndaptin), of an N-terminal module similar to the BAR domain and called F-BAR domain. This domain corresponds to the FCH (Fes/CIP4 homology) domain followed by the CC (coiled-coil) domain previously identified in these proteins and, as the BAR domain, is a membrane binding/bending module (113; 118).

Some BAR proteins have additional motifs that provide further functions. These may enhance membrane association, like the pleckstrin homology (PH) domain (oligophrenin and centaurinβ) or the phox homology (PX) domain (sorting nexins); mediate the interaction with other proteins, like the Src homology 3 (SH3) domain (amphiphysin and tuba); or regulate the activity of small GTPase through GEF or GAP domains (nadrins, tuba, oligophrenin and centaurinβ) (48).

Furthermore, some other proteins belonging to the same family interact with small GTPase and take part in the signalling pathways from them regulated. Arfaptins, for example, bind alternatively Arf1/Arf6 in the GTP-bound form and Rac in the GDP-bound form, and probably mediate the cross-talk between these two GTPases (113; 118). Another example are APPL1 and APPL2 (from adaptor protein containing PH domain, PTB domain and Leucine zipper motif) which are Rab5 effectors (119).

1.3.9 Phosphoinisitides

Phosphatidylinositides (PIs) are important regulatory molecules involved in diverse processes such as signal transduction, cytoskeleton remodeling, cell migration and membrane trafficking. Phosphorylation on different positions of the inositol ring generates different isomers that are heterogeneously distributed in the cell and, together with proteins, especially small GTPase (described earlier in this section), provide additional specificity to the processes indicated above (120; 121).

PIs were initially characterized as mediators of signal transduction events, through the formation on the plasma membrane of second messengers like inositolpolyphosphate 3 (IP3), diacylglycerol (DAG) or arachidonic acid from PtdIns4, $5P_2$ (PI(4,5)P_2)) (122). Later it was clarified that PIs may also act directly in signal transduction, interacting with proteins (effectors) bearing a lipid-binding domain like the pleckstrin homology (PH) domain, the FYVE (from Fab1-YOTP-Vac1-EEA1) domain, the epsin amino terminal homology (ENTH) domain, the phox homology (PX) domain, the C2 (for the homology with PKC) domain or the plant homeodomain (PHD) (123). Various are the examples of the involvement of PIs in membrane trafficking. PI(4,5)P_2 is enriched in regions of the plasma membrane and promotes clathrin-mediated endocytosis, through the recruitment of the adaptor complex AP-2 and accessory proteins with a role in endocytosis (dynamin among them). PI(4,5)P_2 is also involved in secretory granule exocytosis, probably through the proteins synaptotagmins and CAPS (Ca^{2+} dependent activator protein for secretion) and it plays a role in rearrangement of the actin cytoskeleton through ARF6 and the small GTPase Rho (124). Moreover, PI(4)P enriched in the Golgi, is involved in the recruitment of AP-1 to the Golgi and is therefore important for AP-1 dependent functions (125); and PI(3)P, enriched on the early endosomes, plays a role in endocytic trafficking, through the interaction with Rab5 and the recruitment of proteins with a FYVE domain, such as EEA1 (121).

1.4 Constitutive and regulated secretion

The term exocytosis indicates the fusion of a vesicle with the plasma membrane. Constitutive exocytosis occurs in all cells, and it is required for constant delivery of newly synthesized proteins and lipids to the cell surface. In specialized secretory cells a second pathway also exists (regulated secretory pathway) in which soluble proteins and other substances are initially

stored in secretory vesicles, and released only in response to a physiological signal. Fig. 1.12 is a schematical representation of the two pathways.

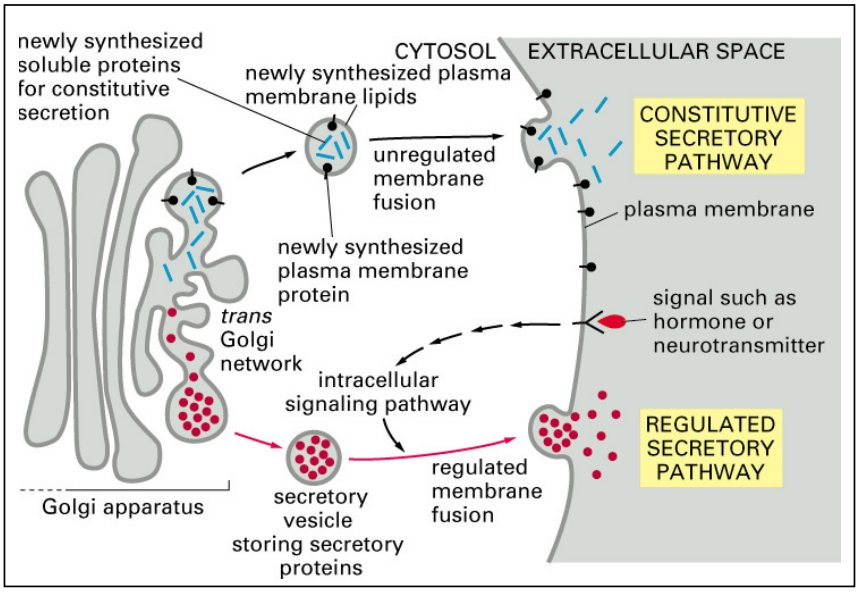

Figure 1.12: **Constitutive and regulated secretory pathways**
The constitutive secretory pathway operates in all cells. Many soluble proteins are continuously secreted by this pathway, which also supplies the plasma membrane with newly-syntethized components. Specialized secretory cells also have a regulated secretory pathway, where secretion happens only in response to appropriate stimuli. Reproduced from (58).

1.4.1 Constitutive secretion

The constitutive secretory pathway assures constant delivery of membrane proteins, receptors and lipids from the TGN to the cell surface. Some extracellular molecules (e.g. plasma proteins, antibodies, extracellular matrix components, lipids for the formation of the myelin sheats, etc.) are also secreted by a constitutive secretory pathway (126). Constitutive exocytosis is observed in non-polarized cells and in polarized cells (to which epithelial cells and neurons belong to), that have two distinct plasma membrane domains. Epithelial cells secrete constitutively mainly through their basal membrane. Neurons secrete constitutively trough their somato-dendritic membrane (127). Recent findings point to the existence of multiple parallel routes in membrane traffic from the TGN to the plasma membrane, even in a non-polarized cell such as a fibroblast: an AP-1- and/or AP-4-based direct route from the TGN to the plasma membrane,

an actin and Cdc42-dependent route, a constitutive transport (e.g. for VSV-G-containing vesicles) to the basolateral membrane involving microtubules and the Exocyst, a constitutive transport to the apical membrane involving Kinesin and Dynamin-2 (e.g. for influenza virus hemoagglutinin(HA)-containing vesicles), and an AP-dependent route from the TGN to the endosomes and from here to the plasma membrane via the recycling endosomes (e.g. for the glucose transporter GLUT-4-containing endosomes in adipocytes) (127; 128).

As described in previous sections (1.1.1 and 1.1.2 on pages 1-3), ultrastructural studies have lead to the widely accepted view that constitutive traffic may proceed through small (60-80 nm) coated vesicles, or through large, pleiomorphic and highly dynamic carriers moving from the perinuclear area to the periphery along microtubule tracks (129). It is still not clear whether clathrin is required or not for constitutive secretion. Likely only some of the routes from the TGN to the plasma membrane (e.g. the one through the recycling endosomes) are regulated by clathrin and AP complexes. A possibility is the involvement of a not yet identified non-clathrin coat on constitutive vesicles (130). Despite original data indicated the constitutive pathway as a default pathway, for which proteins lacking any targeting information would exit the cell constitutively (131), more recent data indicate the existence of sorting signals, although degenerate, for constitutive secretion (127). It is not clear, however, how the active sorting of proteins in the constitutive pathway occurs.

Since constitutive exocytosis is often presented as the opposite of regulated exocytosis, it is widely considered as unregulated. However, constitutive exocytosis is well controlled, as demonstrated in polarized cells by the fact that the sites of fusion at the cell surface are not randomly distributed but subject to control. Studies of constitutive transport in polarized cells and in budding yeast have allowed the identification of multiple regulators of this process. Rab8, Rab13 and Rab11 have been implied in the regulation of the TGN-to-plasma membrane traffic. They could act on different routes of the constitutive pathway, or act sequentially on the same one (128). ARF proteins play a role in the budding of constitutive vesicles from the TGN, as demonstrated by inhibition of their formation by brefeldin A (BFA) (130). Heterotrimeric G-proteins appear to regulate the formation of both constitutive and regulated secretory vesicles from the TGN (132). Protein kinase D (PKD) regulates the fission from the TGN of transport carriers that are directed to the cell surface (133).

1.4.2 Regulated secretion

Constitutive and regulated exocytosis differ by three main characteristics (126). First, regulated secretion is coupled to an extracellular stimulus , which leads to a transient rise in intracellular Ca^{2+} or another second messenger. Second, in regulated exocytosis the cargoes destined to be released are accumulated and concentrated within specialised organelles, which are not ubiquitous among cell types; while a constitutive secretory cell shows up to two-fold concentration of the secretory product from the ER to the secretory vesicle, a cell which secretes in a regulated fashion shows up to 200-fold concentration of the secretory product. Third, regulated secretory cells store secretory vesicles within their cytoplasm even for long periods of time. Regulated secretory cells include neurons, endocrine, neuroendocrine and exocrine cells, mast cells, platelets, large granular lymphocytes and neutrophils (134).

Two routes of regulated secretion can be distinguished (126; 135). One route releases molecules synthesized in the ER, modified in the Golgi and packaged in secretory vesicles at the TGN. The other one releases molecules synthesized in the cytosol and taken up into secretory vesicles. The first pathway is followed by polypeptides (e.g. insulin, glucagon, granins, parathyroid hormone), while the second is for low molecular weight factors, such as neurotransmitters (e.g. cathecolamines, acetylcolin, glutamate). The difference between the two pathways corresponds at the morphological level to two distinct types of organelles. In neurons, based on early observations at electron microscopy, these are defined as small clear synaptic vesicles (SVs), ∼50 nm in diameter, for classical neurotransmitters, and large dense core (for the presence of an electron-opaque content separated or not from the membrane by a clear space) vesicles (LDCVs) or more generically secretory granules (SGs), ∼200 nm in diameter, for neuropeptides (136; 137). In endocrine cells the same organelles are called synaptic-like microvesicles (SLMVs) and LDCVs or SGs, respectively (138). Neurotransmitter and peptide secretion differ also in terms of exocytosis. Exocytosis is fast (∼200 μsec) and short-lasting for SVs, with secretion in restricted synaptic active zones. It is slow (from milliseconds to seconds) and less precisely targeted for LDCVs (135). Concerning the molecular exocytotic machinery, the majority of the proteins that function in regulated exocytosis has been studied in SVs, at synapses. Synaptic vesicles are indeed abundant within nerve terminals and relatively easy to purify. Nevertheless, both SVs and LDCVs share an overall similar molecular composition, not only at the level of components present in their membrane, but also at the level of cytoplasmic and plasma membrane components that participate in the exocytosis (134; 139).

1.4.2.1 Biogenesis of SVs and LDSVs

SVs are known to be docked at specialised area of synaptic plasma membrane, the active sites, where they undergo fast discharge and rapid recycling. They are thought to originate from constitutive vesicles which undergo exocytosis, through local recycling of the plasma membrane. The neurotransmitter, synthesized in the cytosol, is taken up into these vesicles, by active transport through a specific transporter (130; 140). At the active sites, SVs are organized in two distinct pools in dynamic equilibrium: the readily releasable pool (RRP) and a much larger reserve pool. This belief has been proposed already 50 years ago (141), and successively generalized and corroborated (140; 142). The RRP is constituted of vesicles that can be released in response to a stimulus, without further maturation steps. The reserve pool is reversibly anchored to the actin cytoskeleton and can be recruited to the RRP upon completion of maturation (142). Electrophysiological measurements suggest that in the various synapses, the size of the releasable pool varies, thus accounting for different proportions (0.5-10%) of the total vesicles content. The transit from the reserve to the releasable pool is modulated by the action of synapsins, which anchor SVs to the actin cytoskeleton. Upon increase in Ca^{2+} concentration synapsins are phosphorylated. The phosphorylation of synapsins reduces their affinity to actin and allows SVs to redistribute to the RRP (143). In addition to synapsins other proteins, such as the Rab3, have been suggested to regulate SVs movement along the cytoskeleton. The detailed mechanisms of these events, however, is still unclear (140; 143).

As already mentioned, the biogenesis of secretory granules begins in the TGN, where regulated secretory proteins (RSP) are sorted, aggregated and packaged into organelles, defined as immature secretory granules (ISGs), which successively are converted in mature secretory granules (MSGs or simply SGs) (144; 145) (Fig. 1.13).

The precise mechanism of sorting of RSP from the TGN in ISGs (and their retention in the ISGs during maturation) is not clearly understood. The research of common sorting signals in RSP has led to the identification of a conserved N-terminal loop in chromogranins A and B (CgA and CgB) and in another secretory protein, the pro-opiomelanocortin (POMC) (146), which seems to play a role in the sorting of these proteins. Other secretory proteins, however, such as insulin, do not contain this type of loop. A different "sorting domain" seems instead to be present in the B-chain of the mature insulin (147). Moreover, to date, no "sorting receptor" in the TGN has been identified.

A model has been proposed for the formation of ISGs, according to which RSP aggregate in the slightly acidic pH and high Ca^{2+} concentration present in the TGN environment. This

leads to the reorganization of cholesterol-rich microdomains in the TGN and to the budding of ISGs from the TGN (148). Many of the secretory proteins are synthesized as precursors, from which the active protein is liberated by proteolysis: processing usually begins in the TGN and is completed in the ISGs. The processing is operated by pro-hormone convertases (e.g. PC1/3, PC2 and carboxypeptidase E/H (CPE/H)) (149). In the case of insulin, the pro-insulin forms examers in the TGN, and as such it is exported in the ISGs. Aggregation and crystallization occurs only upon processing, in the examers, of pro-insulin to insulin (150). Granins, a family of proteins to which CgA and CgB belong to, seem to play a role as helpers of packaging, sorting and aggregation (151).

ISGs which bud from the TGN, undergo maturation to become MSGs. During this step pro-hormones are processed by endopeptidases known as pro-hormone convertases (PC). ISGs have discontinuous mantle of clathrin, which, however, does not play a role in the budding of ISGs rather in their maturation (146; 152), for the removal, through clathrin-coated vesicles, of soluble peptides, unprocessed pro-hormones, missorted proteins and random material that is not supposed to be in the MSGs. Recently, it has been shown that GGA (described in section 1.3.2 on page 14) is the adaptor protein recruiting clathrin on the ISGs (153). During their maturation the secretory granules change size upon condensation of the soluble content and the removal of material via clathrin-coated vesicles. In cells like chromaffin PC12 cells, ISGs may also undergo homotypic fusion as part of their maturation process (146; 154).

In a few number of cells that undergo to regulated secretion, the pool of SGs is fully releasable upon stimulation: this is the case for mast cell. In most of regulated secretory cells however, at least two distinct pools of SGs exist (in analogy to the SVs): a readily releasable pool (RRP), consisted of immobile granules near the plasma membrane, and a reserve pool. Notably the RRP (1-5% of the total granules) is preferentially composed by newly synthesized granules (155; 156). Microtubules seem to play a role in this phenomenon: newly synthesized granules are preferentially released because they preferentially associate with microtubules and are therefore located closer to the plasma membrane, if compared with "old" granules. As for the SVs, the recruitment of SGs to the RRP is regulated by their trapping in the actin cytoskeleton, in particular in the cortical actin meshwork (the so-called "cell web"). Stimulation of secretion and increase in Ca^{2+} concentration, seems to activate phosphorylation of specific substrates and to reduce the affinity of SGs to actin, allowing SGs to redistribute to the RRP and to be secreted. The molecular players of this mechanism seem to be better understood in insulinoma cells, where SGs are trapped in the actin cortex by the receptor

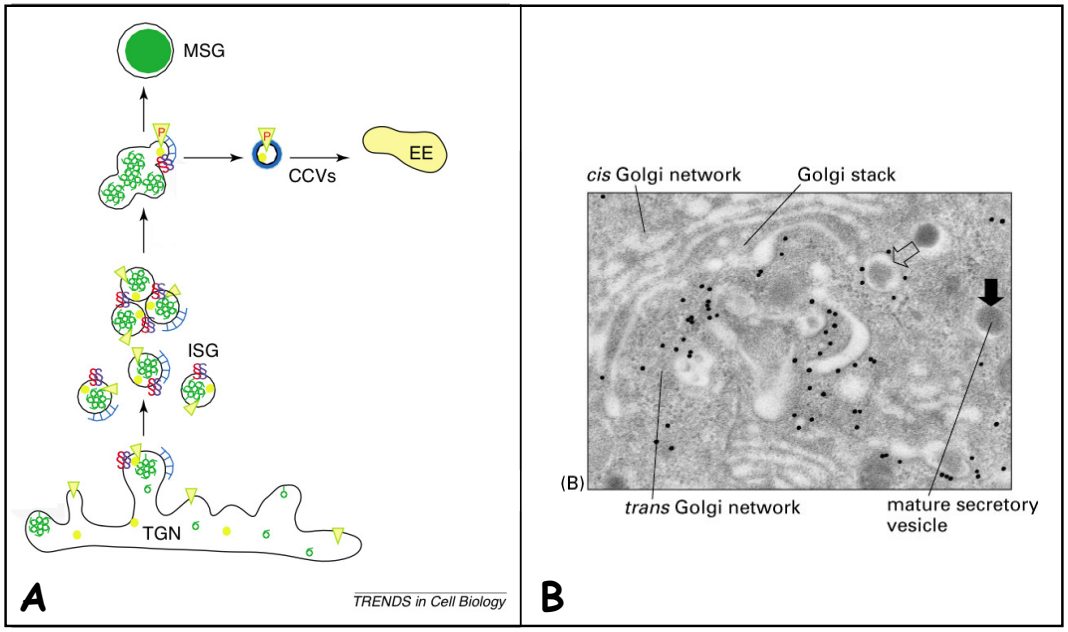

Figure 1.13: **Biogenesis of secretory granules**
A) Immature secretory granules (ISGs) budding from the TGN undergo progressive maturation in secretory granules (MSG) by homoypic fusion and removal of all the ISGs components which are not destined to be part of the SG, by clathrin-coated vesicles (CCVs). During the maturation of the ISGs the secretory proteins mature as well, through cleavage by convertases and aggregation. Modified from (146). B) Electron micrograph showing secretory vesicles forming from the *trans*-Golgi network in a insulin-producing β-cell of the pancreas. The black dots are relative to immuno-gold labeling of clathrin. The ISGS (open arrow), contain clathrin patches, while the mature SGs (solid arrow) do not show this patches anymore, while showing a highly condensed core. Reproduced from (58), by courtesy of L. Orci.

tyrosine phosphatase-like protein ICA512, a transmembrane protein which binds, through β2-syntrophin and utrophin, the actin cytoskeleton. Upon stimulation of insulin secretion, and as result of phosphorylation/dephosphorylation of β2-Syntrophin, the interaction between the latter protein and ICA512 is loosened and SGs can be secreted (157).

1.4.2.2 Exocytosis of SVs and SGs

The stages of regulated exocytosis and the basic fusion machinery involved in this processes have been shown to be essentially the same for the two types of organelles (SVs and LDCVs) (126), although the different kinetics suggests that some specific factors are also needed. As for all the vesicles cycle (described in section 1.3 on page 6), the exocytotic vesicle cycle can be divided into 5 distinct steps, as schematically illustrated in Fig. 1.14 A: targeting, tethering, docking, priming and fusion. Targeting is defined as SVs and LDCVs transport to the release sites. Tethering as the initial, not stable contact between organelles and release sites. Docking is the attachment to the membranes. Priming is the maturation step through which the organelles become competent for final release. Finally the fusion leads to the release of the secretory vesicle content in the extracellular space (134; 139).

The same kind of components already described in section 1.3 on page 6 and seq. (Rab proteins, SNAREs, NSF and SNAPs) are involved in exocytosis, with one important "new entry": the Ca^{2+}-binding proteins. The SNAREs associated with regulated exocytosis are synaptobrevin (also called vesicle-associated membrane protein or VAMP) on the vesicle, and syntaxin1 and SNAP-25 on the plasma membrane (139). It is still not clear which factors are involved in the tethering and docking steps. It is possible that SNAREs are not essential for this steps, since the number of vesicles docked to the plasma membrane is not decreased in cells poisoned with clostridial toxins (known to block neurotransmitter release by cleaving the SNAREs) (158). SNAREs seem instead to be essential for the last steps, the priming and the fusion (104). Other factors, most probably Rab proteins, might be responsible for the tethering and docking steps (159). More in detail, Rab3a for SVs and Rab3a and/or Rab27a for SGs seem to be involved in these processes (139; 160; 161).

Priming events render vesicles competent for fusion with the plasma membrane (primed vesicles constitute the RRP, which undergo to rapid exocytosis in response to an increase in Ca^{2+} concentration). The priming step is ATP-dependent, and involves several processes. NSF (described earlier in section 1.3.7 on page 20) is necessary to dissociate SNARE complexes formed within a single membrane in favor of a productive *trans*-SNARE complex (162). Protein

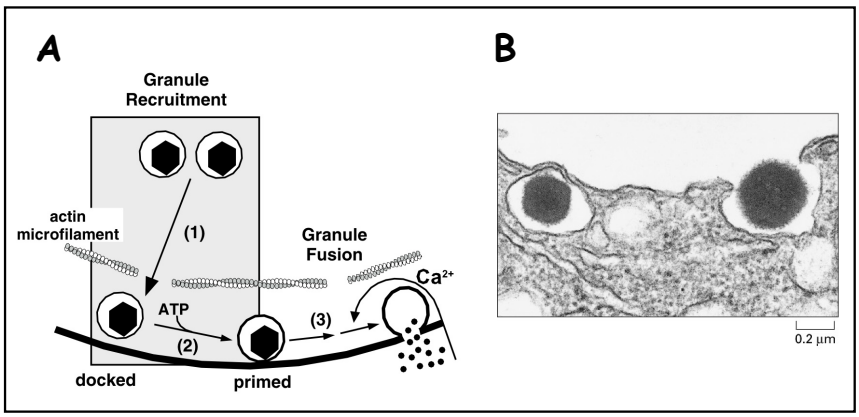

Figure 1.14: **Exocytosis of secretory vesicles**
A) The recruitment of a secretory vesicle to the readily releasable pool (RRP) involves it's tethering and docking to the plasma membrane (1), and it's ATP-dependent priming (2). Following Ca^{2+} signaling the secretory vesicle fuses to the cell surface and discharge its content. Ca^{2+}entry leads also to the disassembly of the cortical actin cytoskeleton, which traps the vesicles reducing the mobility of the secretory vesicles close to the plasma membrane. B) Electron micrograph showing the release of insulin from a pancreatic β-cell. Reproduced from (58), by courtesy of L. Orci.

phosphorylation (Calmodulin -dependent kinase, protein kinase A (PKA) and protein kinase C (PKC)) seem to play a role in priming, as well as phospholipid phosphorylation, and in particular formation of PI(4,5)P_2. PI(4,5)P_2, in turn, binds and regulates Ca^{2+}-binding proteins such as synaptotagmin and CAPS (Ca^{2+} dependent activator protein for secretion) (163; 164). Another event during priming is the action of munc13 (a SM protein described earlier in section 1.3.7 on page 20) in removing the inhibitory effect of munc18 (a SM protein) on syntaxin1 (139).

The central role of Ca^{2+} in regulated exocytosis has been recognized for many years. Most exocytotic fusions are induced, indeed, by an increase in the intracellular concentration of Ca^{2+}. SVs require a higher Ca^{2+} concentration (100-200 μM) than SGs (1-10 μM) (135). In neurotransmission the action potential induces the opening of Ca^{2+}-channels and the increase in Ca^{2+} concentration. Conversly, in secretion of SGs, an extracellular stimulus leads to the opening of Ca^{2+}-channels. Synaptotagmins represent the best and most characterized Ca^{2+}-sensors (165). Synaptotagmins are transmembrane proteins that can bind phosholipids through two C2 domains (similar to the lipid-binding domain in PKC), can bind Ca^{2+}, and in a Ca^{2+}-dependent fashion undergo conformational changes and interact with other proteins involved in regulated exocytosis (e.g. SNAREs) (166). At least 15 synaptotagmins have been identified, and among them two seem to have a main role in SVs and SGs exocytosis, synaptotagmin1 and synaptotagmin3 respectively. Synaptotagmin1, shows low Ca^{2+} affinity, which is consistent with the high Ca^{2+} concentration required for neurotransmitter release (167). Synaptotagmin3, which does not bind pospholipids through the C2 domains, has a higher affinity for Ca^{2+} which makes it a better Ca^{2+}-sensor for secretion of SGs, that requires a much lower Ca^{2+} concentration (168). Notably both synaptotagmins can interact with Ca^{2+}-channels. Synaptotagmin1 interacts with the N-type Ca^{2+}-channel involved in neurosecretion, while synaptotagmin3 interacts with the L-type Ca^{2+}-channel involved in secretion of SGs (169); the same Ca^{2+}-channels also interact with syntaxin1 and SNAP-25: this ensures that Ca^{2+}-entry is restricted to the areas where SVs or SGs are located. CAPS is other putative Ca^{2+}-sensor, specific for SGs. It can bind Ca^{2+} (at low affinity) and PI(4,5)P_2 and it seems to be involved in regulated exocytosis (170).

Mobilization of intracellular Ca^{2+} stores (meaning from the ER) does not seem to be a major determinant in regulated secretion.

Upon Ca^{2+} signaling , and as illustrated in Fig. 1.10 (Ca^{2+} is the factor that in secretory vesicles exocytosis determines the "zipping" of the SNAREs), the SVs and SGs fuse to the cell surface and discharge their content. How the *trans*-SNARE complex, already but not tightly assembled in the priming step, causes fusion is still open to questions. In summary,

the hypotheses may be grouped according to two possible models. In the first proposal, during the assembly of the "trans complex", membranes are so close that the hemifusion state favours their final contact and the formation of a lipidic fusion pore. In the second model, the fusion pore forms a sort of proteinaceous channel connecting the two opposing membranes (171). After fusion, and as already described in section 1.3.7 on page 20, NSF and SNAPs cause the disassembly of the SNARE complex.

After discharge, vesicles are retrieved from membrane surface. SVs are locally recycled and refilled with neurotransmitter for another exocytotic cycle, while the LDCVs are refilled via the Golgi-complex. Two models have been proposed since the early '70s for vesicles recycling at synapses, schematically illustrated in Fig. 1.15. In the first model, recycling occurs through endocytosis via clathrin-coated vesicles (172). According to an alternative model, known as "kiss and run", recycling occurs through coupled exo-endocytosis (173). The recycling through CCVs model involves the dispersal of SV components in the plasma membrane following exocytosis, their reclustering, probably through the adaptor complex AP-2 and the consequent budding of a CCV (174). In the "kiss and run" model, neurotransmitter is released through a fusion pore that transiently and reversibly opens during exocytosis. Vesicles are therefore molecularly preserved and simply need to be refilled by uptake systems present in situ in nerve terminals (173). The same two models have been proposed for the secretion of SGs (175; 176), with addition of an intermediate model, known as "semifusion". This model involves the establishment of a large opening between the SGs and the extracellular space, even though the SGs remain structurally intact (177). Experimental data do not favor either model. CCVs are abundant in nerve terminals and block of clathrin-mediated endocytosis determines paralysis in the mutant known as *shibire* in *Drosophila*. These data would favor the first model (140). On the other hand the first model can explain with some difficulties continuous secretion for sustained stimulation. This consideration, together with capacitance measurements and amperometric assays, favors the "kiss and run" model (178). Recent investigations strongly suggest that both pathways, coated pits and kiss-and-run, are employed in parallel, although at different rates. Both routes coexist in the same terminal, and that the contribution of kiss-and-run increases (up to 80%) at high frequencies of stimulation (179).

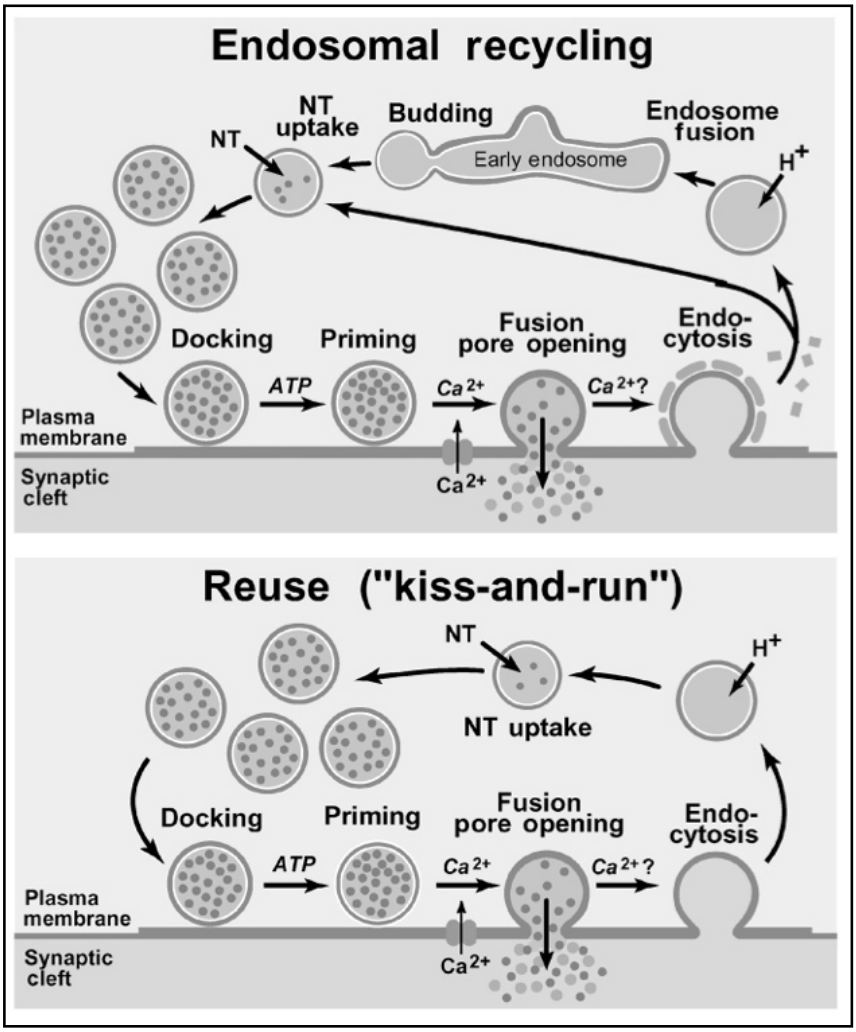

Figure 1.15: **Secretory vesicle recycling**
Two pathways are proposed to explain synaptic vesicle recycling. The first pathway (up) implicates conventional exocytosis, with intermixing of the vesicle and plasma membrane components. Follow clathrin-mediated retrieval of the vesicle components, their delivery to the endosome and the budding of synaptic vesicle from the endosome. In the kiss-and-run model (bottom) the fusion pore is closed shortly after its opening. According to this model, the vesicle maintains its identity and simply needs to be refilled with neurotransmitter. The same two models have been proposed in the secretion of SGs. Reproduced from (140).

1.4.3 Insulin-containing SGs

Insulin[1], the most important hormone for glucose homeostasis, is produced in the β-cells of the pancreatic islets of Langerhans (180). Discovered in 1869 by Paul Langerhans, the islets of Langerhans constitute approximately 1 to 2% of the mass of the pancreas. Each pancreatic islet contains few thousands cells and is 50-500 μm in diameter. Hormones produced in the islets of Langerhans are secreted directly into the blood flow by (at least) four different types of cells (neuroendocrine cells) (181): insulin producing β-cells (70-80% of the islets cells), glucacon-releasing α-cells (15-20%), somatostatin-producing δ-cells (5%), pancreatic polypeptide-producing PP cells also called γ-cells (up to 1%).

Insulin is the primary anabolic hormone, promoting glucose uptake into the cells, glycogen and triglyceride synthesis and inhibiting hepatic gluconeogenesis. Additionally, insulin regulates other cellular events such as protein and DNA synthesis and amino acid (aa) transport (182). Insulin is produced only in β-cells (Fig. 1.16), and the regulation of its expression depends on an elaborate set of transcription factors which tightly regulate insulin gene expression also in response to physiologic signals such as glucose (183). Another important step in the regulation of insulin expression is the post-transcriptional regulation of its mRNA. Stimulation of the β-cells with high glucose leads to an increase in insulin biosynthesis up to 20-fold. Several mechanisms are involved in the increased translation: increase of the initiation of translation and increase in the elongation rate of the nascent peptide, increased binding to the SRP and translocation in ER (184). Recently it has been shown that glucose increases also insulin mRNA stability, through the binding of polypirimidine tract-binding protein (PTB) to its 3'-untranslated region (3' UTR). This mechanism stabilizes also other mRNAs encoding proteins of the SGs (185).

Insulin secretion occurs upon increase of glucose concentration in the blood, (in healthy individuals plasma glucose is on a range between 3.9 and 6.1 nmM (70 and 110 mg/dL)). Glucose is the primary signal that triggers SGs exocytosis. Other signals, however, like amino acids or long-chain acyl-CoA, derived from glucose and from free fatty acid (FFA), play a role in insulin secretion (186). β-cells store insulin in SGs (described earlier in this section). Ultrastructural studies have shown that a single β-cell contains $\sim$13000 granules (187), of which, as described earlier, $\sim$5% belongs to the RRP.

[1]Insulin is the first hormone which has been discovered, in 1922 by the collaboration of Frederick Banting and Charles Best with J.J.R. Macleod and James Collip; in 1923 Banting and Macleod were awarded the Nobel Prize in Physiology of Medicine for the discovery of insulin.

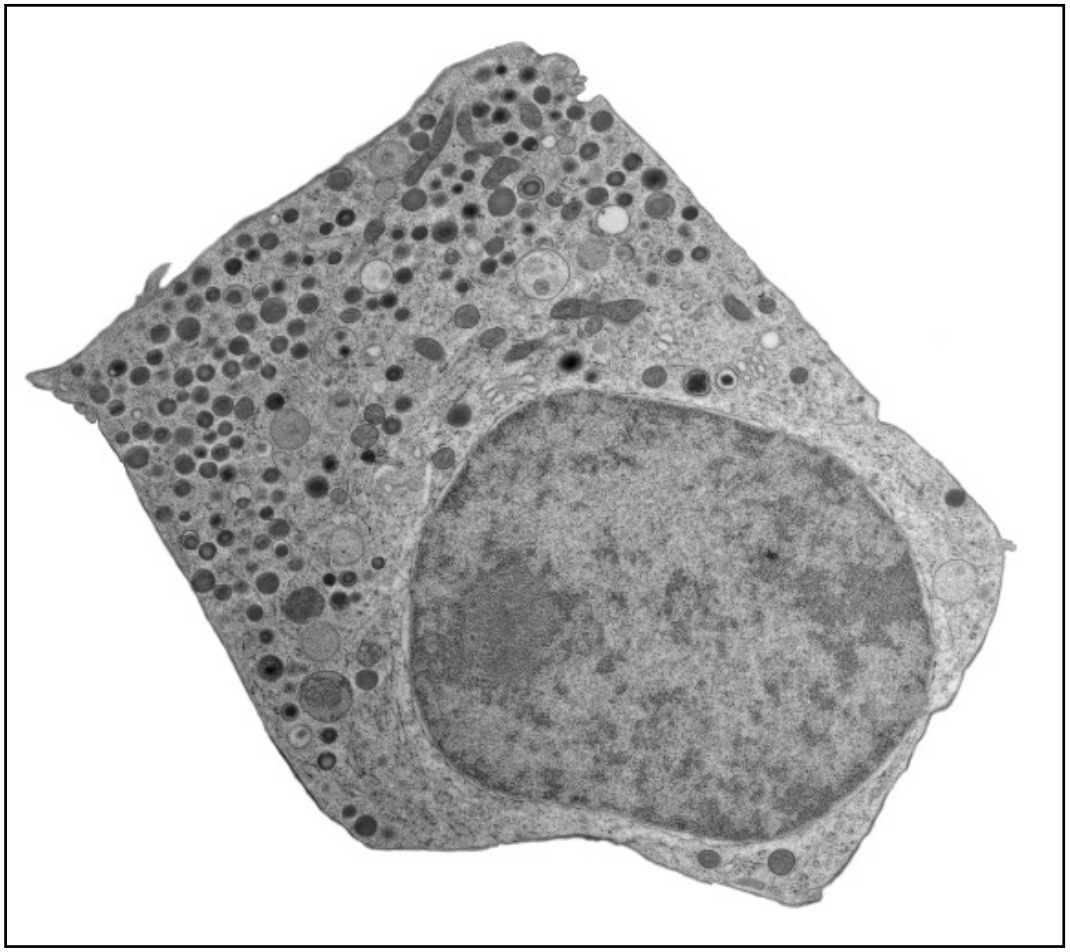

Figure 1.16: **Pancreatic β-cell**
Electron micrograph of a high pressure frozen islet cell (by Joke Ouwendijk).

Glucose enters the β-cell through the low-affinity glucose transporter-type 2 (GLUT-2), and after phosphorylation by glucokinase (GK), it goes into the glycolysis and the respiratory cycle, with consequent ATP production and increase in the ATP/ADP ratio. This controls the closure of ATP-sensitive potassium ($K^+{}_{ATP}$) channels on the plasma membrane. The consequent depolarization of the membrane causes the opening of voltage gated L-type Ca^{2+}-channels. The local increase in Ca^{2+} concentration, in turn, determines exocytosis of SGs (188). Actually, and because of the allosteric regulation of the glycolytic enzyme phosphofruttokinase (PFK), glucose determines oscillations in the ATP/ADP ratio, with consequent oscillations in membrane potential and oscillations in the local Ca^{2+} concentration. This phenomenon gives rise to pulsatile insulin secretion (189; 190). Furthermore patch-clamp and amperometric measurement have established that insulin secretion in response to glucose stimulation is biphasic[1] and consists of a rapid release phase and a slower, sustained phase, during which secretion continues at a lower rate in compared to the first phase (192; 193). The first phase of insulin secretion corresponds to the exocytosis of the RRP, already primed and therefore competent for secretion. The second phase correspond to the exocytosis of the reserve pool. This phase is slower than the first one, reflecting the time SGs need to be recruited, docked and primed at the plasma membrane (164; 169; 194). The molecular machinery involved in insulin secretion has already been described earlier in this section.

β-cells are able to couple the consumption and the production of SGs. Upon stimulation several processes are activated in order to renew granule stores. Recently, a putative mechanism which couples this two processes has been identified in insulinoma cells. The receptor tyrosine phosphatase-like protein ICA512, a transmembrane protein of the SGs, is indeed cleaved after exocytosis of SGs, and the cytosolic fragment generated translocates to the nucleus, binds the transcription factor STAT5 and promotes insulin gene expression. This allows the β-cell to monitorate the consumption of SGs (195; 196).

1.5 Diabetes

Diabetes mellitus (or simply diabetes) is a complex metabolic disorder characterized by hyperglycemia, disturbance of carbohydrate, fat and protein metabolism resulting from defects in insulin secretion, insulin action or both. Diabetes comprehends type 1 diabetes, type 2 diabetes, maturity-onset diabetes of the young and gestational diabetes (197).

[1] Mice deviate from this behavior, showing a first and transient phase in insulin secretion, followed by a very weak second phase (191).

1.5.1 Type 1 diabetes

Type 1 diabetes (T1D) (also known as insulin-dependent diabetes mellitus (IDDM), as immune mediated diabetes (IDM), or as "juvenile diabetes" because it mostly affects individuals already during their childhood-adolescence) accounts for approximately 5-10% of all diabetes cases. T1D results from the autoimmune destruction (by CD4+ and CD8+ T-cells and by macrophages) of the pancreatic β-cells, therefore resulting in insulin deficiency (198). Susceptibility to T1D, indicating the genetic predisposition to T1D, seems to plays a role in the future development of T1D. In the last years a number of loci have been identified as susceptibility loci for T1D and between them the HLA DR/DQ region (199). Another important factor which may lead to T1D is the exposure to environmental factors such as viruses (e.g. enteroviruses, rotavirus and especially rubella) (200), toxins (e.g. nitrosamines) or food (e.g. cereals, gluten and cow's milk proteins) (201).

In T1D the abnormal activation of T-cells leads to insulitis (inflammation of the islets) with consequent and progressive destruction of the β-cells and to the activation of B-cells with production of autoantibodies to β-cell antigens. T1D autoantibodies, pointed out in Fig. 1.17, include antibodies against insulin, CPE/H, islet cell autoantigen 512 (ICA512) and the related phogrin, islet cell autoantigen 69 (ICA69) and glutamic acid decarboxylase 65/67 (GAD 65/67) (202). Autoantibodies appear already in the pre-diabetic phase of the disease, allowing therefore (especially if two or more different autoantibodies are present) the identification of subjects with high risk of developing T1D (203). Nevertheless there is no evidence that any of this antibodies has an active role in the pathogenesis of this disease. Recent studies indicate, on the other hand, that B-cells play an important role in the development of T1D, not as antibody-producing cells, but as antigen-presenting cells, contributing therefore to the expansion of CD4+ and CD8+ T-cells (204).

1.5.1.1 Autoantibodies in T1D

As pointed out earlier, T1D is characterized by the appearance of a specific set of autoantibodies. Many systemic and organ-specific autoimmune diseases are characterized by high-titer autoantibodies against intracellular antigens. A frequent finding is that autoimmune targets of any given disorder are part of the same macromolecular complex. Proteins associated with nucleic acids are, for example, typical autoantigens in systemic lupus erythematosus (205). Centrosomal proteins are associated with rheumatoid arthritis (206). Golgi or nuclear proteins are

characteristic autoimmune targets in Sjögren syndrome (207) or systemic scleroderma (208), respectively.

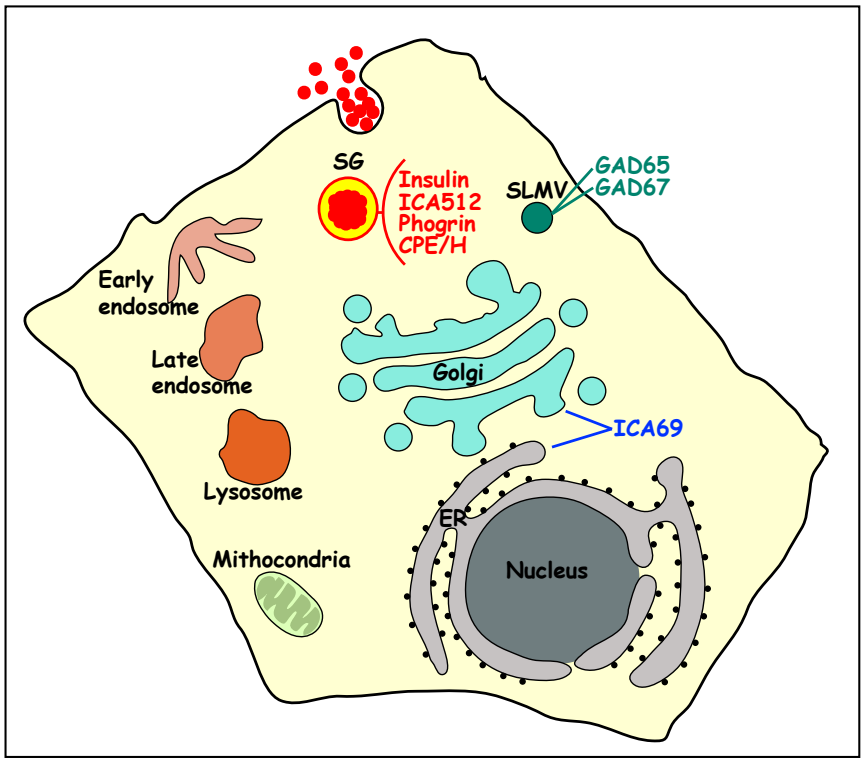

Figure 1.17: **Autoantigens in T1D**
Schematic drawing of a β-cell showing the intracellular distribution of known T1D autoantigens. With the exception of ICA69, all other autoantigens are associated with secretory vesicles. ICA69 seems to be associated with earlier stages of the secretory pathway.

Increasing evidence suggest that autoimmunity in T1D follows a similar pattern. In the case of T1D, humoral autoimmunity seems to preferentially target β-cell proteins that are enriched in Golgi and post-Golgi secretory vesicles, including insulin secretory granules and synaptic-like microvesicles (202) (Fig. 1.17). These findings have been explained by proposing that in the course of the disease humoral autoimmunity spreads from one epitope in a single antigen to many epitopes within the same antigen, as well as to multiple epitopes of associated proteins (209).

1.5.2 Type 2 diabetes

Type 2 diabetes (T2D) is the most common form of diabetes, accounting for approximately 90% of all diabetes cases. T2D is characterized by disorders in insulin secretion and insulin action[1]. In most patients, T2D results from alterations in various genes, each having a partial and additive effect. T2D is indeed a polygenic disease (210). During the last years an increasing number of genes involved in T2D have been identified, some of which are involved in insulin secretion (e.g. GLUT-2, GK, insulin, $K^+{}_{ATP}$ channels), some others in insulin action (e.g. insulin receptor, insulin receptor substrate 1 (IRS1), phosphoinositide 3-kinase (PI3K), hepatocyte nuclear factor 1-α (HNF1α), calpain 10) (211). Another important trigger for the development of T2D is given by environmental factors (including obesity, lack of physical activity, smoke or alcohol intake). As pointed out earlier, insulin resistance, meaning the inability of insulin target tissues to correctly uptake and utilize insulin and the following resistance to the metabolic effects of insulin, is one of the defects in T2D. For the clinical manifestation of T2D, however, insulin resistance must be accompanied by a compromised β-cell compensatory ability (212).

1.5.3 Maturity-onset diabetes of the young

Maturity-onset diabetes of the young (MODY) is a monogenic form of diabetes, caused by specific mutations in one of the MODY-related genes, causing a β-cell dysfunction: MODY-related genes include GK and β-cell-specific transcription factors (e.g. HNF1α and HNF4α) (213).

1.5.4 Gestational diabetes

Gestational diabetes is carbohydrate intolerance associated with hyperglycemia with onset or first recognition during pregnancy. This form of diabetes can have deleterious consequences for both the fetus and the mother (214). The pathogenesis of gestational diabetes resembles that of T2D and it seems to be caused by some of the hormones produced in the placenta, which can have a blocking effect on insulin (the so-called "contra-insulin" effect).

[1] Insulin initiates its effect on target tissues by binding a specific membrane receptor on their plasma membrane, the insulin receptor (IR), thus activating its tyrosine-kinase activity which leads to the phosphorilation of endogenous substrates and in particular IRS-1 (insulin receptor substrate 1). IRS-1, in turn, activate several cytosolic signaling components, including phosphatidilinositol 3-kinase (PI3K) and $p21^{ras}$ (182).

1.6 Islet Cell Autoantigen 69

Islet Cell Autoantigen of 69 kDa (ICA69) was originally identified by screening an islet cDNA expression library with sera of pre-diabetic relatives of patients with T1D (215). ICA69 was shown to migrate as a 69 kDa protein by SDS-PAGE. The corresponding gene, designated as ICA1 in humans and Ica-1 in mice, was mapped on chromosome 7 and 6 in the two species. The rat ICA69 was cloned afterwards, and the correspondent gene was mapped on chromosome 4 (216). Alternatively spliced variants which encode different protein isoforms have been described in different species. However, not all variants have been fully characterized (being the 69 kDa isoform the most studied) (217). As most autoantigens of T1D, ICA69 is primarily expressed in neuroendocrine tissues, with peak levels in brain and in pancreatic islets (215; 218). Recent studies have shown that the tissue expression of this protein is affected by three distinct 5'-untraslated (5' UTR) exons representing three different promoters (exons A, B or C). More in detail, exon A transcript predominate in islet cells, exon B transcripts in neuronal cells (219).

Despite not being a main autoantigen of T1D (whose antibodies are the first to appear in the development of T1D, like insulin, ICA512 and GAD 65 (220)) and not being an obligate autoantigen of T1D, still ICA69 is a target autoantigen[1] in T1D (215). Moreover, nonobese diabetic (NOD) mice (the experimental model for the study of autoimmune diabetes) show a loss of self-tolerance to ICA69 (222). ICA69 is an antigen also in autoimmuno diseases other then diabetes. ICA69 autoantibodies have been shown, indeed, in rheumatoid arthritis and in primary Sjögren's syndrome (223; 224).

ICA69 is partially cytosolic and soluble, although a subfraction appears to be membrane-bound, as shown by subcellular fractionation studies in murin brain tissues and insulinoma cells. More in detail, it appears to be associated, at least partially, with the Golgi complex (225; 226).

ICA69 function is still unknown, but a mutation of its homologue *ric-19* in *Caenorhabditis elegans* confers resistance to the drug aldicarb, an inhibitor of acetylcolinesterase, consistent with a defective neurotransmitter secretion in the mutant and an involvement of ICA69 in neurosecretion (225; 227). Nevertheless ICA69^{null} NOD mice have no obvious phenotype and age normally. ICA69^{null} NOD females develop diabetes at essentially wild-type NOD incidence,

[1] The antigenic determinant in ICA69 is called Tep69 T-cell epitope, encompassing amino acids 36-47 of human ICA69 (221).

by they are highly resistant to cyclophosfamide-induced diabetes progression. How cyclophosfamide accelerates islets destruction is not well understood, but it may require the ICA69 protein (228).

Recently, sequence and structural analyses, have revealed the presence of a BAR domain in the N-terminal region of ICA69 (113; 226). The BAR domain proteins, as described in section 1.3.8 on page 23, are mostly involved in intracellular transport. This finding has provided new motivation in the investigation of the still unknown cellular function of ICA69, and its putative role in intracellular membrane trafficking.

Chapter 2

Aim of the thesis

The main aim of this thesis was to study the role of ICA69 in context of membrane trafficking. Several lines of evidence point to an involvement of this protein in membrane traffic:

- ICA69 was historically identified as a T1D autoantigen. As described in section 1.5.1.1 on page 40, in T1D autoantibodies are preferentially directed against β-cell proteins that are enriched in Golgi and post-Golgi secretory vesicles.

- Even though ICA69 function is still unclear, a mutation of ICA69 homologue in *C. elegans* impairs acetylcholin release at the neuromuscular junctions, thereby suggesting an involvement of ICA69 in regulated secretion.

- Preliminary evidence indicate that ICA69 is associated with the Golgi complex, in agreement with its putative involvement in neurosecretion.

- ICA69 contains, in the N-terminal region, a BAR domain. The BAR domain, described in section 1.3.8 on page 23, is present in several proteins involved in intracellular transport and functions as dimerization motif, provides a general binding interface for different types of GTPases and it is a membrane binding/bending module.

In the course of this thesis it was therefore investigated whether ICA69, similar to other proteins containing a BAR domain, plays a role in intracellular membrane traffic and in particular in the trafficking of proteins targeted to the insulin secretory granules.

Part of the thesis was also devoted to the study of an ICA69 paralogue gene, called ICA69-RP. This is a novel gene whose expression, like that of many components of the regulated

secretory machinery in β-cells, is glucose regulated, therefore pointing to the involvement of this protein in insulin secretion.

In brief, the study of β-cell autoantigens with yet unknown function may provide insight into the secretory machinery of β-cell, and lead to the discovery of novel pathways. Furthermore, the characterization of proteins containing a BAR domain, here the two members of the ICA69 protein family, with emphasis on their interaction with small GTPases, could elucidate novel aspects involved in the trafficking of secretory proteins in β-cells, and more in general in secretory cells.

Chapter 3

ICA69

3.1 ICA69 cellular localization

ICA69[1] cellular localization was investigated in the rat insulinoma cell line INS-1, as ICA69 was shown to be highly expressed in islet-derived cell lines (215).

Confocal microscopy shows a cytosolic distribution of ICA69, the punctate "vesicular" staining consistent with the interaction of a pool of the protein with membranes (225; 226). ICA69 is enriched in the perinuclear region[2], where also markers of the Golgi region are found (Figs. 3.1 and 3.2). More in detail ICA69 partially co-localizes with GM130, marker of the cis-medial Golgi compartment, and with TGN38, marker of the TGN, even though ICA69 shows a broader distribution than these Golgi markers. No significant co-localization is found between ICA69 and concavalin A, a lectin which specifically binds α-mannopyranosyl α-glucopyranosyl sugar residues, or the membrane-anchoring tail of the citocrome b in fusion with GFP (called btail-GFP), both markers of the ER, or β-COP, component of the coatomer and peripherally associated with the Golgi complex.

These results partially confirm previous data (226).

[1] Two previously characterized α-ICA69 antibodies were used in the experiments reported in this thesis: a polyclonal antibody raised against residues 471-483 of human ICA69, and a monoclonal antibody, which recognizes an epitope in the first 230 amino acids of human ICA69 (215; 226). Despite the strong homology at the protein level between ICA69 and ICA69-RP (see Chapter 4), these α-ICA69 antibodies did not crossreact with ICA69-RP (AppendixB, Fig B.1, on page 112). Another antibody was produced in the course of this thesis, raised against the central region of ICA69. This antibody turned out, however, not to be specific for ICA69, and was therefore not used in any of the reported experiments.

[2] The more specific and confined distribution later obtained for ICA69 by immunocytochemistry (compare Figs. 3.1 and 3.2), was due to the use of a new batch of the antibody, in conjunction with a partially modified protocol for the immunocytochemistry, which allowed a clearer visualization of the distribution of ICA69.

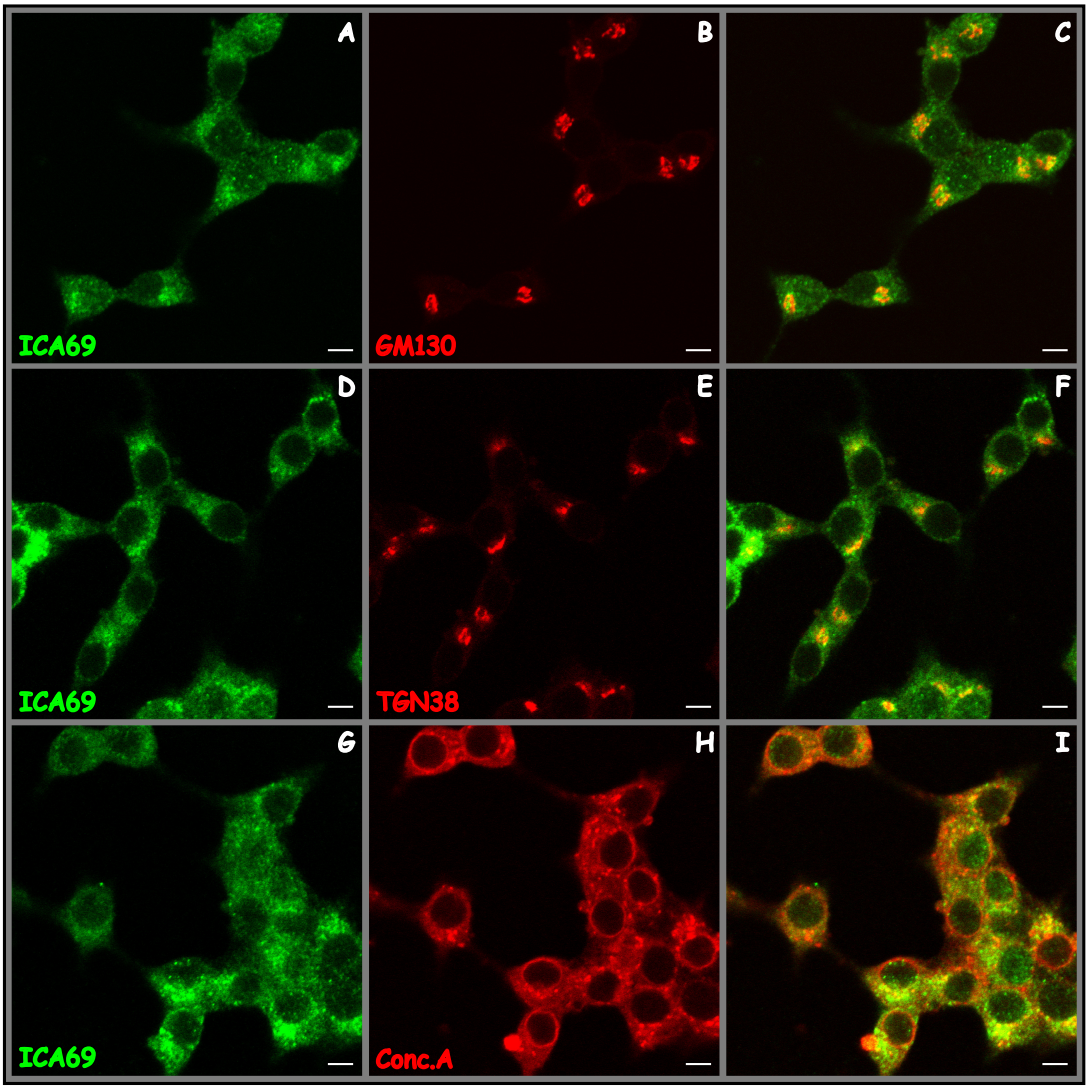

Figure 3.1: **ICA69 cellular localization.1**
Confocal microscopy images from double stained INS-1 cells. A-C: ICA69 (pseudogreen) and GM130 (pseudored). D-F: ICA69 (pseudogreen) and TGN38 (pseudored). G-I: ICA69 (pseudogreen) and concavalin A (pseudored). Merge in C, F, I. Scale bar: 5 μm.

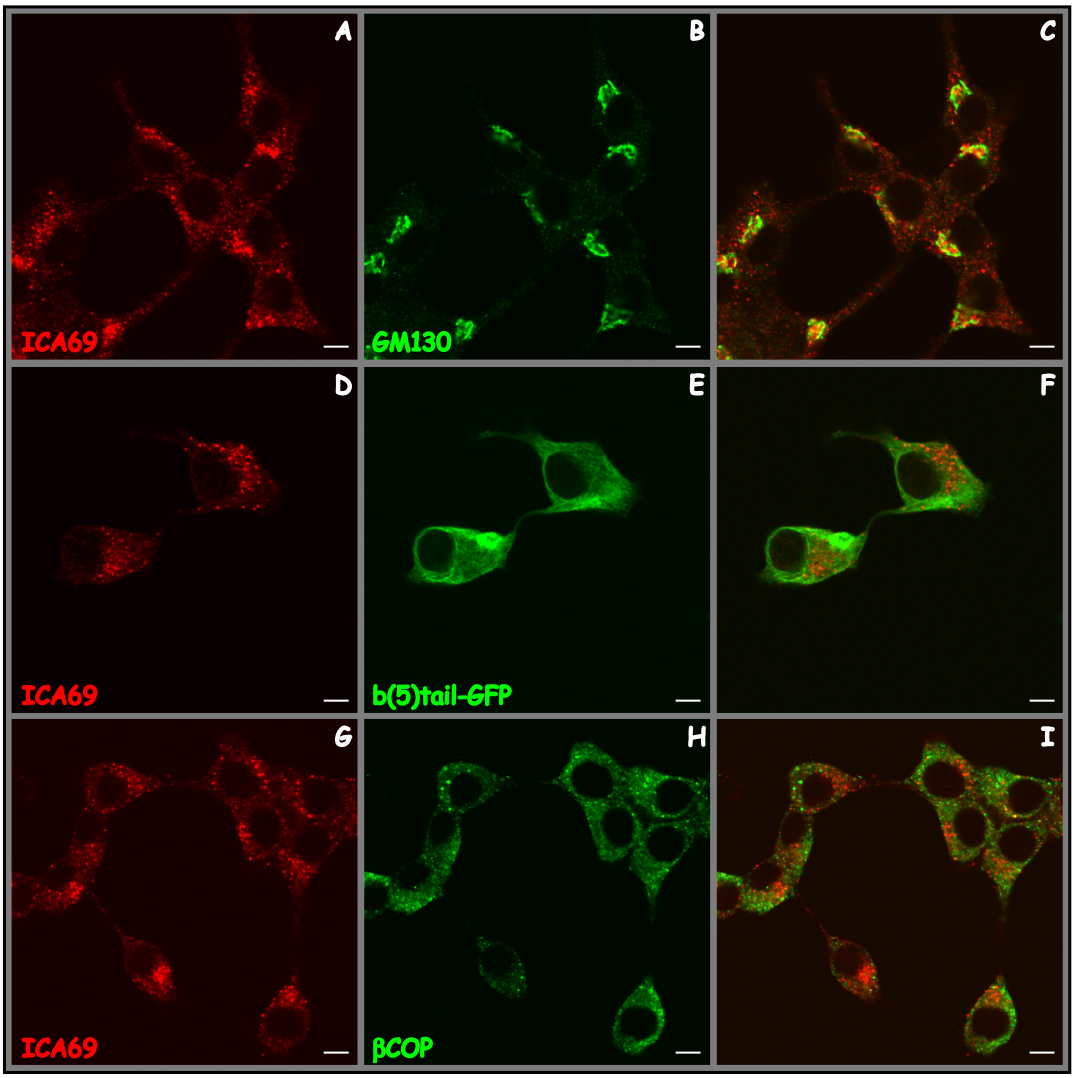

Figure 3.2: **ICA69 cellular localization.2**
Confocal microscopy images from double stained INS-1 cells. A-C: ICA69 (pseudored) and GM130 (pseudogreen). D-F: ICA69 (pseudogreen) and btail-GFP (pseudogreen). G-I: ICA69 (pseudogreen) and β-COP (pseudogreen). Merge in C, F, I. Scale bar: 5 μm.

3.2 Binding of ICA69 to lipids

As described in section 1.3.8 on page 23, relative to proteins with a BAR domain, the BAR domain is a membrane binding/bending module. Therefore ICA69, with a BAR domain at its N-terminus, was likely to bind lipids. In order to elucidate the lipid binding properties of ICA69, a protein-lipid overlay assay was performed. Nitrocellulose filters spotted with various phospholipids (PIP Strips) were incubated with purified ICA69-GST in an overlay assay, and binding of ICA69 to specific phospholipids was detected by blotting with an α-GST antibody. GST was used as negative control. Amphiphysin1-GST, known to bind membrane lipids, was instead used as positive control.

The results of the experiment are reported in Fig. 3.3. ICA69 interacts with several membrane lipids, including PI(3)P, PI(4)P, PI(5)P, PI(3,4)P_2, PI(3,5)P_2, PI(4,5)P_2, PI(3,4,5)P_3. Furthermore, densitometry performed on the PIP strip shown in Fig. 3.3, indicate that the lipid which ICA69 binds the most is PI(4)P, enriched in the Golgi region.

3.3 Binding of ICA69 to Rab2

Previous studies pointed to the interaction of ICA69 with a small GTPase (226) whose identity, however, remained to be established. In the meantime Francis Barr (MPI for Biochemistry, Martinsried, personal communication) found that ICA69 interacts with Rab2 by two-hybrid system in yeast. As Rab2 is involved in the trafficking between the ER and the Golgi complex (30; 63; 229), and ICA69 is associated with the Golgi complex, this interaction was likely to be relevant and therefore further analyzed using *in vivo* and *in vitro* approaches.

3.3.1 Interaction ICA69/Rab2 by immunoprecipitation assays

The putative interaction between ICA69 and Rab2 was first analyzed by immunoprecipitation experiments. For this purpose INS-1 cells were transfected with a plasmid expressing Rab2 in fusion with GFP or with a plasmid expressing GFP as negative control. The Triton X-100 soluble fraction of transfected cells was then incubated with an α-GFP antibody and then with Protein G resin in order to bind GFP, or Rab2-GFP and isolate in this way presumed complexes containing Rab2-GFP and ICA69. Incubation mixtures were washed and then resolved by SDS/PAGE, followed by western blotting. The results of the experiment are reported in Fig. 3.4. ICA69 co-immunoprecipitated with Rab2-GFP (lane 5, from cells transfected with pEGFP-Rab2) but not with GFP (lane 6, from cells transfected with pEGFP-N1).

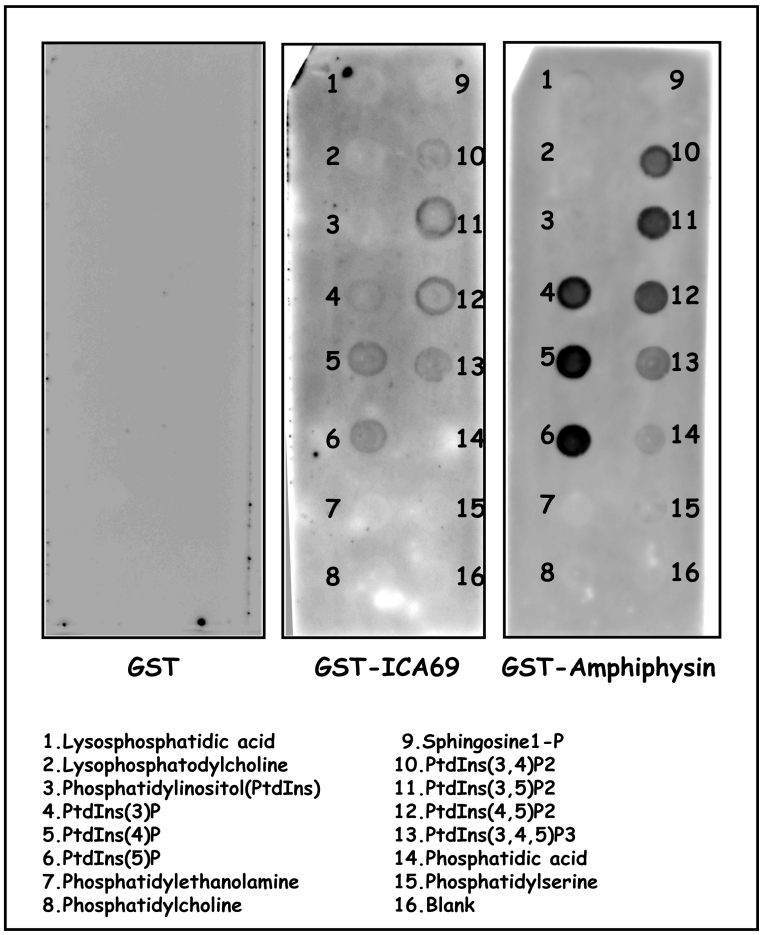

Figure 3.3: **ICA69 binds to membrane phospholipids**
GST, ICA69-GST or amphiphysin1-GST were used in a protein-lipid overlay assay employing PIP strips. The lipids spotted at each position in the PIP strips are indicated at the bottom. The experiment was repeated twice, with similar results.

Therefore ICA69 interacts with Rab2 *in vivo*.

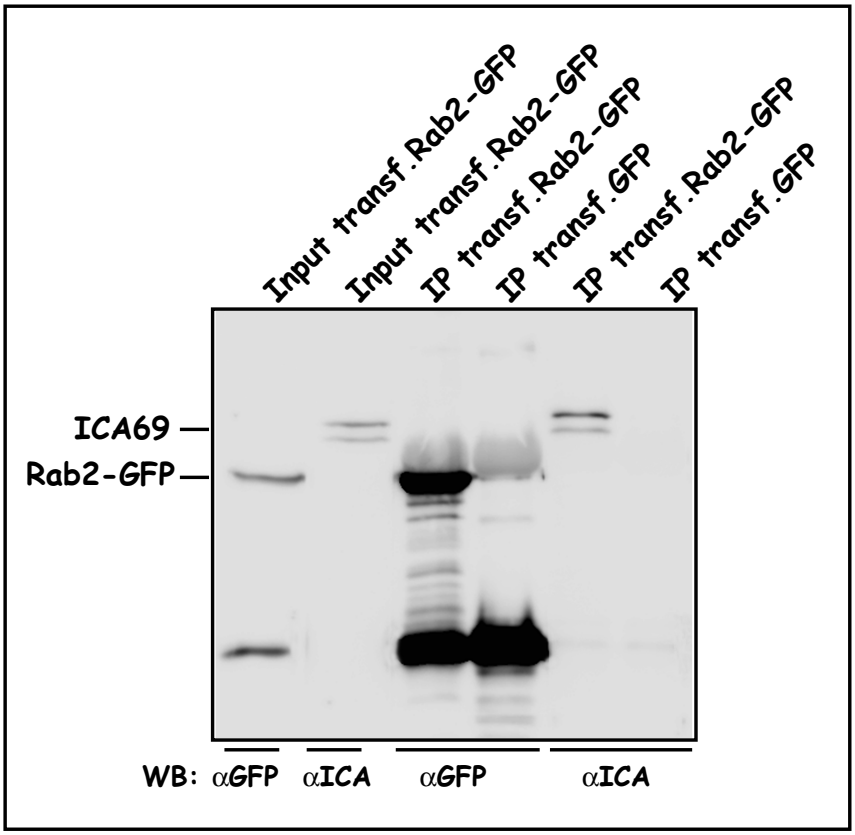

Figure 3.4: **Interaction between ICA69 and Rab2 *in vivo***
INS-1 cells were transfected with pEGFP-Rab2 or with PEGFP-N1, and immunoprecipitations (IP) were carried out using an α-GFP antibody. The antibodies used for the western blotting are indicated at the bottom. Lanes 1 and 2: Rab2-GFP and ICA69 in the input. Lane 3: IP for Rab2-GFP. Lane 4: IP for GFP. Lane 5: co-IP of ICA69 from cells transfected with pEGFP-Rab2. Lane6: absence of co-IP of ICA69 from cells transfected with pEGFP-N1.

3.3.2 Interaction ICA69/Rab2 in pull down assays

The potential *in vivo* interaction was further evaluated with GST pull down assays. Rab2-GST loaded with GDP or with GTPγS, and previously immobilized on beads, were incubated with INS-1 Triton X-100 soluble fraction. Incubation mixtures were washed and then resolved by SDS/PAGE, followed by western blotting. The results of the experiment are reported in Fig. 3.5. Rab2 pulls down ICA69 from the cell extracts, only in its GTP-bound state (lane 4),

but not in its GDP-bound state (lane 3). As an additional negative control, GST alone cannot pull down ICA69 (lane 2). As positive control in this assay, the interaction between Rab2 and GM130 was investigated, as GM130 is reported to be a Rab2 effector (230). Surprisingly GM130 did not appear to interact with Rab2 (data not shown).

Hence, ICA69 interacts with Rab2 *in vitro* and the interaction is GTP-dependent.

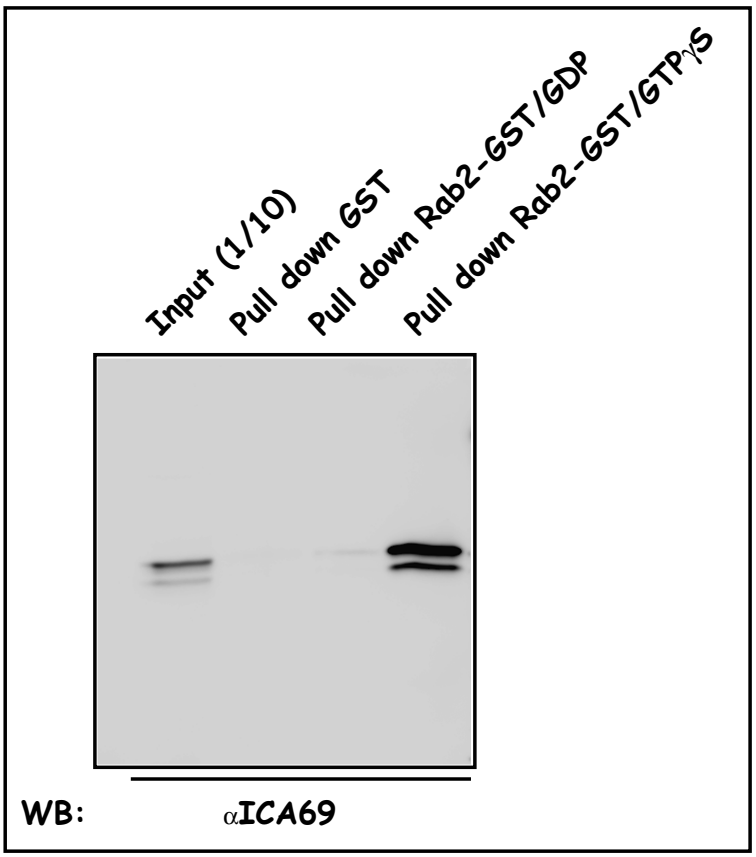

Figure 3.5: **Interaction between ICA69 and Rab2 *in vitro***
GST pull down assay: GST (lane 2), Rab2-GST loaded with GDP (lane 3) and Rab2-GST loaded with GTPγS (lane 4) were immobilized on beads and incubated with INS-1 cells Triton X-100 soluble fraction. Bound proteins were eluted and fractionated by SDS/PAGE, followed by western blotting with an α-ICA69 antibody. The input (10%) is shown in lane 1.

3.3.2.1 Specificity of the ICA69/Rab2 interaction

To investigate the specificity of the interaction between ICA69 and Rab2, pull down assays were performed also with different Rab proteins, verifying their functionality through the binding of the latter to known effectors (Fig. 3.6). The choose of the specific Rab proteins to use for this assay was dictated by their location within the cell, namely Rab proteins which shared similar, though not identical, location and/or function with Rab2, as for Rab1, involved in the anterograde membrane trafficking between the ER and the Golgi complex (61), and Rab6, Golgi-associated and regulating the trafficking between early and late Golgi compartments and a Golgi-to-ER retrograde pathway COPI independent (231) or Rab proteins with a different location and function if compared with Rab2, as for Rab5, required for endosome fusion, and Rab4, with a role in sorting/recycling in early endosomes (88).

The interaction of ICA69 with Rab2 is specific. ICA69, indeed, is not pulled down by Rab1, Rab4, Rab5 or Rab6 (loaded with GDP or GTPγS) (Fig. 3.6, upper panels), being these Rab properly folded and functional as demonstrated by their ability to pull down in their GTP-bound form, GM130, Rabaptin and EEA1, respectively (Fig. 3.6, lower panels). Only in the case of Rab6, it was not possible to demonstrate in the same way its functionality because of the lack of an antibody against a known effector of this protein, to be used in the western blotting. The purification of this Rab protein and its loading with the nucleotide was nevertheless performed in parallel with the purification and the loading of the Rab2 protein used for the pull down showed in Fig. 3.6.

Interestingly, in the conditions used for the pull down experiments, the known effectors of the Rab used as controls clearly interact in a GTP-dependent fashion, but their interaction appears to be quite weaker than the association of Rab2 with ICA69 (compare input and GTPγS in each panel).

3.3.3 Interaction ICA69/Rab2 by immunocytochemistry

ICA69 was found to be enriched in the perinuclear region (Figs. 3.1 and 3.2), while Rab2 is a resident protein of the intermediate compartment (together with ERGIC53), located in proximity of the Golgi complex, in the perinuclear region (232). The interaction between ICA69 and Rab2 was further investigated by immunocytochemistry, to better explore where, within the cell, it occurred.

Confocal microscopy on INS-1 cells transfected with a plasmid encoding Rab2 in fusion with GFP, shows that ICA69 and Rab2-GFP mostly colocalize in particules throughout the

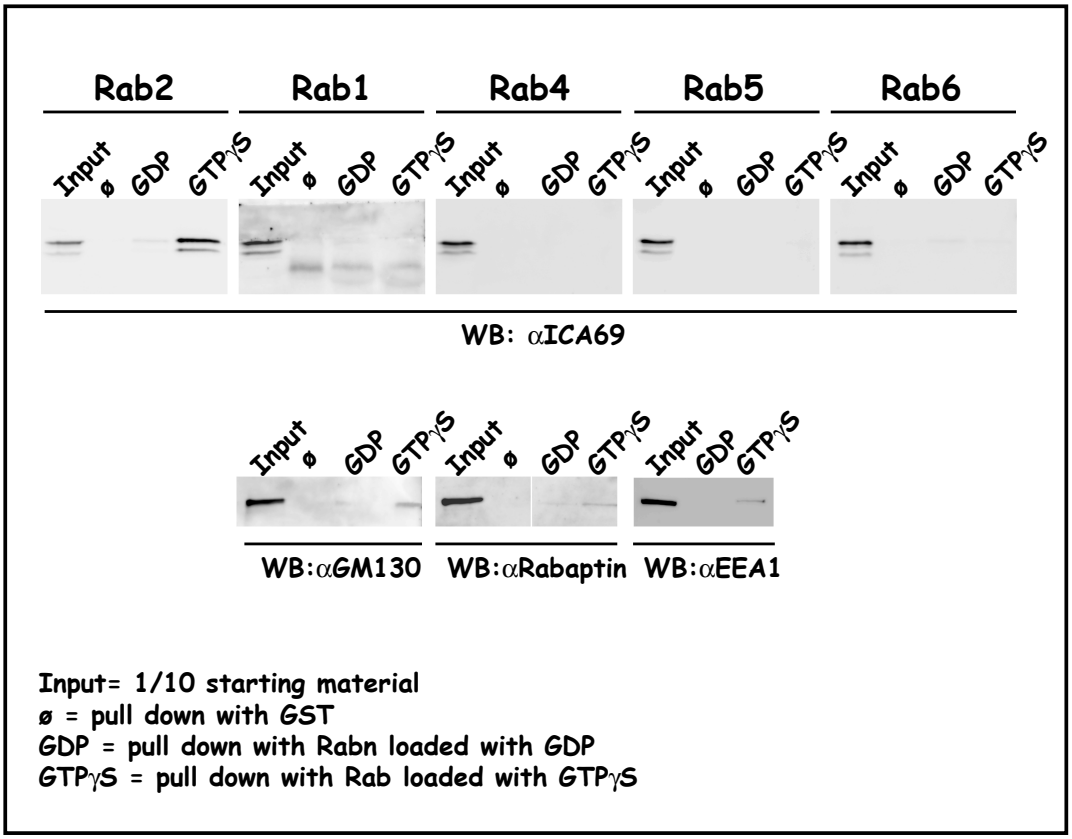

Figure 3.6: **Specificity of the ICA69/Rab2 interaction**
GST pull down assays with Rab2-GST, Rab1-GST, Rab4-GST, Rab5-GST, Rab6-GST. For each panel, but the last bottom panel on the right: GST (lane 2), Rab-GST loaded with GDP (lane 3) and Rab-GST loaded with GTPγS (lane 4) were immobilized on beads and incubated with INS-1 cells Triton X-100 soluble fraction; last bottom panel on the right: Rab-GST loaded with GDP (lane 2) and Rab-GST loaded with GTPγS (lane 3) were immobilized on beads and incubated with INS-1 cells Triton X-100 soluble fraction. Bound proteins were eluted and fractionated by SDS/PAGE. The input (10%) is shown in lane 1. Western blotting was performed using an α-ICA69 antibody (upper panels), or an α-GM130 (for Rab1), α-Rabaptin (for Rab4) or α- EEA1 (for Rab5) antibodies.

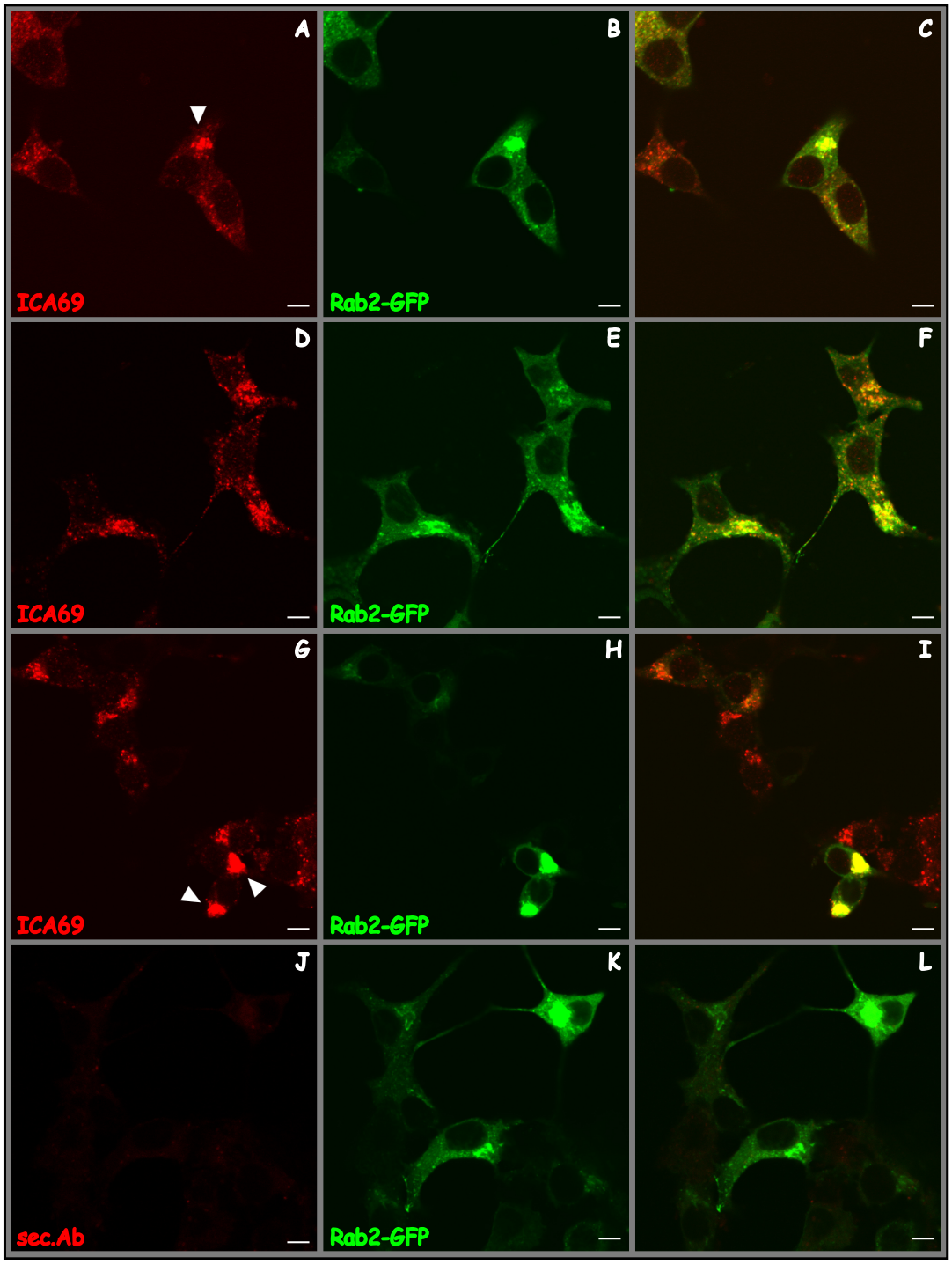

Figure 3.7: **ICA69 cellular localization in Rab2-GFP expressing-INS-1**
Confocal microscopy images from INS-1 cells transfected with pEGFP-Rab2. A, D, G: immunolabeling for ICA69 (pseudored). J: negative control (secondary antibody only). B, E, H, K: GFP fluorescence (pseudogreen). C, F, I, L: merge. Scale bar: 5 μm.

cytoplasm (Fig. 3.7 A-I, transfected cells). Although the identity of these particulates is not entirely clear, being Rab2-GFP over-expressed, they are positive for both ICA69 and Rab2.

Interestingly, in cells expressing the highest levels of Rab2-GFP, ICA69 is especially enriched in a perinuclear structure, where also Rab2 is found (Fig. 3.7 A and G, Fig. 3.13 B-A and Fig. 3.14 G, arrowheads)[1]. ICA69 appears to be concentrated in this compartment only upon over-expression of Rab2-GFP, suggesting a "redistribution"[2] of ICA69 within the cell in a Rab2-GFP dependent fashion. This data is an additional indication that ICA69 binds Rab2.

In order to better define the compartment where ICA69 and Rab2 interacted, additional immunolabeling assays were performed (Fig. 3.8). Surprisingly, despite both Rab2 and ERGIC53 are resident proteins of the intermediate compartment, the signals, obtained by confocal microscopy, for ERGIC53 and Rab2-GFP in INS-1 cells did nor overlap (Fig. 3.8 G-I), as well as the signals for β-COP (component of the coatomer and recruited by Rab2 on the intermediate compartment (63)) and Rab2-GFP (Fig. 3.8 D-F). Consistent with the substantial colocalization of ICA69 with Rab2-GFP, also the signals for ICA69 and β-COP did not overlap (Fig. 3.8 A-C).

3.4 Rab2-dependent ICA69 membrane recruitment

The potential Rab2-dependent "redistribution" of ICA69 within the cell was further investigated by subcellular fractionation. High speed supernatants (HSS, containing cytosolic material) and high speed pellets (HSP, enriched in detergent-soluble particulate material) were prepared from INS-1 cells not transfected or transfected with a plasmid encoding Rab2-GFP and then subjected to SDS/PAGE, followed by western blotting.

The results of the fractionation experiments are showed in Fig. 3.9. In not transfected cells, and in agreement with previous studies (226), ICA69 is mainly cytosolic, but a pool of the protein is membrane-associated (Fig. 3.9 A, lane 1 of the first panel from the top and lane 3 of the second panel). Notably, in cells expressing Rab2-GFP, the signal for ICA69 is decreased in the HSS (Fig. 3.9 A, compare lanes 1 and 2 of the first panel from the top) and concomitantly the signal for this protein is increased in the HSP (Fig. 3.9 A, compare lanes 3 and 4 of the second panel from the top). Fig. 3.9 B shows the quantification of this experiment. Upon

[1] Clearly this was not due to an artifact caused by a bleed-through of the Rab2-GFP signal in the red channel, since this structure was not detectable when ICA69 was not immunolabeled (Fig. 3.7 J-L).

[2] The unchanged ICA69 protein levels in control cells and in cells over-expressing Rab2-GFP (data not shown) indicated that the increased signal for ICA69 in these latter was due to "redistribution" within the cell rather than to increased amount of this protein.

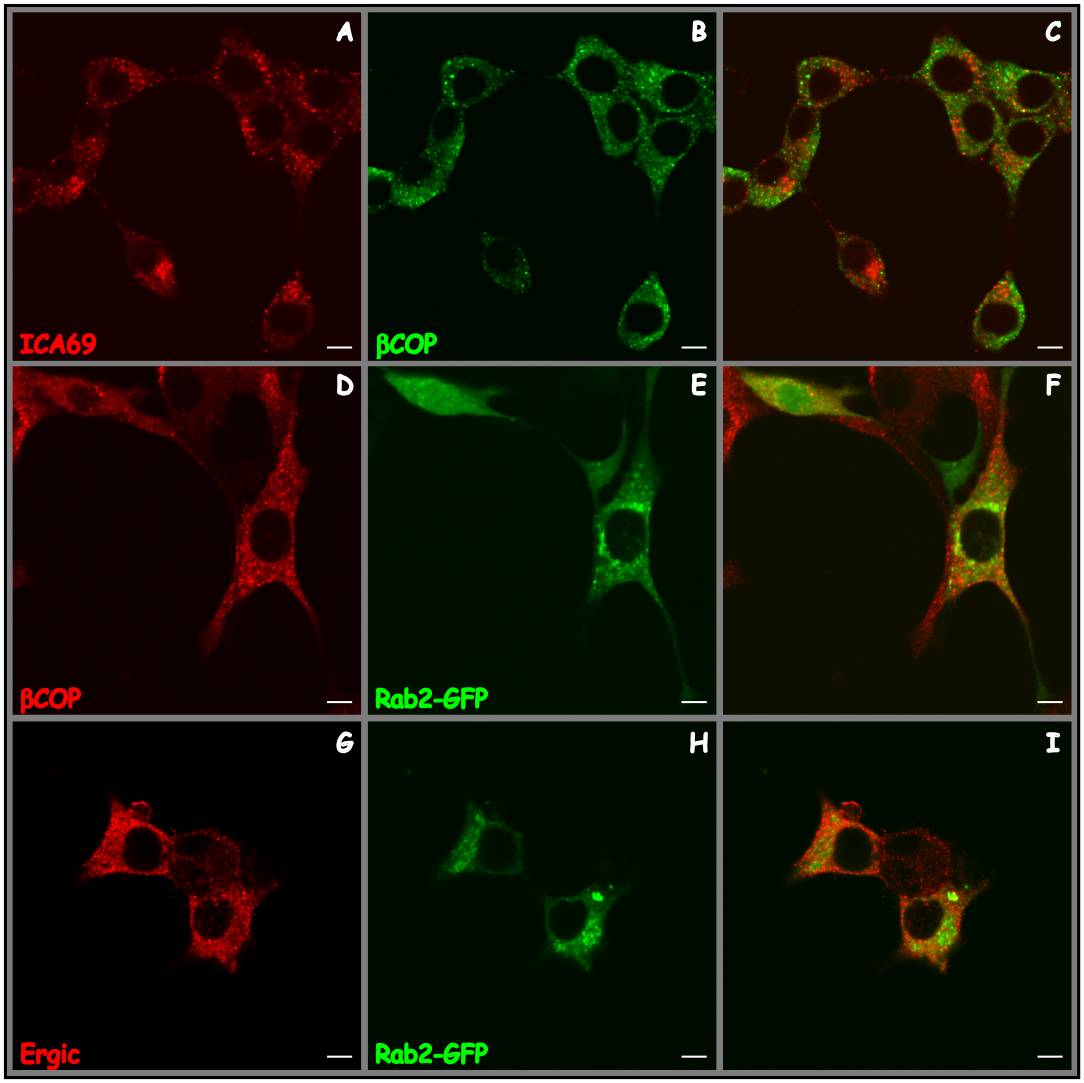

Figure 3.8: **ICA69 and Rab2-GFP cellular localization compared with markers of the intermediate compartment**
Confocal microscopy images from INS-1 cells (A-C) or INS-1 cells transfected with pEGFP-Rab2. (D-I). A, D, G: immunolabeling for ICA69, β-COP and ERGIC53, respectively (pseudored). B: immunolabeling for β-COP (pseudogreen). E, H: GFP fluorescence (pseudogreen). C, F, I: merge. Scale bar: 5 μm.

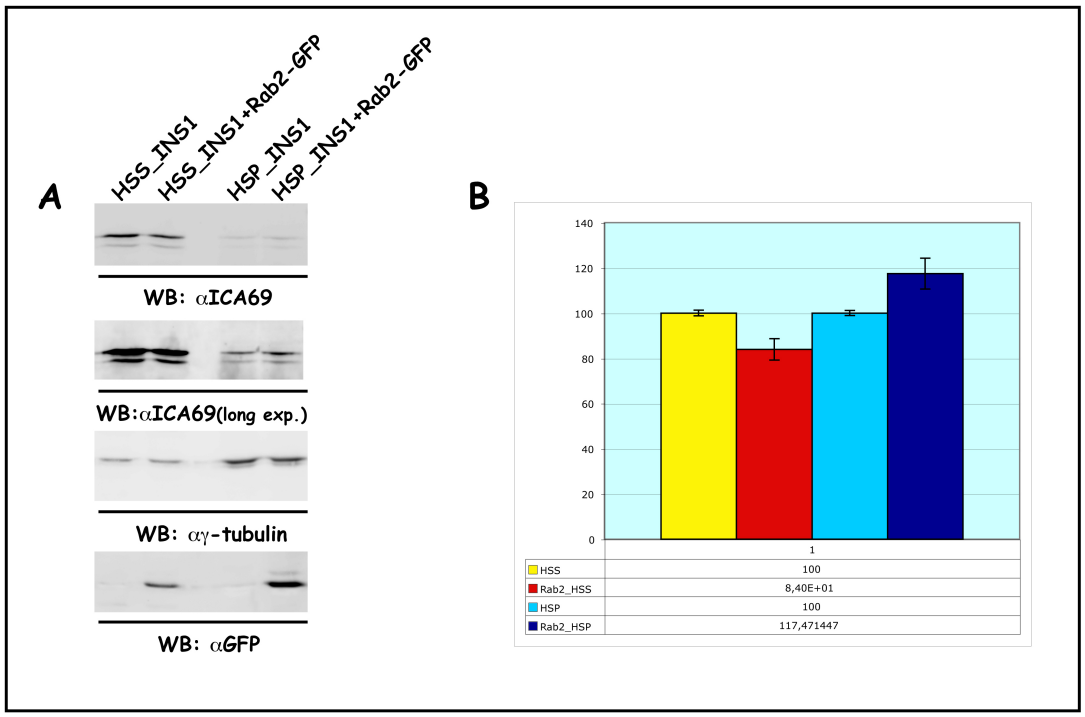

Figure 3.9: **Rab2-dependent ICA69 membrane recruitment**
A) Subcellular fractionation was performed on INS-1 or INS-1 transfected with pEGFP-Rab2, as described in Materials and Methods. Followed SDS/PAGE and western blotting with the antibodies indicated. 20 and 18.5 μg of total protein were loaded on the gel for HSS and HSP, respectively. The first two panels from the top show the same gel exposed for either for a short (3 min) or long (11 min) period of time for the acquisition of the signal, as ICA69 is much more aboundant in the HSS than in the HSP. B) Quantification of three independent experiments, as in A. Amounts were normalized against γ-tubulin, and not transfected cells were equaled to 100%. The error bar indicates the standard deviation (SD) for the not transfected cells, and the standard error of the mean (SE) for transfected cells.

over-expression of Rab2, the signal for ICA69 decreases of 16% in the HSS, and increases of 17% in the HSP. The results are even more significative when the low efficiency of transfection ($\sim 25\%$) is taken in account.

Therefore, subcellular fraction studies indicate that over-expression of Rab2-GFP correlates with an increased recruitment of ICA69 to membranes.

3.5 Mapping, in ICA69, of the domain of interaction with Rab2

Preliminary evidence indicated that the interaction ICA69/Rab2 occurs through the C-terminal region of ICA69 (F. Barr, personal communication), and not through the BAR domain. This was unexpected considering that ICA69 contains a BAR domain and that BAR domains act as binding interfaces for many GTPases (as described in section 1.3.8 on page 23). To verify whether the C-terminus of ICA69 binds Rab2, a deletion mutant of ICA69, which only contains the C-terminal 230 aa of ICA69 was generated (Fig. 3.10) and expressed in INS-1 cells (Fig. 3.11).

The truncated mutant of ICA69 was detected in the Triton X-100 soluble fraction of INS-1 cells as a doublet of ∼34 kDa, despite it has a molecular mass of 23 kDa (Fig. 3.11). The same phenomenon is observed for ICA69, which has a molecular mass of 54 kDa, but an electrophoretic mobility of 60 kDa. Interestingly, also the C-terminal region of ICA69 appears as a doublet on protein gels. The origin of the doublet is still unknown. However, its appearance upon expression of the C-terminal domain of the protein only, suggests it may be due to post-translational modification of ICA69, rather than alternative splicing or alternative initiation of the translation in ICA69 mRNA.

This mutant was thereafter used in GST pull down assays, to locate the region of ICA69 which binds to Rab2. As previously described, GST pull down experiments were performed using Triton X-100 soluble fraction from untransfected INS-1 or from INS-1 expressing the C-terminus of ICA69 (ICA69woBAR, so called because it encompasses the entire protein excluding the N-terminal BAR domain), using Rab2-GST loaded with GDP or with GTPγS. The results of these experiments are reported in Fig. 3.12. Despite Rab2 was functional and properly folded, as demonstrated by its GTP-dependent interaction with endogenous ICA69 (Fig. 3.12, lanes 3 and 6), it does not interact with the C-terminus of ICA69 (Fig. 3.12, lane 6).

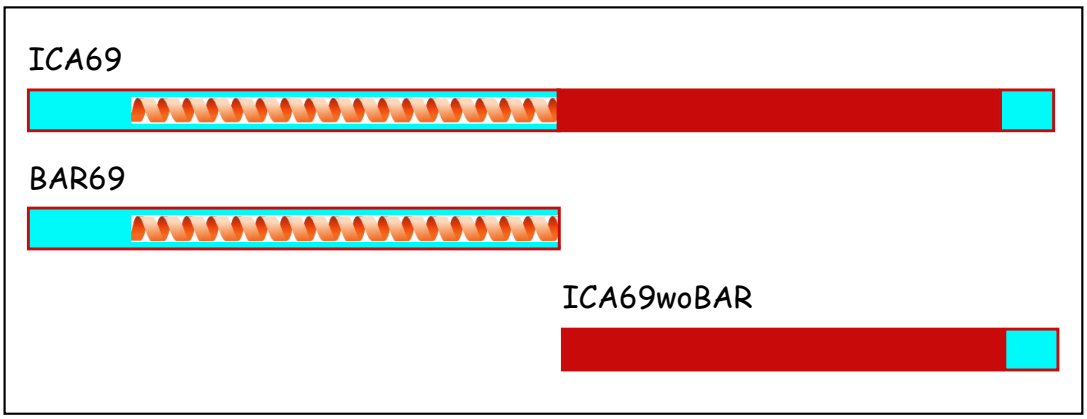

Figure 3.10: **Scheme of ICA69 deletion mutants**
The cartoon is relative to ICA69 and two generated deletion mutants, called BAR69, comprising the N-terminus of ICA69, with the entire BAR domain, and ICA69woBAR, comprising the C-terminus of ICA69. The cyan indicates high homology regions with ICA69-RP. The red indicates the region where ICA69 and ICA69-RP differ the most.

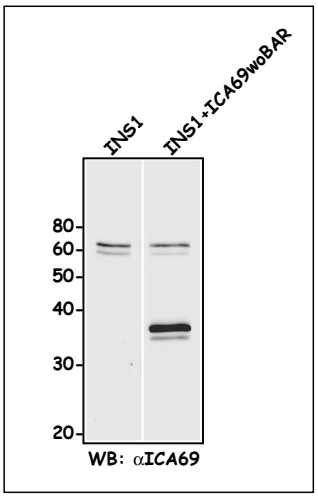

Figure 3.11: **Expression of ICA69 C-terminus in INS-1**
Western blotting on Triton X-100 soluble fraction of INS-1 cells (lane 1) or INS-1 transfected with a plasmid encoding the C-terminus of ICA69 (lane 2), with the polyclonal α-ICA69.

Studies are ongoing to test whether the interaction ICA69/Rab2 occurs through the BAR domain of ICA69. However, all attempts to express the N-terminal half of ICA69 (called BAR69) have failed so far.

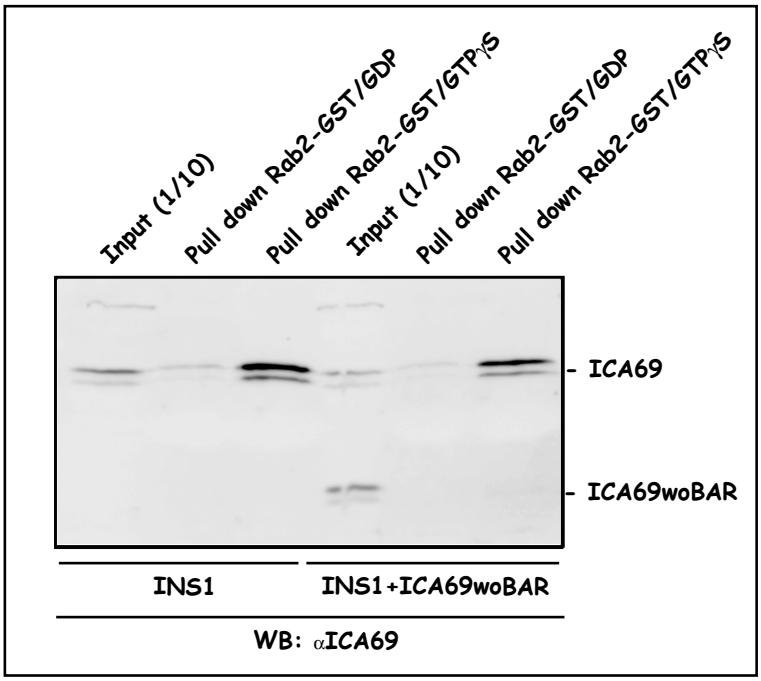

Figure 3.12: **Mapping of the domain of interaction with Rab2**
GST pull down assay: Rab2-GST loaded with GDP (lanes 2 and 5) and Rab2-GST loaded with GTPγS (lanes 3 and 6) were immobilized on beads and incubated with Triton X-100 soluble fraction from INS-1 cells (lanes 2 and 3) or INS-1 cells expressing the C-terminus of ICA69 (lanes 5 and 6). Bound proteins were eluted and fractionated by SDS/PAGE, followed by western blotting with an α-ICA69 antibody. The inputs (10%) are shown in lanes 1 and 4.

3.6 Related behavior of ICA69 and Rab2 upon perturbation of early secretory compartments

The distribution of ICA69 and Rab2-GFP was further investigated upon incubation of INS-1 cells at 15 °C for 80 minutes. Cells were incubated at this reduced temperature to accumulate and enhance visualization of the intermediate compartment by blocking the anterograde ER-to-Golgi transport: at 15 °C, secretory cargo leaves the ER, but instead of being transported to the Golgi apparatus, it accumulates in the intermediate compartment (233).

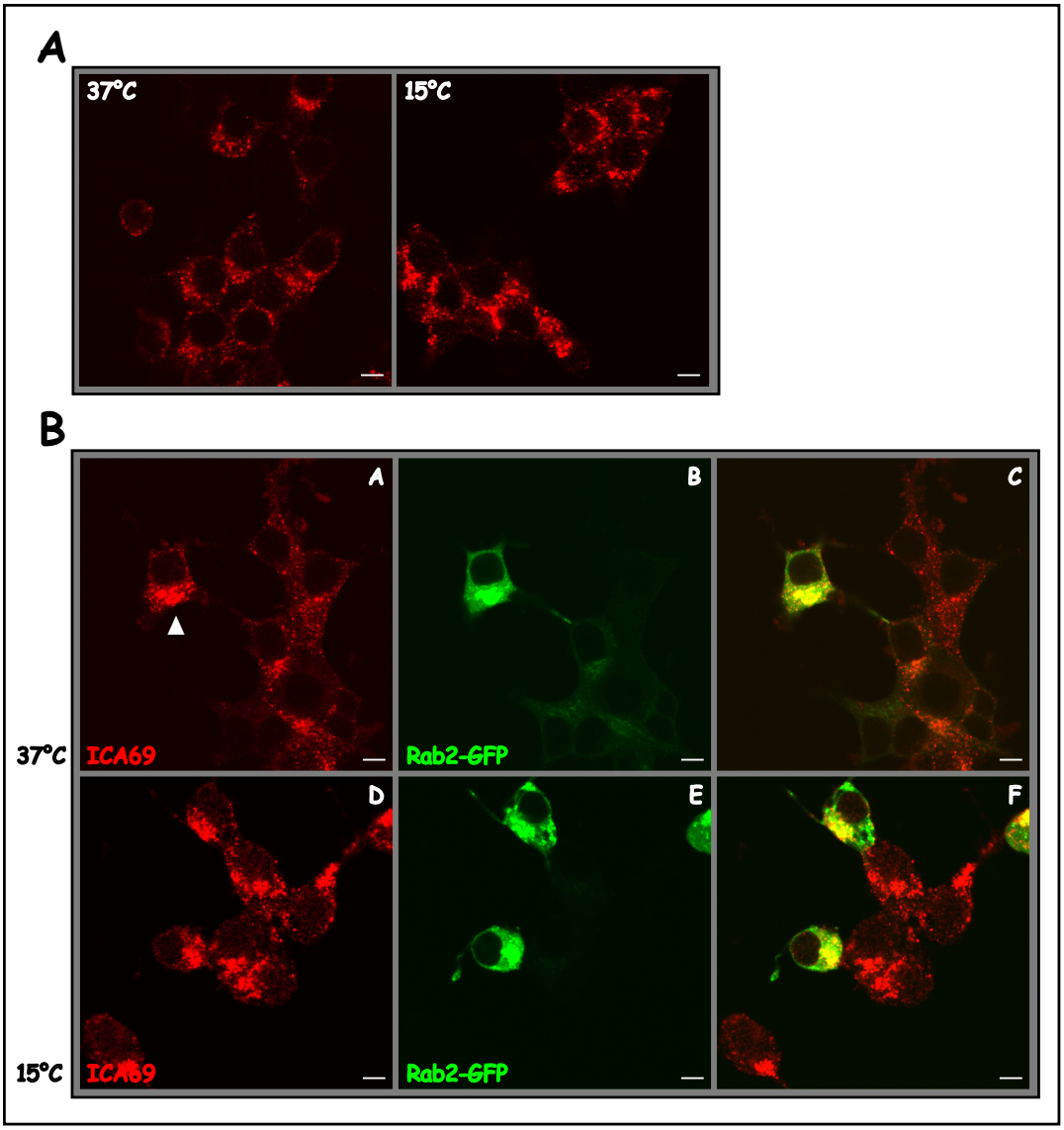

Figure 3.13: **ICA69 distribution upon incubation of INS-1 cells at 15 °C**
A) Confocal microscopy images from INS-1 cells, kept at 37 °C, or incubated at 15 °C, and immunolabeled for ICA69 (pseudored). Scale bar: 5 μm. B) Confocal microscopy images from INS-1 cells transfected with pEGFP-Rab2, kept at 37 °C (A-C), or incubated at 15 °C (D-F). A and D: immunolabeling for ICA69 (pseudored). B and E: GFP fluorescence (pseudogreen). C and F: merge. Scale bar: 5 μm.

Immunocytochemistry was performed on control INS1 and INS-1 cells over-expressing Rab2-GFP, upon incubation at the reduced temperature, and the results are shown in Fig. 3.13. In control cells ICA69 has a perinuclear distribution (Fig. 3.13 A, 37 °C and Fig. 3.13 B (A and C)) with an enrichment in a perinuclear structure were also Rab2 is found in cells over-expressing Rab2-GFP (Fig. 3.13 B (A-C)). Upon incubation of the cells at 15 °C, both in control INS-1 and in INS-1 over-expressing Rab2-GFP, ICA69 accumulates to a perinuclear structure resembling that observed upon over-expression of Rab2-GFP (compare (Fig. 3.13 B (A-C) and Fig. 3.13 B (D-F)).

This data further corroborate the recruitment of both ICA69 and Rab2 to the intermediate compartment.

Additional immunocytochemistry experiments were performed upon treatment of INS-1 cells with BrefeldinA (BFA) (Fig. 3.14). BFA, which is synthesized by a variety of fungi, inhibits guanine-nucleotide exchange on ARF1 and consequently prevents the binding of COPI proteins to the Golgi membranes. This, in turn, causes the loss of the Golgi structure, with the redistribution of Golgi enzymes to the ER, while Golgi matrix proteins, such as GM130, remain associated with punctate cytoplasmic structures called "Golgi remnants" (234).

Following treatment of INS-1 cells with BFA (3 μg/ml, 45 min), the signals of both ICA69 (Fig. 3.14 D-F and J-L) and Rab2-GFP (Fig. 3.14 K-L) decreases, consistent with their re-distribution in the cytosol and their dependence on the integrity of the ER and the Golgi complex.

3.7 Functional studies on ICA69

The data reported above point to ICA69 as a downstream effector of Rab2. Studies were conducted and are currently ongoing to test whether the phenotype resulting from the over-expression of ICA69 over-expression resembles that observed upon the over-expression of Rab2, and investigate in such way ICA69 function. To this aim, a plasmid encoding full length ICA69, tagged at its N-terminus with the X – press^{TM} epitope and the poly-histidine tag followed by glycin, was generated. As shown in Fig. 3.15, this tagged form of ICA69, called ICA69-HisMAX, is expressed in INS-1 cells, and is detectable by antibodies directed either against ICA69 or one of the two tags.

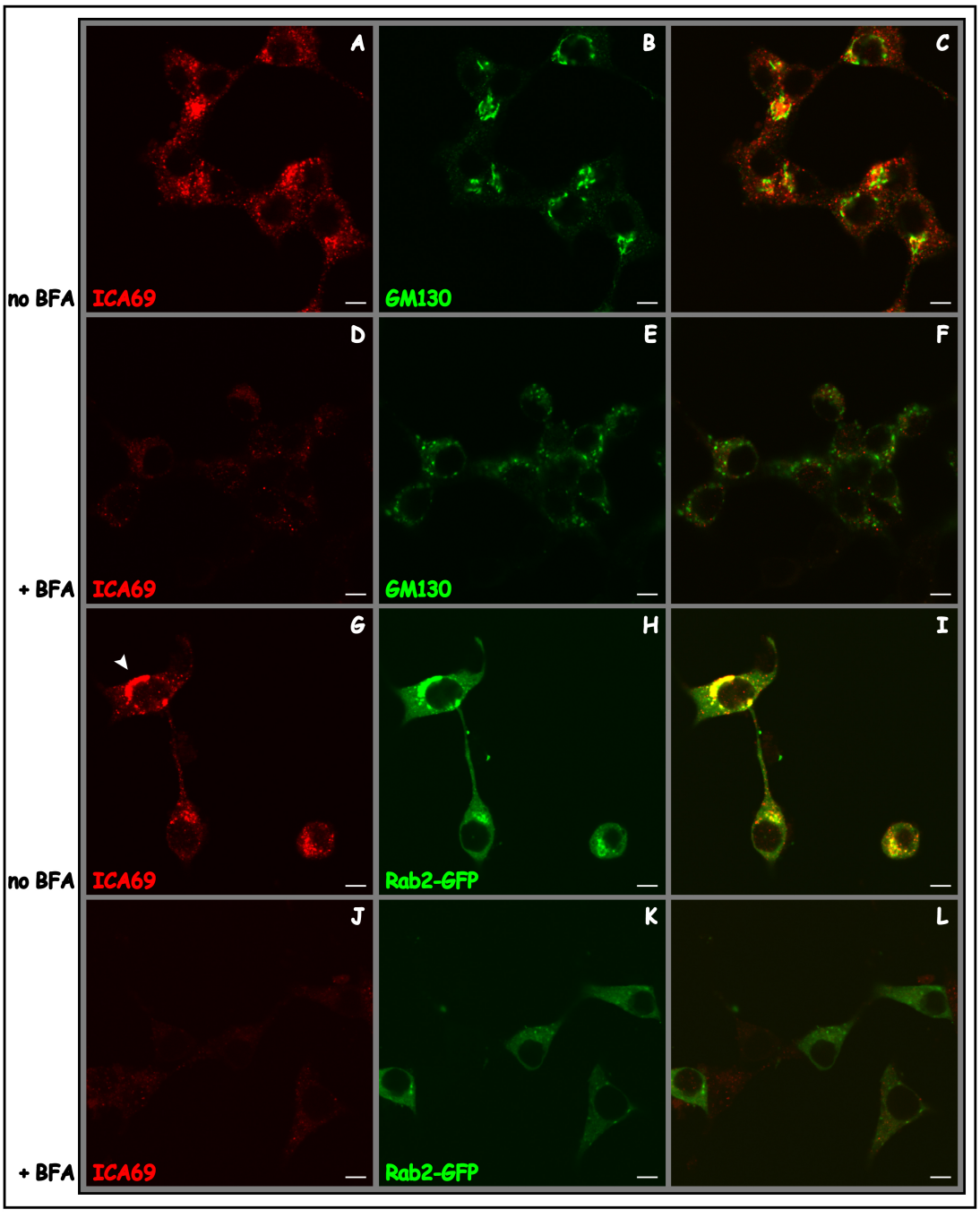

Figure 3.14: **ICA69 distribution upon incubation of INS-1 cells with BFA** Confocal microscopy images from INS-1 cells (A-F) or INS-1 cells transfected with pEGFP-Rab2 (G-L). Cells were incubated or not with BFA, as indicated. A, D, G and J: immunolabeling for ICA69 (pseudored). B and E: immunolabeling for GM130 (pseudogreen). H and K: GFP fluorescence (pseudogreen). C, F, I, L: merge. Scale bar: 5 μm.

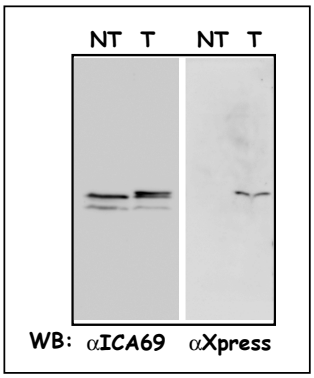

Figure 3.15: **Expression of ICA69-HisMAX in INS-1**
Western blotting on Triton X-100 soluble fraction of INS-1 cells (NT) (lanes 1 and 3) or INS-1 transfected with a plasmid encoding the ICA69-HisMAX (T) (lanes 2 and 4), with the polyclonal α-ICA69 and an α-X − press^{TM} antibody.

3.7.1 ICA512 conversion

The effect of ICA69 or Rab2 over-expression on the early secretory pathway was analyzed by examining the conversion of pro-ICA512 into the mature form of the protein[1].

To this aim, control INS-1 cells or INS-1 over-expressing Rab2, ICA69 or ICA69woBAR were kept at rest for 1 hour, stimulated for 30 min to induce the biosynthesis of pro-ICA512, and then returned to resting medium, for up to 1.5 hours, in order to follow its conversion in the mature form while trafficking from the ER to the SGs, through the Golgi.

The result of this experiment is shown in Fig. 3.16. Stimulation of control cells induces an increase in the levels of pro-ICA512 (compare R and S), which is progressively converted in the mature form, with consequent consumption of pro-ICA512. Ninety min after stimulation, cells are depleted of both the pro-form and the mature form of ICA512. In cells over-expressing Rab2-GFP, instead, the levels of pro-ICA512 do not change in the course of the experiment. Likewise the levels of ICA512-TMF remain constant after the stimulation, though its levels are strongly diminished if compared with those of control cells. In cells over-expressing ICA69, this effect is amplified. The amount of pro-ICA512 is indeed increased, as only a smaller fraction of

[1]ICA512 is a N-glycosilated T1D autoantigen investigated in the laboratory were this thesis was carried on. Pro-ICA512 is synthesized as a glycoprotein of 110 kDa. Along the secretory pathway pro-ICA512 is first converted into a protein of 130 kDa, with a very short half-life, and then during the maturation of the SG from the Golgi towards the plasma membrane, is cleaved at a consensus site for furin-like convertase. The resulting transmembrane fragment (ICA512-TMF) has a molecular weight of ∼70 kDa (235).

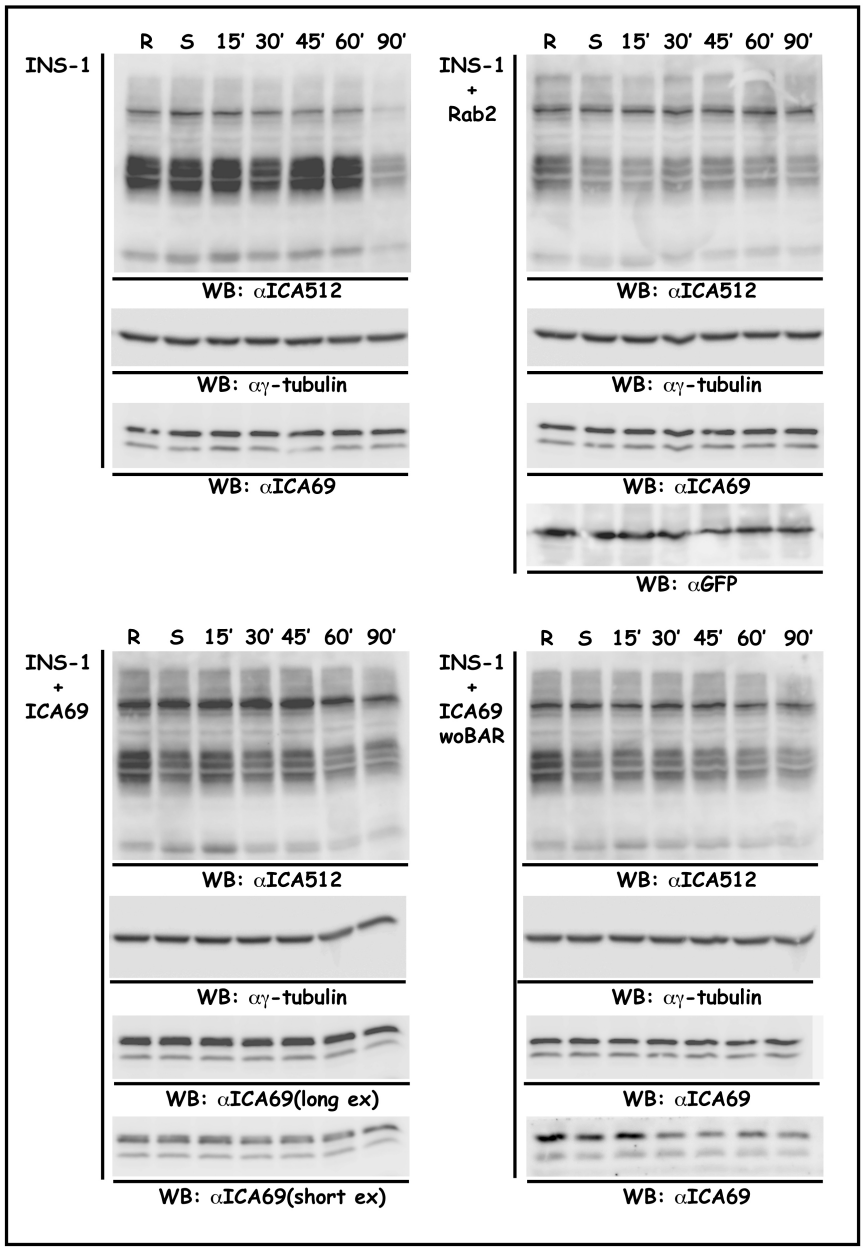

Figure 3.16: **ICA512 maturation upon Rab2 or ICA69 over-expression**
Western blotting on Triton X-100 soluble fraction of INS-1 cells (up, left) or INS-1 transfected with a plasmid encoding Rab2-GFP (up, right) or ICA69-HisMAX (bottom, left) or ICA69woBAR (bottom, right). Cells were at rest (R) in resting medium (no glucose, 5 mM potassium) for 1.5 hours, or at rest for 1 hour and stimulated with high glucose (25 mM) and high potassium (55 mM) for 30 min (S), or at rest for 1 hour, stimulated for 30 min, and returned in resting medium for the time indicated, up to 90 min. The antibodies used for the western blotting are also indicated.

the protein is converted into ICA512-TMF. In cells over-expressing the C-terminus of ICA69, the rise in pro-ICA512 levels and its reduced conversion in the mature form of the protein, are intermediate between the two last cases.

These data point to a partial block in the trafficking of ICA512 beyond the Golgi complex upon over-expression of Rab2, ICA69 or ICA69woBAR.

3.7.2 Insulin secretion

The over-expression of Rab2 correlates, even if not unequivocally, with a partial block of the trafficking between ER and Golgi (62). To investigate whether Rab2 or ICA69 over-expression determine an alteration of trafficking in β-cells, insulin secretion was measured in control (not transfected) INS-1 cells or in INS-1 cells over-expressing Rab2 or ICA69. As indicated in Fig. 3.17, the over-expression of Rab2 correlates with ∼28% decrease in glucose stimulated insulin secretion, while the over-expression of ICA69 correlates with a ∼11% decrease in insulin secretion upon stimulation of the cells.

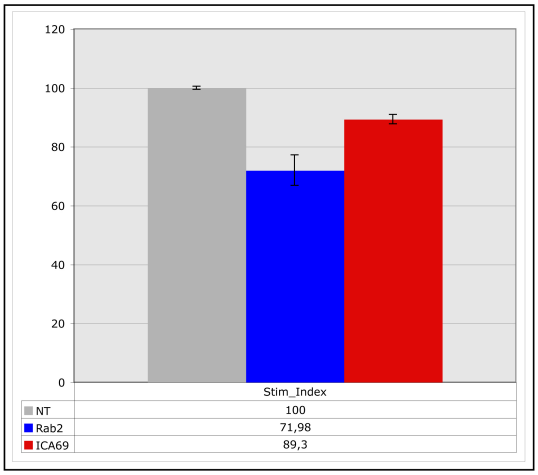

Figure 3.17: **Insulin secretion upon Rab2 or ICA69 over-expression**
Insulin secretion in INS-1 cells, measured as stimulation index upon stimulation of the cells with 25 mM glucose and 55 mM potassium for 2 hours, as described in Materials and Methods. Grey: control cells (not transfected). Blue: cells over-expressing Rab2-GFP. Red: cells over-expressing ICA69-HisMAX. The quantification refers to three independent experiments. Not transfected cells were equaled to 100%. The error bar indicates the SD for the not transfected cells, equaled to 100% and the SE for transfected cells.

Therefore, ICA69 over-expression appears to impair insulin secretion from INS-1 cells, even if less than Rab2 over-expression.

3.7.3 Recruitment of β-COP on membranes

Previous data in the literature indicated Rab2 over-expression being coupled with an increase in membrane-associated β-COP, more in detail with an increase in vesicle-associated β-COP, and a decrease in ER, IC and Golgi-associated β-COP. These data suggested therefore a role for Rab2 in the formation of COPI-vesicles from the IC (229; 236). To investigate whether this effect was reproducible, the same subcellular fractionation protocol described in (236) was applied to control (not transfected) INS-1 cells or INS-1 cells transfected with a plasmid encoding Rab2-GFP or ICA69-HisMAX. Briefly, post nuclear supernatants (PNS) where subjected to sequential centrifugation at $20,000 \times$ g and $100,000 \times$ g. The first pellet (P1) contains rapidly sedimenting membranes (ER, IC and Golgi compartments), while the second pellet (P2) contains vesicles.

The results of this experiment are reported in Fig. 3.18. At variance with the data obtained in HeLa or Normal Rat Kidney (NRK) cells (236), Rab2 over-expression correlates with an increase of ER, IC and Golgi-associated β-COP (Fig. 3.18 C, compare P1-NT with P1-Rab2), and a decrease in the vesicle-associated β-COP (Fig. 3.18 C, compare P2-NT with P2-Rab2). No significant changes were observed in the amount of β-COP in the cytosolic fraction. ICA69 over-expression is coupled with an even larger increase of ER, IC and Golgi-associated β-COP (Fig. 3.18 C, compare P1-NT with P1-ICA69), and a larger decrease in the vesicle-associated β-COP (Fig. 3.18 C, compare P2-NT with P2-ICA69). Moreover ICA69 over-expression was associated with an increase of β-COP in the cytosolic fraction.

These data suggest a similar repartitioning of β-COP following the over-expression of Rab2 or ICA69, with a redistribution between fast sedimenting membranes, vesicles and cytosol which is more pronounced upon over-expression of ICA69 than upon over-expression of Rab2.

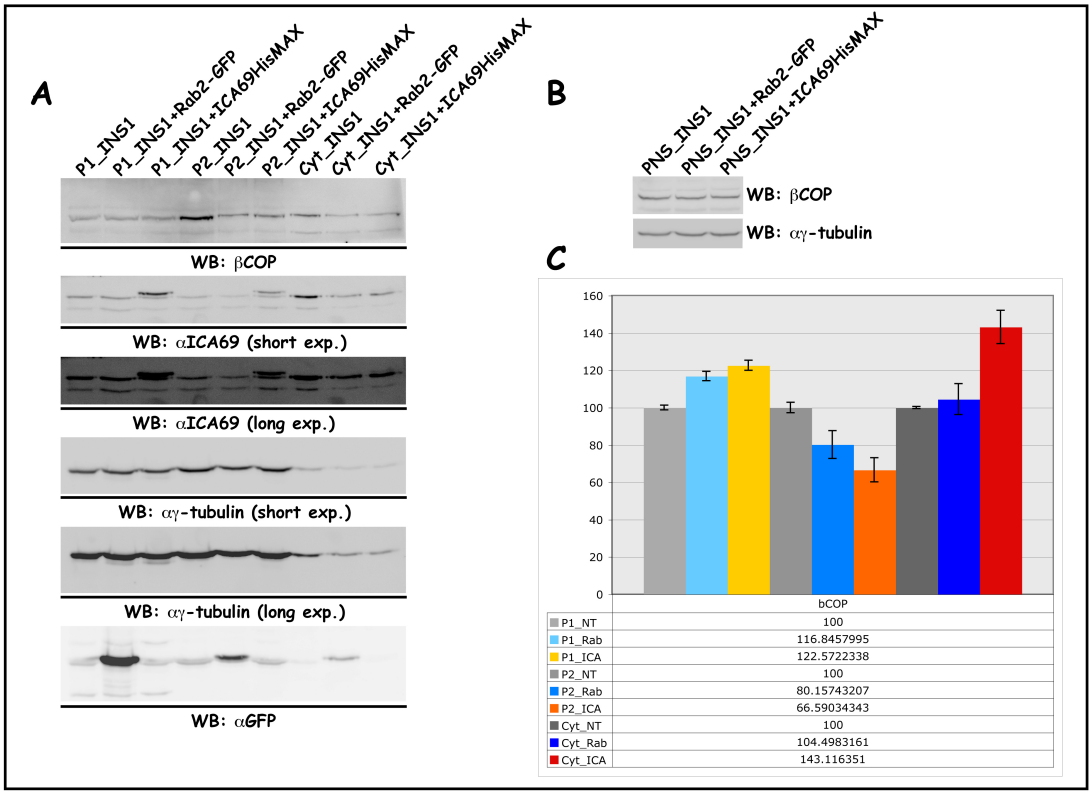

Figure 3.18: **β-COP distribution in different cellular fractions uopn Rab2 or ICA69 over-expression**

A) Subcellular fractionation was performed on INS-1 or INS-1 transfected with pEGFP-Rab2, or pcDNA4/HisMAX-ICA69 as described in Materials and Methods. Followed SDS/PAGE and western blotting with the antibodies indicated. 23, 18 and 7 μg of total protein were loaded on the gel for P1, P2 and cytosol, respectively. With the α-ICA69 and the α-tubulin antibodies, the same gel was exposed for either for a short or long period of time for the acquisition of the signal. B) PNS from INS-1 or INS-1 transfected with pEGFP-Rab2, or pcDNA4/HisMAX-ICA69, subjected to SDS/PAGE, followed by western blotting with the antibodies indicated. C) Quantification of three independent experiments. Amounts were normalized against γ-tubulin. The error bar indicates the SD for the not transfected cells, equaled to 100% and the SE for transfected cells.

Chapter 4

ICA69 Related Protein

4.1 ICA69-RP gene

Through sequence alignments, it was discovered, in mammals, the existence of a novel gene encoding an ICA69 orthologue/paralogue[1], henceforth termed ICA69 Related Protein (ICA69-RP). ICA69-RP gene is located in position 2q33.1 in humans, 1c2 in mice and 9q31 in rats (ICA69 is located in positions 7p22, 6A1-A2 and 4q21 respectively, in the same animals). Both genes are predicted to encode alternatively spliced isoforms in humans, mice and rats, as indicated in the Ensembl database (http://www.ensembl.org/index.html).

4.1.1 Phylogenetic tree

As a defined secretory phenotype was observed in *C.elegans* upon mutations of *ric19*, but ICA69^{null} mice had no obvious phenotype, there was the possibility ICA69-RP could have been the real homolog of *ric19*, being therefore involved in the process of neuroendocrine secretion via association with secretory vesicles. In order to address this question a phylogenetic tree was generated.

The tree is reported in Fig. 4.1 and was obtained using ClustalW, a multiple sequence alignment program, at the European Bioinformatic institute (EBI). According to this analysis, ICA69 is evolutionary closer to *ric19* than ICA69-RP, thereby suggesting the initial hypothesis was not correct. Partially redundant functions between ICA69 and ICA69-RP or between

[1] Both paralogues and orthologues are genes related by duplication within a genome. Orthologues retain the same function in the course of evolution, whereas paralogues evolve new functions, even if these are related to the original one.

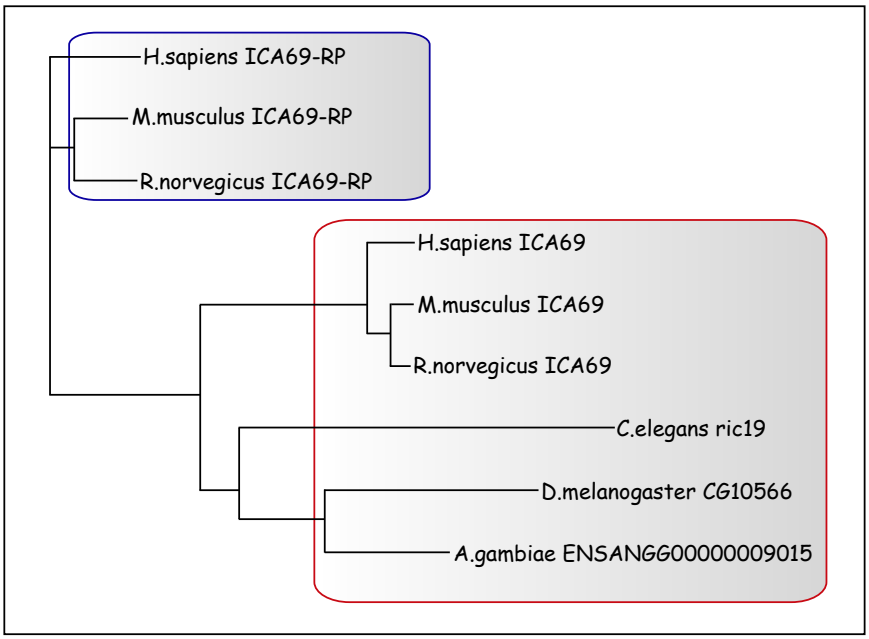

Figure 4.1: **ICA69 protein family genealogical tree**
Genealogical tree for ICA69 family members in *Homo sapiens*, *Mus musculus*, *Rattus norvegicus*, *Caenorabitis elegans*, *Drosophila melanogaste*r and *Anopheles gambiae*. The blue rectangle indicates ICA69 paralogues, the red one indicates ICA69 homologs. The tree shows the relatively small "evolutionary time" (indicated by the length of the horizontal lines) between ICA69-RP homologs and ICA69 homologs respectively in humans, mice and rats, and a bigger "evolutionary time" between ICA69 mammalian and not mammalian homologs. Accession numbers (NCBI): *H.sapiens* ICA69-RP: NP_612477.3; *M.musculus* ICA69-RP: NP_081683.2; *R.norvegicus* ICA69-RP: NP_955432.1; *H.sapiens* ICA69: NP_071682.1; *M.musculus* ICA69: NP_034622.2; *R.norvegicus* ICA69: NP_110471.1; *C.elegans* ric19: NP_491216.2; *A.gambiae* ENSANGG00000009015: XP_316657.2.

ICA69 and some yet unidentified protein, on the other hand, may account for the lack of a phenotipe in ICA69^{null} mice.

4.1.2 Cloning of ICA69-RP cDNA

According to the SOURCE database (http://source.stanford.edu/cgi-bin/source/sourceSearch) ICA69-RP was predicted to be highly expressed in brain. Thus, the ICA69-RP cDNA was cloned by PCR from a rat brain cDNA library. The sequence of the cloned cDNA encodes a protein of 435 aa, and points to an exon-intron structure of the ICA69-RP gene partially different from the one deposited at the time in the public databases, and which was generated by automated computational analysis of the yet incomplete rat genome.

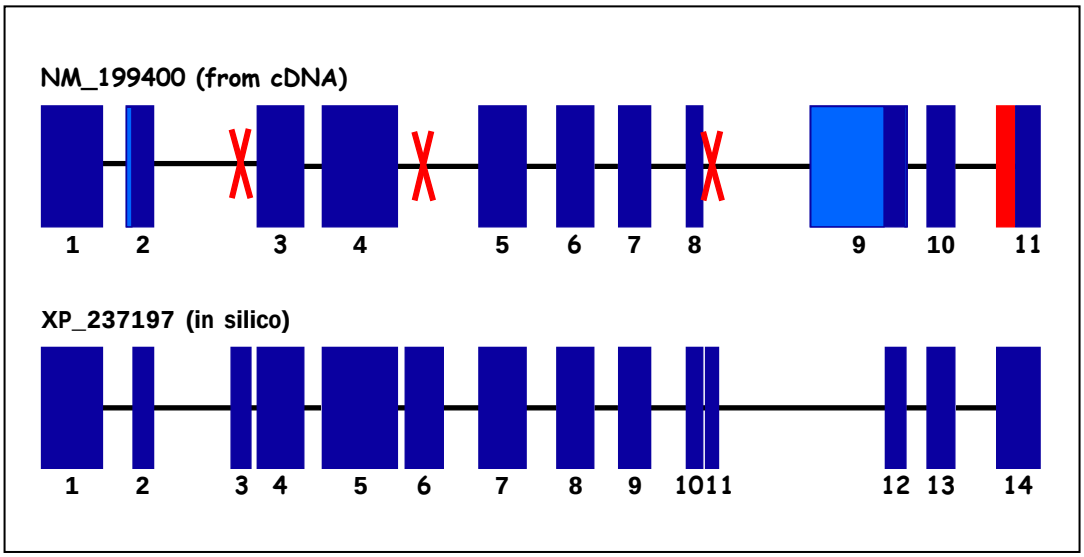

Figure 4.2: **ICA69-RP gene structure**
Exon-intron structure of ICA69-RP gene (on the top) as deduced by sequencing the cDNA obtained from a rat brain cDNA library, and now deposited in the public database. It differs from the predicted structure of the gene derived by automated computational analysis (on the bottom). The red crosses indicate exons which are missing in the new structure. The light blue rectangles are regions found to belong to the coding sequense and not to introns. The red rectangle is a sequence found to belong to an intron and not to the coding sequence.

The differences between the two gene structures are reported in Fig. 4.2. More in detail:

- exon 2 extends 19 nucleotides before the predicted 5' site

- exons 3 ,6 and 11 of the old structure are missing
- exon 9 extends 201 nucleotides before the predicted 5' site and 2 nucleotides after the predicted 3' site
- exon 11 extends 51 nucleotides after the predicted 3' site

The coding sequence of rat ICA69-RP, as predicted by the rat genome sequencing project, contained several large gaps compared to human and mouse ICA69-RP. The experimental data did not confirm anymore the original prediction. The comparison of ICA69-RP amino acidic sequences in these species, as present nowadays in the public databases, is reported in Appendix A .

4.2 ICA69-RP versus ICA69

Both ICA69 and ICA69-RP genes are predicted to encode alternatively spliced isoforms in humans, mice, and rats. In reference to the most common isoforms, ICA69-RP includes 482 aa in humans (predicted MW: 54 kDa), 431 aa in mice (predicted MW: 49 kDa), and 435 aa in rats (predicted MW: 50 kDa). As illustrated in table 4.1 and table 4.2, ICA69 and ICA69-RP are highly conserved among humans, mice and rats, and between each other.

	ICA69	ICA69-RP
% similarity within the homologs	97.0 %	93.0 %
% identity within the homologs	88.5%	76.5 %

Table 4.1: ICA69-RP in human, mouse and rat

	human	mouse	rat
% similarity within the paralogs	96.8%	75.5%	79.0 %
% identity within the paralogs	47.8%	50.0%	52.0 %

Table 4.2: ICA69-RP versus ICA69

More in detail (Fig. 4.3 and AppendixA), ICA69 and ICA69-RP are highly conserved in their N-terminal region (first 250 aa) containing a BAR domain which is almost identical in ICA69 and ICA69-RP, and in the C-terminal region (last 22 aa), while they are quite divergent in the central region, with two gaps of 22 and 9 aa respectively in ICA69-RP, compared to ICA69.

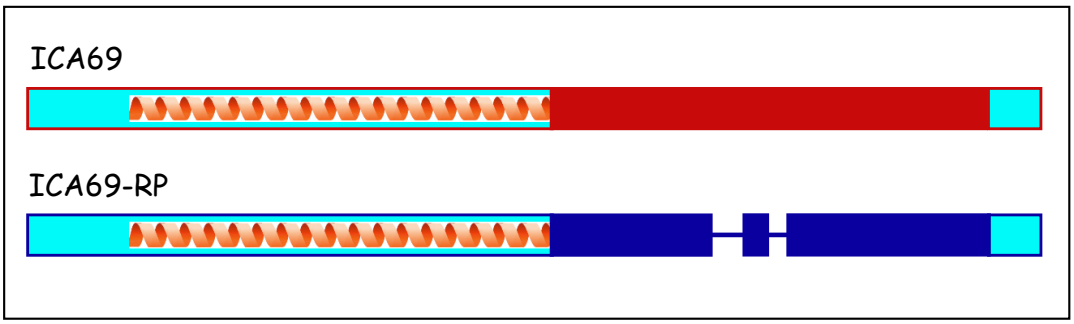

Figure 4.3: **Schematical representation of ICA69 and ICA69-RP**
The cartoon in relative to ICA69 and ICA69-RP proteins. The helix indicates the N-terminal BAR domain. The cyan, at the N-terminal and C-terminal of the two proteins, encompassing also the BAR domain, indicates high homology regions; the red and the blue indicate the regions were ICA69 and ICA69-RP, respectively, differ the most.

4.3 ICA69-RP tissue expression

4.3.1 Rat tissues

In order to study the tissue expression of ICA69-RP, RT-PCR analyses were performed on RNA prepared from various rat tissues (Fig. 4.4). The data obtained[1] indicate that both ICA69 and ICA69-RP are expressed in brain and pancreatic islets, with much higher expression levels in brain. Interestingly it is possible to detect ICA69-RP but not ICA69 expression in the hearth. Furthermore, ICA69-RP cDNAs in hearth and brain are slightly different in size, suggesting a differential tissue expression of ICA69-RP isoforms, which however was not further investigated.

4.3.2 Human tissues

RT-PCR analyses were performed on various total human RNA purchased from BD Bioscience. The data obtained (Fig. 4.5), which are consistent with those in the SOURCE database, indicate that ICA69-RP is expressed mainly in the brain, including the cerebellum, in the testis and in the spinal cord.

Taken together these data indicate that ICA69-RP has the typical distribution pattern of genes that are preferentially expressed in neuroendocrine cells.

[1] Ins indicate the rat insulinoma cell line INS-1. The results of the RT-PCR from this cells will be discussed in section 4.4 on page 76.

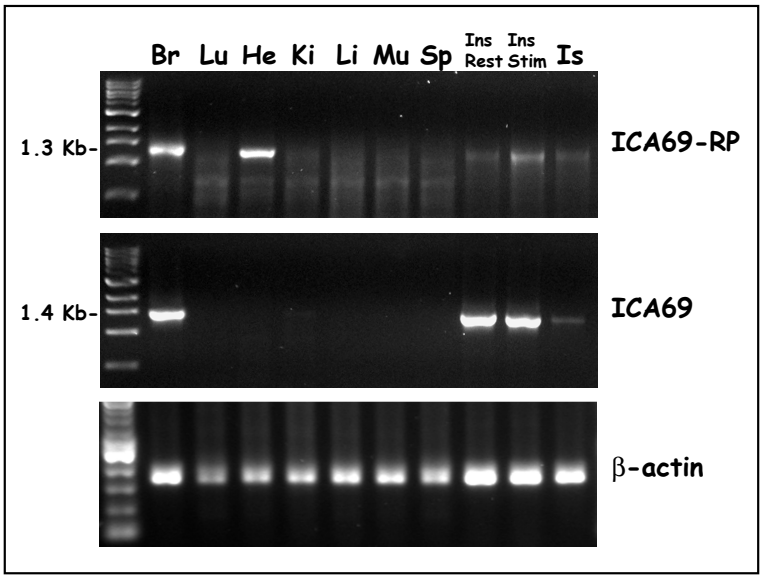

Figure 4.4: **ICA69-RP expression in rat tissues**
Semi-quantitative RT-PCR analysis on RNA prepared from various rat tissues. Br=Brain, Lu=Lung, He=Hearth, Ki=Kidney, Li=Liver, Mu=Muscle, Sp=Spleen, Ins Rest=INS1 cells in resting conditions, INS Stim=INS1 cells stimulated with high glucose, Is=Islets. ICA69, ICA69-RP and the house keeping gene β-actin were PCR-amplified.

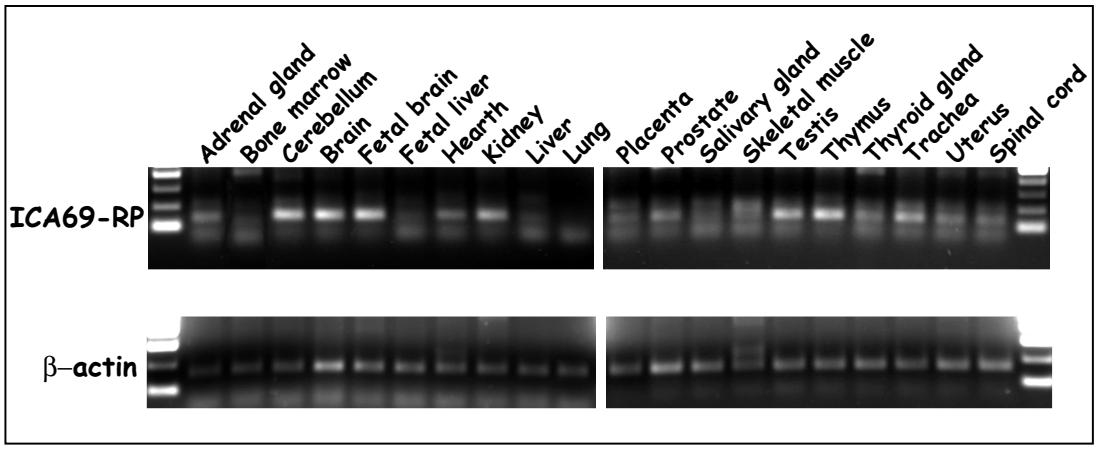

Figure 4.5: **ICA69-RP expression in human tissues**
Semi-quantitative RT-PCR analysis on total human RNA from the tissues indicated, as purchased from BD Biosciences. Segments of approximately 150 bp for both ICA69-RP and the house keeping gene β-actin respectively, were PCR-amplified.

4.4 ICA69-RP glucose regulation

Fig. 4.4 suggested a glucose regulation of ICA69-RP. Iits mRNA increased upon stimulation of INS-1 cells with high glucose (25 mM) for two hours (compare INS Rest and INS Stim in Fig. 4.4, top panel) . As already described in section 1.4.3 on page 36 regarding insulin-containing SGs, glucose is the primary physiological stimulator of insulin secretion. It triggers SGs exocytosis and activates transcriptional and post-transcriptional mechanisms in order to upregulate the expression of secretory granule genes and renew granule stores which undergo depletion following exocytosis. More in detail, increased translation of mRNA accounts entirely for the up-regulation of SG components biosynthesis within the first two hours after stimulation, typically within 20-30 min from the beginning of the stimulation, whereas activation of transcription is a slower process (237; 238). The putative glucose regulation of ICA69-RP was therefore of relevance for its possible involvement in the trafficking and secretion of insulin.

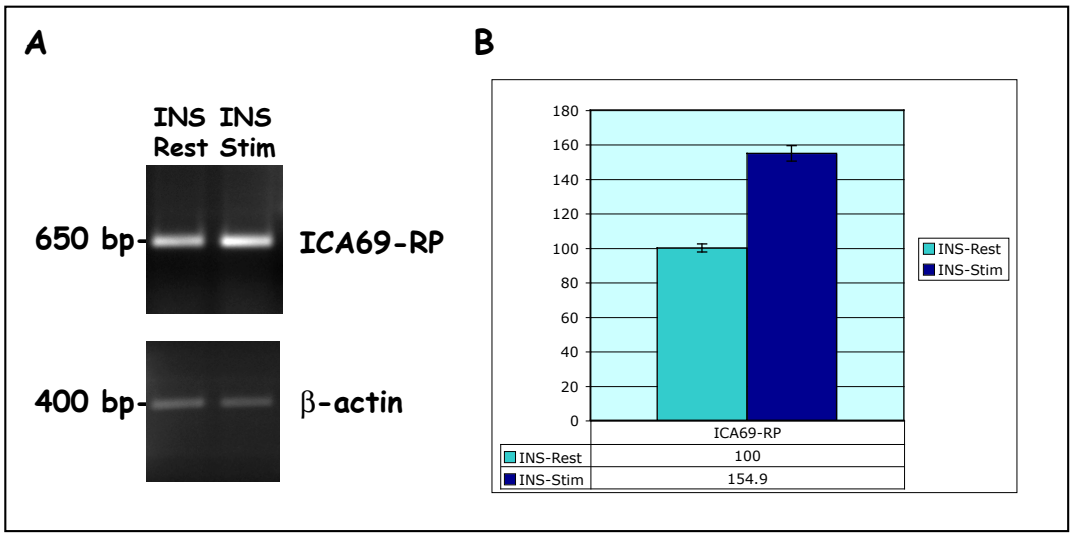

Figure 4.6: **ICA69-RP glucose regulation**
A) Semiquantitative RT-PCR analysis from INS-1 cells kept at rest (0 mM glucose) or stimulated (25 mM glucose). B) Quantification of three independent experiments; amounts were normalized against β-actin. The error bar indicates the SD for the resting condition, equaled to 100%, and the SE for the stimulated condition.

To further investigate this issue, additional semiquantitative RT-PCRs were performed on INS-1 cells in resting condition or stimulated for two hours with high glucose (the stimulation

of the cells also with high potassium was not necessary for the purposes of this experiments, as it determines depolarization of the membrane and insulin secretion, but does not have any transcriptional or post-transcriptional effect). Moreover two sets of oligos were chosen to carry out the RT-PCR experiments, giving a PCR product of 650 and 550 base pairs (bp) respectively. The results of the experiment relative to the 650 bp PCR product (identical values were obtained using the other set of oligos) are reported in Fig. 4.6. ICA69-RP mRNA increases 1.55 fold in INS-1 cells stimulated with high glucose for two hours. These data indicate that ICA69-RP is glucose-regulated.

Many mRNA encoding proteins of the SGs are stabilized, upon stimulation, through the binding of the protein polypirimidine tract-binding protein (PTB) to their 5' or 3'-untranslated regions: this leads to their increased translation. Bioinformatic searches did not reveal any putative binding site for PTB. ICA69-RP, however, could also be regulated by glucose but indipendenly from PTB.

4.5 ICA69-RP antibodies

4.5.1 Production of a polyclonal α-ICA69-RP antibody

In order to obtain α-ICA69-RP specific antibodies a construct expressing a fusion protein between GST and the amino acids 266-402 of ICA69-RP was generated (Fig. 4.7). The construct was expressed in bacteria, the GST fusion protein purified (Appendix B, Fig. B.2 on page 113) and sent to Eurogentec to be injected into rabbits.

As showed in Fig. 4.3 (the blue region in ICA69-RP), the region of ICA69-RP chosen for the expression in bacteria is the most divergent region from ICA69, and its use as immunogen in rabbits provided high probability of obtaining antibodies which would not have cross-reacted with the orthologue/paralogue gene product.

4.5.2 Characterization of the polyclonal α-ICA69-RP antibody

The reactivity of the crude rabbit antisera against ICA69-RP was first evaluated using a fusion protein between ICA69-RP and GFP (AppendixB, Fig. B.3 on page 114). Briefly, the antibody was affinity purified and tested by western blotting and immunocytochemistry on INS-1 cells, human epidermal keratinocytes (HEK cells) and transformed african green monkey kidney fibroblasts (COS-7 cells) cells transiently transfected with a plasmid expressing ICA69-RP in fusion with GFP.

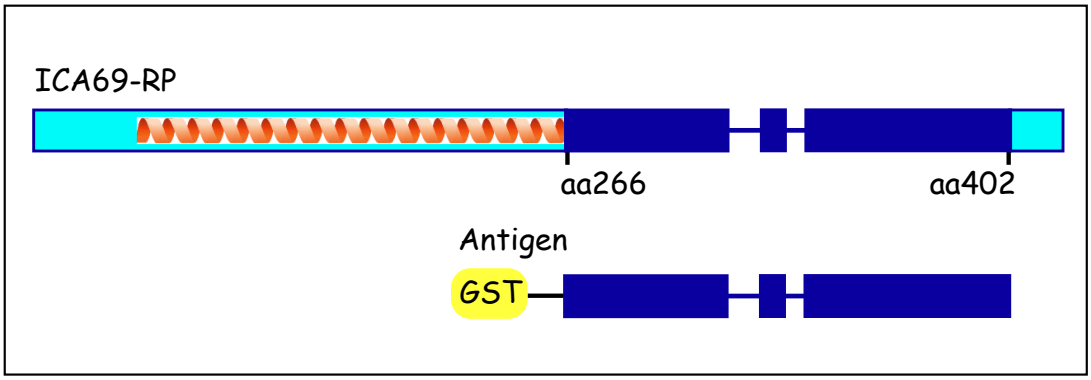

Figure 4.7: **Schematic representation of ICA69-RP-antigen**
The cartoon indicate the region in ICA69-RP (named ICA69-RP-antigen) which, in fusion with GST, was used as immunogen to inject rabbits and produce α-ICA69-RP specific antibodies.

By western blotting (Fig. 4.8 A) ICA69-RP-GFP was detected in the Triton X-100 soluble fraction of cells as a ~80 kDa protein using an α-GFP antibody or the affinity purified α-ICA69-RP antibody. Considering the fusion with GFP, which has a molecular weight of ~27 kDa, this mobility is consistent with the expected size of 50 kDa for ICA69-RP.

By immunocytochemistry the α-ICA69-RP antibody only reacted with cells that were also positive for GFP (compare Fig. 4.9 A and D with Fig. 4.9 B and E, respectively. Compare also, in Fig. 4.11 B, A-C (top) with D-F (bottom)), thereby confirming the specific reactivity of this antibody.

4.5.3 Detection of endogenous ICA69-RP

Despite the encouraging evidences obtained with the above described α-ICA69-RP antibody, the same did not recognized a *bonafide* endogenous ICA69-RP by western blotting on Triton X-100 soluble or insoluble fractions of INS1-cells, grown either in normal medium, or in resting (0 mM glucose) or stimulating (25 mM glucose, 55 mM KCl) buffers. ICA69-RP was also not detectable in cells treated with a proteasome inhbitor.

A commercial monoclonal antibody against ICA69-RP, which in the meantime become available, was also similarly tested. Despite recognizing ICA69-RP overexpressed in cells, this antibody also failed to detect the endogenous ICA69-RP (Fig. 4.8 B) probably because the expression levels of this protein in all attempted conditions were too low.

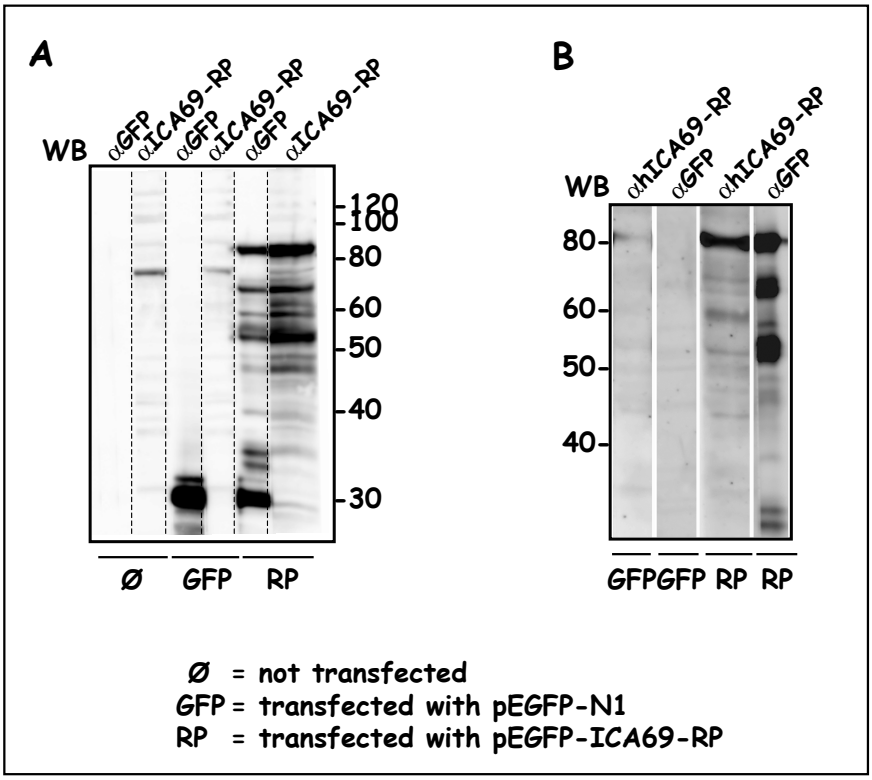

Figure 4.8: **Recognition of ICA69-RP by two antibodies: Western Blot**
A) Western blotting on HEK cells Triton X-100 soluble fraction with a α-GFP antibody or with the polyclonal α-ICA69-RP antibody. Lanes 1 and 2: not transfected cells. Lanes 3 and 4: cells transfected with pEGFP-N1. Lanes 5 and 6: cells transfected with pEGFP-ICA69-RP. B) Western blotting on INS-1 cells Triton X-100 soluble fraction with a α-GFP antibody or with the commercial monoclonal α-ICA69-RP antibody. Lanes 1 and 2: cells transfected with pEGFP-N1. Lanes 3 and 4: cells transfected with pEGFP-ICA69-RP. It should be noted that the α-GFP antibody does not detect GFP ($\sim$27 kDa) in lanes 2 and 4 because the portion of the gel shown in the figure does not include proteins with a molecular weights lower than 30 kDa).

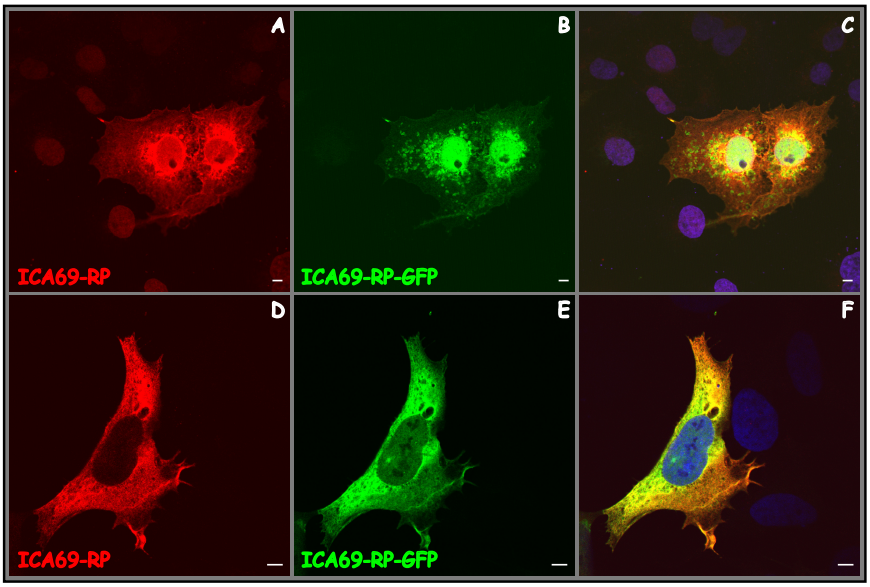

Figure 4.9: **Recognition of ICA69-RP by an affinity purified antibody: Immunocytochemistry**
Confocal microscopy images from COS-7 (A-C) and HEK (D-E) cells transfected with pEGFP-ICA69-RP. A and D: immunolabeling for ICA69-RP (pseudored). B and E: GFP fluorescence (pseudogreen). C and F: merge - nuclei counterstained with DAPI (pseudoblue). Scale bar: 5 μm.

Comparable negative results were obtained using both antibodies for visualization of endogenous ICA69-RP in INS-1 cells by immunofluorescence microscopy (data not shown).

4.6 Generation of a cell line expressing ICA69-RP-GFP

To continue investigating the properties of ICA69-RP, while obviating the inability to detect the endogenous protein, INS-1 cells stably expressing ICA69-RP fused with GFP were generated. Of several stable ICA69-RP-GFP expressing INS-1 clones originally generated (Fig. 4.10), two clones expressing high and low levels of ICA69-RP-GFP were further analyzed.

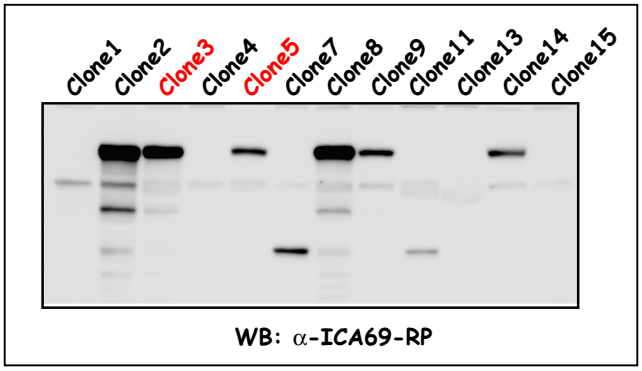

Figure 4.10: **INS-1_ICA69-RP-GFP stable cell line: different clones**
Western blotting on Triton X-100 soluble fraction of INS-1 cells stably expressing ICA69-RP-GFP using the polyclonal α-ICA69-RP antibody. Of all the clones, clone 3 and clone 5 were further analyzed.

4.6.1 Immunocytochemistry on the stable cell line

Confocal microscopy indicated that ICA69-RP-GFP is mostly cytosolic (Fig. 4.11 A (C and D) and B (A-C)) and does not significantly colocalize with markers of the ER (PDI), cis-medial Golgi (GM130), TGN (TGN38), secretory granules (insulin and CPH/E), and synaptic-like microvesicles (synaptophysin) (data not shown). The staining pattern, however, suggests that ICA69-RP-GFP may not be entirely soluble. As previously shown for COS-7 and HEK cells expressing ICA69-RP-GFP, the α-ICA69-RP antibody only reacted, by immunocytochemistry, with cells positive for GFP (Fig. 4.11 B).

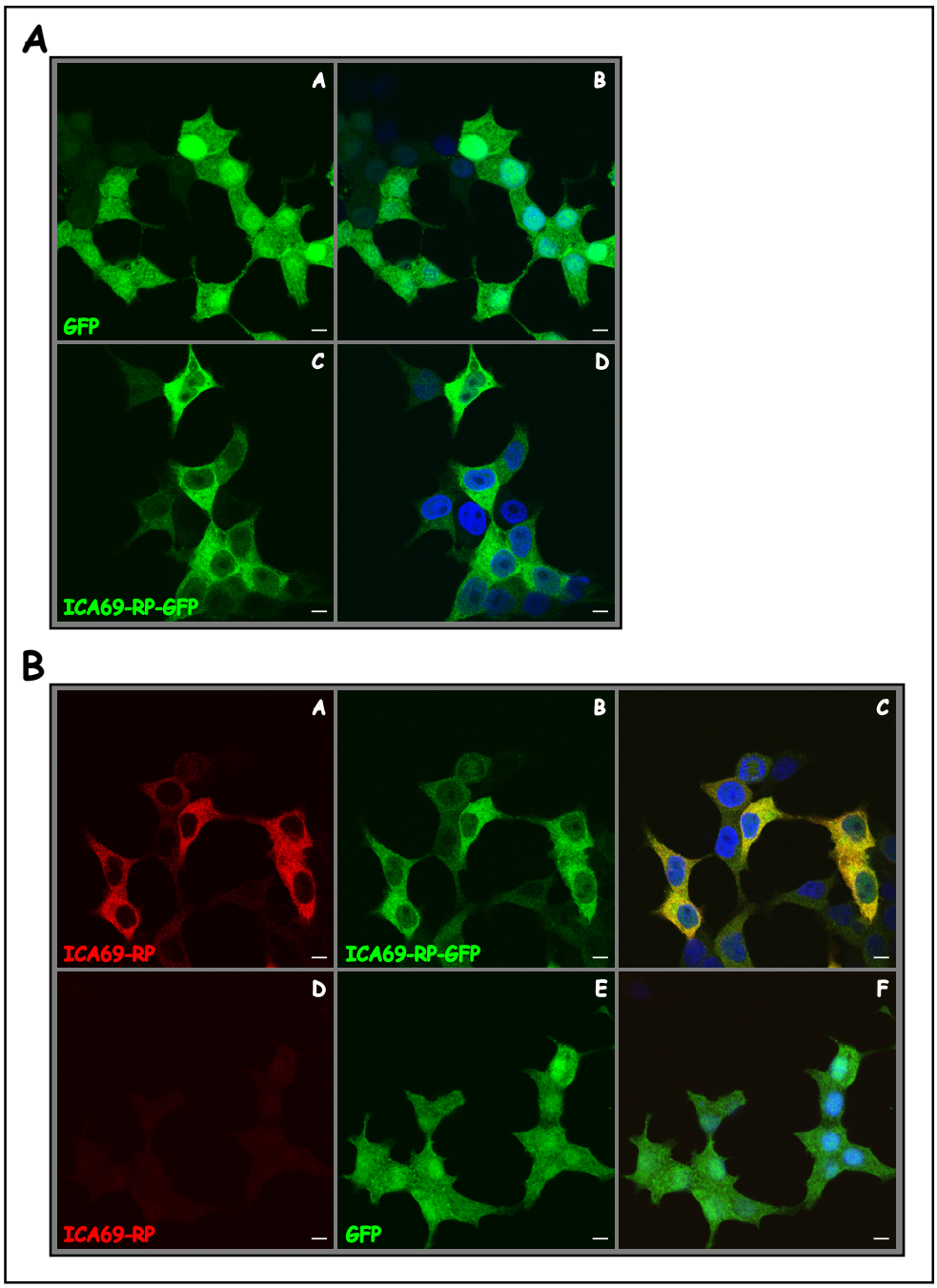

Figure 4.11: **INS-1_ICA69-RP-GFP stable cell line**
Confocal microscopy images from INS-1 cells stably expressing GFP or ICA69-RP-GFP. Scale bar: 5 μm. A) A and B: INS-1 stably expressing GFP. C and D: INS-1 stably expressing ICA69-RP-GFP. A and C: GFP fluorescence (pseudogreen). B and D: merge (nuclei counterstained with DAPI (pseudoblue)). B) A-C: INS-1 stably expressing ICA69-RP-GFP. D-F: INS-1 stably expressing GFP. A and D: immunolabeling for ICA69-RP (pseudored). B and E: GFP fluorescence (pseudogreen). C and F: merge (nuclei counterstained with DAPI (pseudoblue)).

4.7 Interaction ICA69/ICA69-RP

Arfaptin 1 and 2, as well as amphiphysin 1 and amphiphysin 2 homo/heterodimerize and bind small GTPases through their BAR domain (48; 239). Thus, it was possible that ICA69 and ICA69-RP would have formed heterodimers. This hypothesis was investigated by performing immunoprecipitation experiments from insulinoma cells and fibroblasts overexpressing ICA69-RP-GFP using an α-GFP antibody or the two α-ICA69-RP antibodies and western blotting for ICA69 (Fig. 4.12).

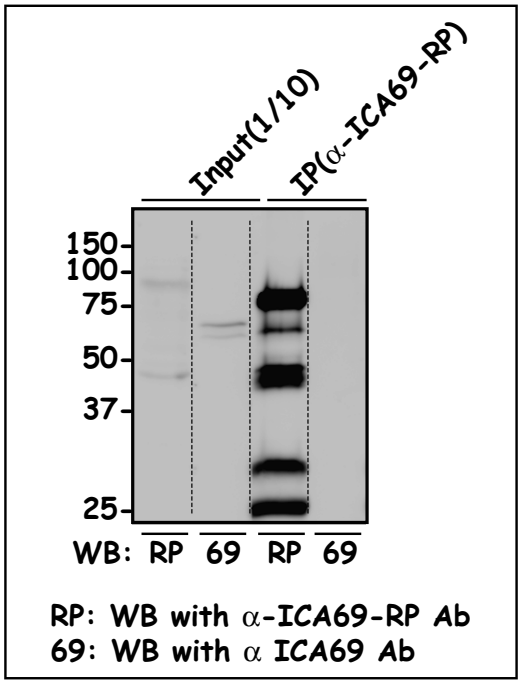

Figure 4.12: **Interaction ICA69/ICA69-RP**
Immunoprecipitation experiment from Triton X-100 soluble fraction of INS-1 transiently transfected with ICA69-RP-GFP, using the monoclonal α-ICA69-RP antibody (identical results were obtained with the polyclonal antibody). Lanes 1 and 2: input (10% of the cell extract used for the immunoprecipitation). Lanes 3 and 4: immunoprecipitations. The antibodies used for the western blotting are indicated.

Up to now the attempts to detect an ICA69/ICA69-RP heterodimer did not produce any positive result.

4.8 Interaction of ICA69-RP with Rab proteins

Using the same approaches as for ICA69 (section 3.3 on page 50), i.e. immunoprecipitations and pull- down assays, the possible interaction of ICA69-RP with Rab2 (as in the case of ICA69) or with Rab1 (the other Rab involved in ER-Golgi transport) was investigated. These assays did not provide any positive result (data not shown). On the other hand it is possible that ICA69-RP interacts with a different Rab protein, or more in general with a different small GTP-binding protein.

Chapter 5

Conclusions and Discussion

This thesis characterized the two members of ICA69 protein family, ICA69 and ICA69-RP, and initiated the elucidation of their role in membrane traffic in pancreatic β- cells.

5.1 Focus on ICA69

As outlined in the Chapter 2, several existing lines of evidence point towards a role of ICA69 in secretion. The two most suggestive results are: the presence of a BAR domain in ICA69, which is a membrane binding/bending module found in proteins involved in intracellular transport (48); and the specific secretory phenotype of a *C. elegans* mutant lacking the ICA69 homologue (225).

In this thesis it was shown that ICA69 is distributed in a punctuate manner within cells. ICA69 was found to be more enriched in the perinuclear region, where also markers of the Golgi region are present. Previous studies failed to demonstrate the association of ICA69 with regulated secretory vesicles of pancreatic β-cells, including SVs (225) and the insulin-containing SGs (226). However, this does not exclude the possibility that ICA69 may be involved in earlier stages of membrane trafficking. The cellular localization of ICA69 as reported in this thesis supports indeed this hypothesis. Impaired protein transport along the early secretory pathway may still results in deficient regulated secretion and account for the involvement of ICA69 in both neurotransmitter secretion, justifying the defective release of acetylcholine in the *C. elegans* mutant despite the absence of ICA69 on SVs, and secretion of insulin, a property, this latter, shared with other autoantigens of T1D.

In this thesis it was shown that ICA69 interacts with several membrane lipids, including PI(3)P, PI(4)P, PI(5)P, PI(3,4)P_2, PI(3,5)P_2, PI(4,5)P_2, PI(3,4,5)P_3 in a protein-lipid overlay

assay. In view of the limit of this assay, this data should be taken with caution: for instance, control binding assays showed a similar broad binding pattern for amphiphysin 1, despite the fact that this protein is known to interact preferentially with PI(4,5)P_2. Yet, the protein-lipid overlay assay results suggest the possibility that ICA69 binds phospholipids, as expected in the case of proteins containing a BAR domain. A similar phospholipid binding pattern has been found with the BAR domain-containing proteins RICH-1 (240) and arfaptin2 (Giovanni D'Angelo, Consorzio Mario Negri Sud,-Italy, personal communication). In particular, the BAR domains of ICA69 and arfaptin 2 are very similar and both proteins appear to interact preferentially with PI(4)P. This phosphoinositide, in turn, is enriched on the Golgi complex and is required for the budding of secretory vesicles from this compartment (121). The work presented herein supports the emerging picture that ICA69 associates with Golgi membranes (226).

In this thesis several biochemical and imaging techniques were applied to investigate the interaction between ICA69 and Rab2. This was motivated by earlier reports of preliminary data that pointed to the interaction of ICA69 with a small GTPase (226) and a two-hybrid screening in yeast identified ICA69 as a putative binding partner of Rab2 (F. Barr, personal communication). Rab2 is a small GTPase that is known to associate with the intermediate compartment (IC) (232). It is involved in the trafficking between the ER and the Golgi complex, while Rab1, found in the ER, IC and early compartments of the Golgi complex, plays a role in the anterograde trafficking between the ER and the Golgi, through COPII vesicle formation (241). Rab2, in particular, recruits β-COP for vesicle formation (229) and was originally proposed to participate, as the COPI coat itself, in the retrograde transport between the ER and Golgi complex[1] (242). Several evidence, however, indicate that Rab2 may be involved also in the anterograde transport (30; 62; 63). With respect to Rab1, Rab2 could therefore function in a parallel or sequential fashion in regulating the ER-to-Golgi transport (62). Thus it is apparent that the molecular mechanism of Rab2 action remains unclear, with only few effectors of Rab2 identified. E. Tisdale and coll., who performed most of the studies on Rab2, suggested that Rab2 stimulates vesicle formation by enhancing the recruitment of β-COP to the membranes of the intermediate compartment (229). For this interaction to occur it is essential that Rab2 binds to its effector protein kinase C PKCι/λ (63). Another Rab2 effector is glyceraldehyde-3-phosphate dehydrogenase (GAPDH), which is believed to be involved in the trafficking between the ER and Golgi independently of its glycolytic activity (243), even

[1]The possible function of COPI-coated vesicles in the anterograde transport, as well as in the retrograde transport, was discussed in the introduction, subsection 1.3.1.2, on page 10.

though its function in this respect remains unclear. F. Barr and coll., on the other hand, showed the GTP-dependent interaction of Rab2 with GM130[1], GRASPP55 and golgin-45, all Golgi proteins, and propose a role for the GRASPP55-golgin45-Rab2 complex in anterograde protein transport and Golgi structure (230).

In this thesis Rab2 was found to co-immunoprecipitate with ICA69 from INS-1 cells extracts. This approach is usually regarded to be inappropriate for the identification of Rab effectors, because in the course of the experiment Rab proteins which are not loaded with the non-hydrolyzable analogue of GTP, GTPγS, would hydrolyze GTP. Thus, the putative interactors found with this assay, would be considered to bind the Rab protein in their GDP-bound state and not be considered to be functionally relevant[2]. Nevertheless, it should also be taken into account that the hydrolitic activity of diverse Rab proteins may vary. Specifically, Rab2 has a very slow hydrolytic activity, such that most of it may remain in a GTP-boud state during the immunoprecipitation procedure (F. Barr, personal communication). Additional Rab effectors that have been found to co-immunoprecipitate with their respective Rab without addition of GTPγS include GAPDH with Rab2 (243), as well as Rabaptin4 with Rab4 (244).

In order to substantiate the interaction between ICA69 and Rab2, GST pull down assays were performed according to the classic procedure described in (245). This analysis demonstrated the GTP-dependency of this interaction, as the two proteins could interact only when Rab2 was loaded with GTPγS, but not when loaded with GDP. In similar pull down assays, this association was shown to be specific. ICA69 did not interact with other Rab proteins, such as Rab1, Rab4, Rab5 and Rab6.

Additional confirmation of the ICA69/Rab2 interaction was obtained by immunocytochemistry experiments. Confocal microscopy showed indeed that ICA69 and Rab2 colocalized extensively in particulate structures throughout the cytoplasm.

Furthermore the results of two independent experimental procedures suggested that Rab2 recruits ICA69 to membranes. By immunocytochemistry it was found that in cells expressing the highest levels of Rab2-GFP, and only upon over-expression of Rab2-GFP, ICA69 was enriched in a perinuclear structure, where also Rab2-GFP was found. This result suggested a "redistribution" of ICA69 within the cells that is Rab2 dependent. Furthermore, subcellular

[1] Surprisingly, the GTP-dependent interaction of Rab2 and GM130 was not reproducible in this thesis, as pointed out in the Results, subsection 3.3.2, on page 50.

[2] Rab effectors, as already described in subsection 1.3.5 on page 17, are proteins that only interact with Rabs in their active, GTP-bound state.

fractionation studies showed that over-expression of Rab2 correlated with an increased recovery of ICA69 in the membrane-bound fraction of cell extracts, consistent with a Rab2-mediated recruitment of ICA69 to membranes.

It is known that by inhibiting nucleotide exchange on ARF1 and thereby preventing the binding of COPI proteins to Golgi membranes, BFA causes the loss of the Golgi structure, with the retrieval of the Golgi enzymes into the ER, while Golgi matrix proteins, such as GM130, remain associated with punctate cytoplasmic structures called "Golgi remnants" (234). Upon treatment of INS-1 cells with BFA, the signals for both ICA69 and Rab2 were strongly decreased, consistent with the redistribution of both proteins to the cytoplasm. These results, in accordance with those on Rab2 (246) and β-COP (234), suggest a similar sensitivity of β-COP, Rab2 and ICA69 to BFA and point again to the related behavior of ICA69 and Rab2.

Taken together, the results shown in the thesis suggest that Rab2, in its GTP-bound form, recruits ICA69 to a membrane compartment. It could be that this compartment is the intermediate compartment, where anterograde and retrograde transport first segregate from each other (63). Additional evidence supporting this hypothesis was obtained by immunostaining of INS-1 cells incubated at 15 °C for 80 min. The incubation at this reduced temperature blocks the transport between the ER and the Golgi complex, and leads to the accumulation of the intermediate compartment, thereby facilitating its visualization (233). In these conditions ICA69 accumulated in perinuclear structures resembling those observed upon over-expression of Rab2. The appearance of this structures following the 15 °C-block, suggests, but do not conclusively prove, their identity as the intermediate compartment. Notably however, the morphology of the perinuclear structures where Rab2-GFP accumulated in cells kept at 37 °C and the perinuclear structures where ICA69 was found in cells incubated at 15 °C differ. Thus, it cannot be excluded that at physiological temperature the bulk of Rab2 and ICA69 may be associated with structures distinct from the intermediate compartment.

The BAR domain of arfaptin, the first one been solved, was crystalized as a dimer (118). In general, proteins including a BAR domain are thought to form homodimers as well as heterodimers with their close paralogues (48). Similar to previous work on proteins with a BAR domain (239; 247; 248), two different approaches were used in the course of this thesis to attempt the detection of ICA69 homodimers: comparisons between native and denaturing gels or co-immunoprecipitations of the endogenous ICA69 and a tagged form of it. Both attempts, however, were unsuccessful (data not shown). Thus, additional information concerning the

possible dimerization of ICA69 may come from crystallographic or equilibrium density ultracentrifugation studies, as reported for other proteins containing a BAR domain (48; 118; 249). Moreover, it should be considered that the dimerization constants found in the case of some proteins with a BAR domain suggest that these proteins mostly exist as monomer in the cell, while forming dimers only transiently, when associated with membranes (50).

As already described in the Introduction (subsection 1.3.4 on page 15), the cytoskeleton has an important role in vesicle transport. Kinesin has been shown to be the motor involved in the microtubule-mediated retrograde transport between the Golgi and the ER (83). Yet, the molecular connection between kinesin and COPI vesicles is still unknown. In the course of this thesis it was tested therefore whether ICA69, recruited on membranes by the active form of Rab2, was also associated with kinesin. Immunoprecipitation experiments, however, did not provide any evidence this interaction (data not shown).

Preliminary data by two-hybrid screening in yeast indicated that ICA69 binds to Rab2 through its C-terminal region (F. Barr, personal communication), rather than through its BAR domain. This finding is quite surprising, since the BAR domain usually acts as a binding interface for different GTPases (113; 118; 119). On the other hand, this raises the possibility that ICA69 acts as a scaffold protein that interacts independently with two small GTPases, through its BAR domain and its C-terminal region, thereby mediating a cross talk between such GTPases and their associated pathways. However, GST pull down assays failed to demonstrate the interaction of Rab2 with a truncated mutant containing only the C-terminal region of ICA69. It is possible, anyway, that the C-terminal domain of ICA69, when expressed alone, is either not properly folded or anyway not functional, and thus cannot bind to Rab2 in absence of the remaining part of the protein. Additional experiments will be necessary to conclusively map the domain of ICA69 that binds to Rab2. Studies are ongoing to test whether the interaction ICA69/Rab2 actually occurs through the BAR domain of ICA69. However, all attempts to express the N-terminal half of ICA69 have so far been unsuccessful. If the binding to Rab2 occurrs through the C-terminal domain of ICA69, it would be interesting to test whether the BAR domain of ICA69 can in turn bind another small GTPase. The interaction between ICA69 and ARF1 has already been tested, with negative result (data not shown). This candidate gene approach for the identification of small GTPases binding to ICA69 could be extended by performing immunoblots of proteins co-immunoprecipitating or pulled down together with ICA69. Attention would be placed on GTPases that are localized in the ER and Golgi region. These

include Arl1, which is important for Golgi structure and function[1] (250); Rab33B, which has a putative role in intra-Golgi trafficking (251); Rab30, which is Golgi-associated (252); and/or Sar1p, that is required for the formation of COPII-coated vesicles (69). An alternative unbiased approach could be to use recombinant ICA69-GST for large-scale affinity chromatography and subsequent screening of the eluate for small GTPases and other potential interactors, by western blotting and mass-spectrometry.

As pointed out earlier, Rab effectors are defined as proteins that interact with the GTP-bound form of a Rab protein and transduce the signal of the Rab protein in the transport mechanism (88). To investigate whether ICA69 was actually a novel Rab2 effector, and to initiate to dissect ICA69 function, several approaches were used. In all cases it was evaluated whether ICA69 over-expression resembles that of Rab2, therefore suggesting their belonging to the same pathway.

Results reported previously, indicated that Rab2 over-expression leads to a decrease of 25% in the processing of the glycoprotein VSV-G from an endoglycosidase H-sensitive form to an endoglycosidase H-resistant form. Endo H-sensitive species are those present in the ER and carrying an high mannose precursor oligosaccharide, while endo H-resistant species are those present in the Golgi and at the plasma membrane (62; 236).

In this thesis the conversion of the pro-form of the T1D autoantigen ICA512 from an endo H-sensitive to an endo H-resistant form was investigated in control cells and in cells over-expressing Rab2 or ICA69 (data not shown). This approach, however, was unsuccessful, as even in the control cells, it was not possible to detect the endo H-resistant form of pro-ICA512. The very rapid conversion of 130 kDa endo H-resistant pro-ICA512 into ICA512 TMF in the Golgi complex, as pointed out in section 3.7.1 on page 65, explains this result, while indicating the inappropriateness of the chosen glycoprotein. In future studies a different protein, such as VSV-G, should be used for this type of analysis.

To evaluate the effect of ICA69 and Rab2 over-expression on the transport along the secretory pathway a different approach was therefore used. Specifically, the conversion of the pro-form of ICA512 in the mature form (ICA512-TMF) was analyzed in cells in which the expression of ICA512 was induced by glucose only for a short time (pulse) (235) and that were subsequently placed in resting buffer for various periods of time (chase). Control cells showed an increase in the levels of pro-ICA512 upon stimulation, which decreased over time because

[1] ARF1 and Arl1 share some common effectors, and have patially overlapping functions.

of its conversion to ICA512-TMF. Cells over-expressing Rab2 exhibited over the time a constant amount of the pro-form of ICA512, which was most likely less converted into the mature form. The levels of ICA512-TMF, conversely, decreased when compared with control cells. These data indicate a partial impairment in the Golgi trafficking of ICA512 upon Rab2 over-expression. Strikingly, this effect was magnified upon ICA69 over-expression, with an increase of pro-ICA512 levels over time, and a corresponding decrease in the levels of ICA512-TMF. These results confirm that ICA69 and Rab2 are involved in the same pathway, and identify ICA69 as a transducer of Rab2 signaling.

Furthermore, the over-expression of the C-terminus of ICA69 led to an increase in the levels of pro-ICA512 and a decrease in the levels of ICA512-TMF that were intermediate between those observed by over-expression of Rab2 or ICA69. While it was not possible to demonstrate the interaction between the C-terminal region of ICA69 and Rab2 *in vitro*, it can not be excluded that the C-terminal region of ICA69 does indeed function as a translator of the effects of Rab2.

Both Rab2 and ICA69 over-expression correlated with an impaired insulin secretion, with a decrease of 28% in insulin secretion upon Rab2 over-expression, and a more confined 11% decrease in insulin secretion upon ICA69 over-expression, indicating an alteration in the trafficking in β-cells following their over-expression. Although these decreases are limited in size, they are likely to be informative because of their high reproducibility.

To further investigate whether the phenotype resulting from the over-expression of ICA69 resembled that observed upon over-expression of Rab2, subcellular fractionation experiments according to the procedure described in (236) were performed. Contrary to the data reported in the literature (236), Rab2 over-expression correlated with an increased association of β-COP with fast sedimenting membranes (conceivably ER, IC and Golgi), and a decreased association of β-COP with slow sedimenting membranes (conceivably vesicles). Notably, this phenotype was even more pronounced upon ICA69 over-expression. Furthermore, ICA69 over-expression, unlike Rab2 over-expression, correlated with an increase in β-COP levels in the cytoplasm. Published data indicate a role for Rab2 in the recruitment of the coatomer and the stimulation of vesicle formation from the intermediate compartment (229; 236). The data obtained here did not allow to establish a correlation between Rab2 or ICA69 with β-COP, and thus to COPI vesicles. This conclusion is supported by the immunocytochemistry data, which did not show an overlapping distribution between β-COP and Rab2 or ICA69 in INS-1 cells.

Taken together, the functional studies presented here indicate that the effects of ICA69 over-expression resemble and in some cases amplify those observed in Rab2 over-expressing

INS-1 cells. They conclusively identify ICA69 as a novel effector of Rab2, and therefore may contribute to the understanding of the still poorly characterized mechanism of action of Rab2.

5.2 Focus on ICA69-RP

The second part of this thesis focused on an ICA69 paralogue, called ICA69-RP. As with each novel gene, some descriptive work was required before more-in-depth biological questions could be addressed. The chromosomal location for ICA69-RP in humans, mice and rats was investigated. ICA69-RP cDNA was cloned from a cDNA library, and the exon-intron structure of the relative gene was deduced, pointing to a coding sequence for this gene partially different from the sequence deposited at the time in the public databases, and now replaced by the new one.

The defective neurotransmitter secretion upon mutation of *ric19*, a putative ICA69 homologue in *C. elegans* (225), and the lack of a defined (secretory) phenotype in ICA69^{null} mice (228), led to the hypothesis that ICA69-RP could be the real homologue of *ric19*, being therefore involved in neuroendocrine secretion. However, analysis of a genealogical tree generated with several members of the ICA69-protein family in different species showed that this was not the case. Partially redundant functions between ICA69 and ICA69-RP or between ICA69 and some yet unidentified protein, on the other hand, may account for the lack of a phenotype in ICA69^{null} mice.

ICA69-RP tissue expression was investigated, both in rat and human tissues. ICA69-RP mRNA was detected primarily in neuronal tissues such as total brain, cerebellum and spinal cord, in pancreatic islets and in the testes (consistent with the reported similarity between human brain and testis gene expression patterns (253)). These results, in accordance with the SOURCE databases (http://source.stanford.edu/cgi-bin/source/sourceSearch) reflect the expression pattern of a gene preferentially expressed in neuroendocrine cells, as already found in the case of ICA69 (215; 218).

Unlike ICA69, ICA69-RP appears to be glucose regulated. Its mRNA increases 1.55 fold in INS-1 cells stimulated with 25 mM glucose for two hours. This is a characteristic shared by many genes associated with the secretory machinery of β-cells. For example, after two hours of glucose stimulation, insulin mRNA increases 1.43 fold, and ICA512 mRNA increases $\sim$2.3 folds (185). It is known that glucose stimulation of β-cells prompts the activation of

post-transcriptional mechanisms[1] in order to quickly up-regulate the expression of secretory granule genes and consequently renew granule stores. This is achieved in part by increasing the stability of mRNAs encoding SGs components through a mechanism involving the mRNA binding protein PTB (185) (as detailed in section 1.4.3 on page 36), and in part by up-regulating the expression and/or activity of factors involved in the expression and transport of molecules along the secretory pathway. The increased expression of ICA69-RP upon glucose stimulation of cells may be part of this process.

Unfortunately, all attempts of investigating the intracellular localization of endogenous ICA69-RP, either with a commercial antibody or with an antibody produced in the course of this thesis, failed, probably because of the low expression levels of the protein. Insights into the localization of ICA69-RP could also not be obtained by over-expressing a fusion protein between ICA69-RP and GFP. In transfected cells ICA69-RP-GFP appears to be mostly cytosolic, with no significant enrichment in any particular compartment. The differences in the staining obtained for ICA69-RP-GFP and for GFP suggest that ICA69-RP may not be entirely soluble. Unlike in the case of ICA69, however, a punctate "vesicular" staining, could not be readily discerned. Subcellular fractionation studies are in progress to address this question.

Using the same approaches as for ICA69, ICA69-RP did not show any interaction either with Rab2 or Rab1, which are involved in ER-to-Golgi transport. It is thus possible that ICA69-RP interacts with Rab proteins other then these, or in general with a different small GTP-binding protein.

To this date, there is no indication that ICA69-RP binds a small GTPase. In order to investigate this possibility, it would be interesting to immunoprecipitate ICA69-RP-GFP from transfected cells and then perform GTP overlay assays on the co-immunoprecipitated material. Unlike in the case of ICA69, a candidate gene approach for the identification of ICA69-RP interactors may not be recommended, given the broad cytosolic distribution of ICA69-RP-GFP. An alternative approach would be to use recombinant ICA69-RP-GST for large-scale affinity chromatography and consequent search in the eluate of small GTPase by mass-spectrometry. As in the case of ICA69, preliminary information about physiological interactors may also be obtained by two-hybrid screening in yeast.

[1] Post-transcriptional mechanisms account entirely for the up-regulation of SGs genes within the first 2 hours after stimulation, whereas activation of transcription is a slower process.

Chapter 6

Material and Methods

6.1 Cell culture

Rat insulinoma INS-1 cells were grown in RPMI 1640 medium (with L-glutamine) (Gibco-Brl or PAA Laboratories GmbH) supplemented with 10 mM HEPES (MERK KGaA) pH 7.4, 10% heat-inactivated fetal bovine serum (FBS) (Gibco-Brl or PAA Laboratories GmbH), 2 mM L-glutamine (PAA Laboratories GmbH), 100 U/ml penicillin (PAA Laboratories GmbH), 100 μg/ml streptomycin (PAA Laboratories GmbH), 1 mM sodium pyruvate (PAA Laboratories GmbH) and 50 μM 2-mercaptoethanol (Sigma Chemical Co.) (254) and incubated at 37 °C in a humidified 95% air-5% CO_2 atmosphere. For trypsinization, cells were separated by exposure to 0.5 mg/ml trypsin-EDTA (PAA Laboratories GmbH) in phosphate buffer saline (PBS) (Gibco-Brl or PAA Laboratories GmbH) for 3 minutes (min) at room temperature (RT). Trypsin was inactivated by adding the growth medium indicated above. Cells were usually passaged every 4 days, and medium was changed 2 days after splitting.

For stimulation experiments, and unless otherwise stated, cells were pre-incubated in resting buffer (5 mM KCl, 120 mM NaCl, 24 mM $NaHCO_3$, 1 mM $MgCl_2$, 2 mM $CaCl_2$, 1 mg/ml ovalbumin, 15 mM HEPES pH 7.4) for 1 hour at 37 °C. The cells were then incubated for additional 2 hours at 37 °C in resting buffer or in stimulating buffer (25 mM glucose, 70 mM NaCl, 24 mM $NaHCO_3$, 1 mM $MgCl_2$, 2 mM $CaCl_2$, 1 mg/ml ovalbumin, 15 mM HEPES pH 7.4, w/o 55 mM KCl, depending on the purposes) (235).

For the time-course stimulation, cells were pre-incubated in resting buffer for 1 hour at 37 °C.

The cells were then incubated for additional 30 min at 37 °C in resting buffer or in stimulating buffer (25 mM glucose, 55 mM KCl), and then, only the latter, in resting buffer for 15, 30, 45, 60 or 90 min.

Human Epidermal Keratinocytes (HEK) cells and Transformed African Green Monkey Kidney Fibroblast Cells (COS-7) cells were grown in Dulbecco's modified Eagle's minimal essential medium (DMEM) (with L-glutamine, 1,000 mg/L D-glucose, sodium pyruvate) (Gibco-Brl) supplemented with 10% heat-inactivated FBS, 100 units/ml penicillin and 100 μg/ml streptomycin (255; 256) and incubated at 37 °C in a humidified 95% air-5% CO_2 atmosphere. For trypsinization cells were washed once with PBS and separated by exposure to 0.025% trypsin-EDTA in PBS for 4-5 min at RT. Trypsin was inactivated by adding the growth medium indicated above. Cells were usually passaged every 3 days.

Cells were grown in 175 and 75 cm^2 flasks or 6-well plates (BD Falcon^{TM} - BD Biosciences).

6.1.1 Transfection

Cells were counted using a Neubauer hemacytometer (Reichert).

INS-1 cells were electroporated with an Amaxa nucleoporator (Amaxa Biosystems, Inc.) using the Cell line nucleofector kit V (Amaxa Biosystems, Inc.) and the program T-20 (transfection efficiency ~50%) according to the manufacturers protocol. 4×10^6 cells were electroporated with 4 μg of plasmid DNA (unless otherwise stated), then gently resuspended in 2 wells of a 6-well plate containing 2 ml of the growth medium indicated above and grown for 3-4 days before harvesting. INS-1 cells stably expressing GFP were selected with 600 μg/ml gentamicin (Gibco-Brl) and cloned by limiting dilution. INS-1 cells stably expressing ICA69-RP-GFP were selected with 500 μg/ml gentamicin and cloned by limiting dilution. Two clones expressing high and low levels of ICA69-RP-GFP, as assessed by western blotting, were further characterized. During the last period of the thesis, INS-1 cells were occasionally electroporated with a Laboratory Pulse Agile® Electroporation System, model PA-3,000 (Cytopulse Sciences, Inc.) using the Cytoporation media (formula T) kit (Cytopulse Sciences, Inc.), at 580 Volt (V), 2 x (4 x 300 μsec (0.2 sec pause)) (1.5 min pause) (transfection efficiency ~25%); the same number of cells, amount of DNA and conditions for resuspension indicated above were applied.

HEK and COS-7 cells were transfected using FuGENE 6 transfection reagent (Roche Diagnostic GmbH) according to the manufacturers protocol. For each well of a 6-well plate 2.5×10^5 HEK cells or 2×10^5 COS-7 cells, 3 μl of Fugene 6 and 1 μg of plasmid DNA were used.

6.1.2 Insulin radioimmunoassay

The insulin content in cells and in medium (resting or stimulation buffer) was measured wit the Sensitive Rat Insulin Radioimmunoassay (RIA) Kit (Linco Reseach, Inc.) according to the manufacturer's recommendations. Cell proteins were extracted upon incubation in acid-ethanol (75% EtOH, 1.5% concentrated HCl, 23.5% H_2O overnight at $-20\,^{\circ}C$. The stimulation index (S.I.) was calculated as follows:

$$S.I. = \frac{\%IRstim}{\%IRrest} \tag{6.1}$$

where:

$$\%IRstim = \frac{Istim}{Istim + ICstim} \tag{6.2}$$

and

$$\%IRstim = \frac{Irest}{Irest + ICrest} \tag{6.3}$$

with

%IR = % Insulin secreted (in resting or stimulated conditions)

Istim = Secreted insulin in stimulating buffer (ng/ml)

ICstim = Cell insulin content in stimulated cells (ng/ml)

Irest = Secreted insulin in resting buffer (ng/ml)

ICrest = Cell insulin content in resting cells (ng/ml)

The stimulation index from control cells was equaled to 100%.

6.2 Animals

6.2.1 Islets isolation

Pancreatic islets from female Wistar rats, were isolated and cultured (400/60 mm culture dish (BD Falcon^{TM} - BD Biosciences)) as described (257). Briefly, a liberase solution containing 100 μl Liberase RI (Roche Diagnostic GmbH) in 6.5 ml RPMI 1640 was injected in the bile duct. Dissected pancreas was incubated at 37 °C in a water bath shaking every 10 min, for ~26 min. After washing 3 times with cold wash media (RPMI 1640 supplemented with 10% FBS) islets were filtered through a cell dissociation sieve, collecting the flow through. The pellet after centrifugation was resuspended in Histopaque 1077 (Sigma Chemical Co.), applied on a gradient generated by 12 ml Histopaque overlayed by 13-14 ml of cold RPMI 1640, and centrifuged at 2,400 rpm for 20 min at 10 °C in a Heraeus Multifuge KS-R centrifuge (Kendro

- Thermo Electron Corp.). The interface layer was collected, washed with cold RMPI 1640 and resuspended in RPMI 1640 medium supplemented with 20 mM HEPES pH 7.4, 10% heat-inactivated FBS, 100 U/ml penicillin, 100 μg/ml streptomycin. Purified islets were hand picked under a stereomicroscope.

6.2.2 Tissues isolation

Rats were euthanized in agreement with the German Welfare Law and approved by the Government Authority of Saxony. Tissues were excised, flash-freezed in liquid nitrogen and immediately transfered to -80 °C.

6.3 Cell extracts

6.3.1 Triton X-100 soluble fraction

Cells were washed twice with ice cold PBS and sedimented by centrifugation at 1,100 rpm for 6 min at 4 °C in a Heraeus Multifuge centrifuge. Triton X-100 soluble fraction was extracted upon incubation of the cells in 50 μl (for 1 well of a 6-well plate) or 800 μl (for a 175 cm^2 flask, 90% confluent) of lysis buffer (10 mM Tris-HCl pH 8.0, 140 mM NaCl, 1% Triton X-100 (Sigma Chemical Co.), 1mM EDTA, 1mM phenylmethylsulfonyl fluoride (PMSF) (Sigma Chemical Co.), 1% protease inhibitor cocktail (Sigma Chemical Co.)) for 30 min at 4 °C and centrifugation at $25,000 \times$ g for 20 min at 4 °C in a centrifuge 5417R (Eppendorf AG).

Protein concentration was assessed with the Bio-Rad Protein Assay Reagent (Bio-Rad Laboratories) or with the BCA^{TM} protein assay kit (PIERCE Biotechnology, Inc.) using an Ultrospec 3300 Pro spectrophotometer (Amersham Bioscience).

6.3.2 Subcellular fractionation

Two different protocols for subcellular fractionation were applied, to investigate the Rab2 dependent ICA69 membrane recruitment and the β-COP redistribution upon Rab2 or ICA69 over-expression, respectively. According to the first method, cells were washed twice with ice cold PBS, sedimented and resuspended in 1.5 ml (for a 175 cm^2 flask) of homogenization buffer (0.32 M sucrose in 10 mM HEPES pH 7.5, 1% protease inhibitor cocktail). Cells were homogenized with 20 strokes in a ball bearing homogenizer (ball diameter 0.0016 inches, clearance

0.0012 inches) (H. Issel, Inc.). Cell homogenates were centrifuged at $3,000 \times$ g for 10 min at 4 °C in the centrifuge 5417R. 1 ml of the resulting post-nuclear supernatant (PNS) was spun at $150,000 \times$ g for 60 min at 4 °C in an Optima^{TM} MAX Ultracentrifuge (Beckman Coulter, Inc.). High-speed pellets (HSP) were resuspended to the original volume (1 ml) in homogenization buffer. According to the second protocol, described in (236), cells were washed twice with ice cold PBS, sedimented and resuspended in 550 μl (for a 75 cm^2 flask) of homogenization buffer (0.32 M sucrose in 10 mM HEPES pH 7.5, 1% protease inhibitor cocktail). Cells were homogenized with 20 passes of a 27-gauge syringe. Cell homogenates were centrifuged at $500 \times$ g for 10 min at 4 °C in the centrifuge 5417R. 550 μl of the resulting post-nuclear supernatant (PNS) was spun at $20,000 \times$ g for 20 min at 4 °C in the centrifuge 5417R. The pellet (P1) was resuspended in 100 μl of homogenization buffer, and the resulting supernatant was centrifuged at $150,000 \times$ g for 60 min at 4 °C in the Optima^{TM} MAX Ultracentrifuge. The so-obtained pellet (P2) was resuspended in 60 μl of homogenization buffer.

Protein concentration was assessed in both cases with the Bio-Rad Protein Assay Reagent, as indicated above.

6.4 RNA isolation and reverse transcription

Total RNA was isolated from INS-1 cells or from rat tissues using the RNeasy® Mini Kit (QIAGEN, Inc.), following the producer's instructions. Total RNA from different human tissues was purchased (Human Total RNA Master Panel II, BD Biosciences). Reverse transcription was carried out on RNA prepared from INS-1 cells or rat tissues or from human RNA using the SuperScript^{TM} RNaseH$^-$ reverse transcriptase (Invitrogen Corp.), following the manufacturer's recommendations.

6.5 Cloning

6.5.1 Purification of plasmid DNA

Plasmid DNA was purified in large scale (Maxi-prep) and small scale (Mini-prep) using the EndoFree Plasmid Maxi Kit (QIAGEN, Inc.) and the QIAprep® Mini-prep Kit (QIAGEN, Inc.) respectively, following the producer's instructions. The DNA purity and concentration were assessed using a Nanodrop ND1000 spectrophotometer (PeqLab Biotechnologie GmbH).

6.5.2 Restriction enzyme digestion of DNA

Restriction enzyme digestions were performed by incubation the DNA with the appropriate restriction enzyme(s) (NEB), using 5 units of enzyme per μg of DNA for 2-3 hours at 37 °C, unless a different digestion temperature was indicated. After digestion, the resulting DNA fragments were separated by agarose gel electrophoresis.

6.5.3 DNA gel electrophoresis

PCR products, DNA inserts and plasmids were run on a suitable agarose gel, stained with ethidium bromide; images of the gels were acquired with GeneGenius BioImaging system (Syngene - Synoptics Ltd) and quantified, if required, with the GeneSnap software (Syngene - Synoptics Ltd). When necessary, the desired bands were excised from the gel and DNA was isolated using a QIAquick® gel extraction kit (QIAGEN, Inc.) according to the manufacturer's recommendations.

6.5.4 PCR

The typical reaction mixture for PCR was composed of 50 ng template DNA, 100 pmol forward and reverse primers, 200 μM dATP, dCTP, dGTP, dTTP, 1X PCR buffer with $MgCl_2$ and 2 units DNA polymerase in H_2O (50 μl final volume). Taq DNA Polymerase (Roche Diagnostic GmbH), Expand high fidelity PCR system (Roche Diagnostic GmbH) or ThermalAce^{TM} (Invitrogen Corp.) were used according to the different needs of the PCR experiment. PCRs were carried out in the thermal cycler Mastercycler epgradient thermal cycler (Eppendorf AG), and the thermal profile used for the amplification was adjusted in order to obtain a discrete and clean PCR product. PCR products were purified using the QIAquick®gel extraction kit or a QIAquick® PCR purification kit (QIAGEN, Inc.) according to the manufacturer's recommendations.

6.5.5 Ligation of DNA

The typical ligation reaction was composed of 100 ng vector DNA, insert DNA (in a ratio 3:1 to the vector DNA), 1X ligase buffer and 1 μl T4 DNA ligase (Invitrogen Corp.) in H_2O (50 μl final volume); the reaction was carried out overnight (ON) at 16 °C in the thermal cycler.

6.5.6 Transformation of plasmid DNA

Heat shock transformation of XL10 − Gold® Ultracompetent cells (Stratagene) was performed according to the manufacturer's recommendations. Heat shock transformation of BL21 cells was performed as for the XL10-Gold cells, but without addition of β-mercaptoethanol.

6.5.7 Construction of expression vectors

6.5.7.1 pCRII-ICA69-RP

Rat ICA69-RP was amplified from a rat brain 5'-stretch plus cDNA library (Clontech Laboratories, Inc.) using the following primers:
RPfor: 5'-CACCATGGATTCCTTTGAGCACCTC-3'
RPrev: 5'-GGCATTCAGAAGCTCGTCATCTGAG-3'
and the program: 94 °C, 5 min; 5 x (94 °C, 30 seconds (sec) ; 48 °C, 30 sec; 72 °C, 1 min 30 sec); 30 x (94 °C, 30 sec; 57 °C, 30 sec; 72 °C, 1 min 30 sec); 72 °C, 7 min; 4 °C, hold forever. The fresh PCR product was cloned in the pCRII − TOPO® vector, according to the manufacturer's recommendations for the TOPO TA Cloning® kit (Invitrogen Corp.).

6.5.7.2 pEGFP-ICA69-RP

Rat ICA69-RP was amplified from the pCRII-ICA69-RP using the following primers:
RP-GFPfor: 5'-CGAATTCATGGATTCCTTTGAGCACCTCA-3'
RP-GFPrev: 5'-TGGATCCATGGCATTCAGAAGCTCGT-3'
and the program: 94 °C, 3 min; 5 x (94 °C, 30 sec; 48 °C, 30 sec; 72 °C, 1 min 30 sec); 30 x (94 °C, 30 sec; 58 °C, 30 sec; 72 °C, 1 min 30 sec); 72 °C, 7 min; 4 °C, hold forever. The PCR product was digested with EcoRI and BamHI (NEB), gel purified and subcloned in the plasmid pEGFP-N1 (Clontech Laboratories, Inc.) digested with the same enzymes and dephosphorylated with Phosphatase, alkaline (Roche Diagnostic GmbH).

6.5.7.3 pCRII-ICA69

ICA69 was amplified from cDNA retro-transcribed from rat islets (as described above) using the following primers:
ratICAfor: 5'-TCTCGAGATGTCAGGACACAAATGTTATTCC-3'
ratICArev: 5'-ATTGTCGACTCATGCATTGAGCAATTCGTG-3'

and the program: 94 °C, 3 min; 5 x (94 °C, 30 sec; 54 °C, 30 sec; 72 °C, 1 min 30 sec); 30 x (94 °C, 30 sec; 59 °C, 30 sec; 72 °C, 1 min 30 sec); 72 °C, 7 min; 4 °C, hold forever. The fresh PCR product was cloned in the pCRII – TOPO® vector, according to the manufacturer's recommendations of the TOPO TA Cloning® kit.

6.5.7.4 pGEX-ICA69

ICA69 was amplified from the pCRII-ICA69 cDNA using the following primers:
69GSTfor: 5'-TCTCGAGATGTCAGGACACAAATGTTATT-3'
69GSTrev: 5'-TGCGGCCGCTCATGCATTGAGCAATTCGT-3'
and the program: 94 °C, 3 min; 5 x (94 °C, 30 sec; 56 °C, 30 sec; 72 °C, 1 min 30 sec); 30 x (94 °C, 30 sec; 60 °C, 30 sec; 72 °C, 1 min 30 sec); 72 °C, 7 min; 4 °C, hold forever. The PCR product was digested with XhoI and NotI (NEB), gel purified and subcloned in the plasmid pGEX-4T-1 (Amersham Biosciences) digested with the same enzymes and dephosphorylated.

6.5.7.5 pGEX-Amphiphysin1

The cDNA encoding human Amphiphysin1 was excised from the plasmid pcDNA3-HA -Amphiphysin1 (a gift from P. De Camilli, Yale University, New Haven, USA) using the restriction enzymes XbaI and BamHI (NEB). Briefly the plasmid DNA was digested with XbaI, purified using the PCR purification kit, filled in using the ThermalAce polimerase, digested with BamHI, again purified and subcloned in the plasmid pGEX-4T-1 digested with BamHI and SmaI (NEB) and dephosphorylated.

6.5.7.6 pGEX-RPantigen

The term "RPantigen" indicates the region in ICA69-RP which was used as immunogen in order to obtain α-ICA69-RP specific antibodies. RPantigen was amplified from the pCRII-ICA69-RP using the following primers:
antGSTfor: 5'-TGGATCCACTCCAGGCAATCTCACTG-3'
antGSTrev: 5'-CGAATTCTCAATTGAACCAGGCTGACATGT-3'
and the program: 94 °C, 3 min; 5 x (94 °C, 30 sec; 45 °C, 30 sec; 72 °C, 1 min); 30 x (94 °C, 30 sec; 54 °C, 30 sec; 72 °C, 1 min); 72 °C, 7 min; 4 °C, hold forever. The PCR product was digested EcoRI and BamHI (NEB), gel purified and subcloned in the plasmid pGEX-4T-1 digested with the same enzymes and dephosphorylated.

6.5.7.7 pcDNA3.1V5His-ICA69woBAR

ICA69woBAR Rat ICA69-RP indicates the C-terminal domain of ICA69 (missing the first 253 aa). ICA69woBAR was amplified from the pCRII-ICA69 cDNA using the following primers:
69V5for: 5'-CACCATGTCAGGACACAAATGTTATTCC-3'
69stopV5rev: 5'-TCATCATGCATTGAGCAATTCGTGTTCTT-3'
and the program: 94 °C, 3 min; 5 x (94 °C, 30 sec; 55 °C, 30 sec; 72 °C, 1 min 20 sec); 30 x (94 °C, 30 sec; 56 °C, 30 sec; 72 °C, 1 min 20 sec); 72 °C, 10 min; 4 °C, hold forever. The fresh PCR product was cloned in the pcDNA3.1D/V5-His vector, according to the manufacturer's recommendations the pcDNA3.1Directional TOPO Expression kit (Invitrogen Corp.).

6.5.7.8 pcDNA4/HisMAX-ICA69

ICA69 was amplified from the pCRII-ICA69 cDNA using the following primers:
69Maxfor: 5'-ATGTCAGGACACAAATGTTATTCCTGGG-3'
69Maxrev: 5'-TCATCATGCATTGAGCAATTCGTGTTCTTTA-3'
and the program: 94 °C, 3 min; 5 x (94 °C, 30 sec; 48 °C, 30 sec; 72 °C, 1 min 30 sec); 30 x (94 °C, 30 sec; 57 °C, 30 sec; 72 °C, 1 min 30 sec); 72 °C, 7 min; 4 °C, hold forever. The fresh PCR product was cloned in the pCDNA4/HisMAX – TOPO® vector, according to the manufacturer's recommendations for the pCDNA4/HisMAX – TOPO® TOPOTACloning® kit (Invitrogen Corp.).

6.5.8 Preparation of competent BL21

A single colony of *Escherichia Coli* coli BL21 was used to inoculate 10 ml of Luria-Bertani broth (LB medium, (258)) which was grown ON at 37 °C with shaking (200 rpm). The day after the culture was diluted to 100 ml l of LB medium and grown at 37 °C with shaking until an OD_{600} of 0.25 was measured. Cells were quickly cooled down to 4 °C on ice and then collected by centrifugation at 3,500 rpm for 10 min at 4 °C in the Heraeus Multifuge centrifuge; the resulting pellet was gently resuspended in 40 ml of ice cold TfB1 buffer (100 mM RbCl, 50 mM $MnCl_2$, 30 mM K-acetate, 10 mM $CaCl_2$, pH 5.8), spun again by centrifugation, resuspended in 8 ml of TfB2 buffer (10 mM RbCl, 75 mM $CaCl_2$, 10 mM MOPS, pH 6.5, 15% glycerol), incubated for 15 min on ice. 100 μl aliquots were rapidly frozen in liquid nitrogen and stored at −80 °C.

6.6 Tissue expression

10 % of the first-strand reaction obtained by reverse transcription, obtained as described, was used for PCR.

6.6.1 Rat tissues

For ICA69 were used the following primers:
ratICAfor: 5'-TCTCGAGATGTCAGGACACAAATGTTATTCC-3'
ratICArev: 5'-ATTGTCGACTCATGCATTGAGCAATTCGTG-3'
and the program: 94 °C, 3 min; 5 x (94 °C, 30 sec; 50 °C, 30 sec; 72 °C, 1 min 30 sec); 30 x (94 °C, 30 sec; 59 °C, 30 sec; 72 °C, 1 min 30 sec); 72 °C, 7 min; 4 °C, hold forever.

For ICA69-RP were used the following primers:
RPfor: 5'-CACCATGGATTCCTTTGAGCACCTC-3'
RPrev: 5'-GGCATTCAGAAGCTCGTCATCTGAG-3'
and the program: 94 °C, 3 min; 5 x (94 °C, 30 sec; 50 °C, 30 sec; 72 °C, 1 min 30 sec); 30 x (94 °C, 30 sec; 59 °C, 30 sec; 72 °C, 1 min 30 sec); 72 °C, 7 min; 4 °C, hold forever.

For β-actin were used the following primers:
actfor: 5'-ACCCACACTGTGCCCATCTA-3'
actrev: 5'-GCCACAGGATTCCATACCCA-3'
and the program: 94 °C, 3 min; 30 x (94 °C, 30 sec; 55 °C, 30 sec; 72 °C, 45 sec); 72 °C, 7 min; 4 °C, hold forever.

6.6.2 Human tissues

For ICA69-RP were used the following primers:
RPex1for: 5'-TACCCAAGAATGCCAGACTGCC-3'
RPex1rev: 5'-TTGTTGAACGCTCCAGCCAC-3'
or alternatively:
RPex2for: 5'-AATGCCAGACTGCCTTTGGG-3'
RPex1rev: 5'-TTGTTGAACGCTCCAGCCAC-3'
and the program: 94 °C, 3 min; 35 x (94 °C, 30 sec; 56 °C, 30 sec; 72 °C, 45 sec); 72 °C, 7 min; 4 °C, hold forever.

For β-actin were used the following primers:
ACTexfor: 5'-GCACCACACCTTCTACAATGAGC-3'

ACTexrev: 5'-TAGCACAGCCTGGATAGCAACG-3'
and the program: 94 °C, 3 min; 30 x (94 °C, 30 sec; 58 °C, 30 sec; 72 °C, 45 sec); 72 °C, 7 min; 4 °C, hold forever.

6.7 Glucose regulation of ICA69-RP mRNA

10 % of the first-strand reaction obtained by reverse transcription, obtained as described, was used for PCR.

For ICA69-RP were used the following primers:
BARfor: 5'-GATTCCTTTGAGCACCTCAGA-3'
BARrev: 5'-TTGGGACATCATTTGAGCCGTT-3'
and the program: 94 °C, 3 min; 20 x (94 °C, 30 sec; 59 °C, 30 sec; 72 °C, 45 sec); 72 °C, 7 min; 4 °C, hold forever.

For β-actin were used the following primers:
actfor: 5'-ACCCACACTGTGCCCATCTA-3'
actrev: 5'-GCCACAGGATTCCATACCCA-3'
and the program: 94 °C, 3 min; 20 x (94 °C, 30 sec; 55 °C, 30 sec; 72 °C, 45 sec); 72 °C, 7 min; 4 °C, hold forever.

6.8 Immunocytochemistry

Cells grown on coverslips were fixed with 3% paraformaldehyde (PFA) (MERK KGaA) in 120 mM Na-phosphate pH 7.4 for 20 min at 4 °C, washed once with PBS, incubated in quencing buffer (0.1 M glycin in PBS) for 20 min at RT, washed once with PBS, once with low salt (LS) buffer (150 mM NaCl, 10 mM Na-phosphate pH 7.4) and twice with high salt (HS) buffer (1M NaCl, 40 mM Na-phosphate pH 7.4). Unspecific binding sites for the antibody were blocked by incubation in the blocking solution GSDB (16.6% goat serum, 0.1% saponin, 20 mM Na-phosphate pH 7.4, 450 mM NaCl) for 45 min at RT. The cells were then immunostained with the primary antibody (in GSDB) for 2 hours at RT. The following antibodies were used: rabbit α-ICA69 (215) (1:40); mouse α-GM130 (BD Transduction Laboratories) (1:25); α-TGN38 (BD Transduction Laboratories) (1:25); mouse α-β-COP (clone maD) (Sigma Chemical Co.) (1:50); mouse α-CPH (Transduction Laboratories) (1:500); mouse α-Synaptophysin (Synaptic System) (1:1,000); rabbit α-p58 (or ERGIC) (gift from K.Svensson) (233) (1:50). After washing 3

times with HS buffer, cells were incubated with α-mouse or α-rabbit, Alexa488- or Alexa568-conjugated IgGs (Molecular Probes, Inc.) or with concavalin A, Alexa594-conjugated, in GSDB (w/wo DAPI (Sigma Chemical Co.-Aldrich) to counterstain nuclei) for 1 hour at RT, and washed 3 times with HS buffer and twice with 120 mM Na-phosphate and mounted with ProLong Gold antifade reagent (Molecular Probes, Inc.).

Images were acquired with a Zeiss Axioverted 200 M (inverted) confocal microscope (Carl Zeiss, Inc.) and arranged using Adobe Photoshop 7 and Adobe Illustrator CS softwares.

6.9 Immunoprecipitation

Cells were washed twice with ice cold PBS and sedimented by centrifugation in the Heraeus Multifuge centrifuge. The Triton X-100 soluble fraction was extracted by incubating the cells in 800 μl (for a 175 cm^2 flask 90% confluent) of immunoprecipitation (IP) lysis buffer (50 mM Tris-HCl pH 8.0, 150 mM NaCl, 1% Triton X-100, 1% protease inhibitor cocktail) for 30 min at 4 °C and centrifugation at 25,000 × g for 20 min at 4 °C in the centrifuge 5417R. The Triton soluble fraction (750 μg of total protein were used for each IP) was then precleared with 100 μl of 50% ProteinA Sepharose 4 Fast Flow (Amersham Biosciences) or ProteinG Sepharose or 25% ProteinA/25% ProteinG Sepharose[1] in PBS for 1.5 hour at 4 °C with shaking and beads were then sedimented by centrifugation at 500 × g for 6 min at 4 °C in the Heraeus Multifuge centrifuge. A rabbit, mouse, goat or chicken antibody (10 or 20 μg, depending on the antibody) was added to the precleared cell extract and the mixture was then incubated ON at 4 °C, with rocking. The material was then washed 5 times with IP washing buffer (50 mM Tris-HCl pH 7.4, 300 mM NaCl, 0.1% Triton X-100, 5 mM EDTA, 0.02% Na-azide) and once with PBS at 4 °C. Beads were sedimented, bound material was eluted with SDS sample buffer (258) and loaded on SDS-polyacrilamide gel.

6.10 Western blotting

Proteins were separated by 8-12% SDS-polyacrylamide Gel Electrophoresis (SDS-PAGE), transferred to nitrocellulose filters (Schleicher&Schuell BioScience GmbH), at 100 Volt (V) for 2 hours or 40 mA ON, at 4 °C (258). Membranes were blocked with blocking solution (4% non fat dry

[1]The binding strenght of IgGs from various species to Protein G and protein A changes: Protein A and Protein G was used in the IP with rabbit or mouse antibodies, Protein G was used in IP with goat antibodies.

milk (AppliChem GmbH), 0.1% Tween-20 (MERK KGaA) in PBS) for 1 hour at RT, and incubated with the primary antibody (in 3% Albumin fraction V (Carl Roth GmbH), 0.1% Tween-20, 0.02% Na-azide in PBS) for 2 hours at RT or ON at 4 °C. The following antibodies were used: rabbit α-ICA69 (226) (1:500); mouse α-ICA69 (1:150) (226); rabbit α-ICA69-RP (described in section 6.13) (1:500); chicken α-ICA69-RP (GenWay Biotech, Inc.) (1:500); mouse α-GM130 (BD Transduction Laboratories) (1:250); goat α-GFP (Protein Expression Facility / MPI-CBG, Dresden) (1:3,000); mouse α-GFP (Clontech Laboratories, Inc.) (1:1,000); rabbit α-GST (Molecular Probes, Inc.) (1:2,000); mouse α-γ-tubulin (Sigma Chemical Co.) (1:5,000); mouse α-Rabaptin4 (gift from M.Zerial) (1:1,000); mouse α-EEA1 (Transduction Laboratories) (1:2500); mouse α-ICA512 (259) (1:75). After washing 3 times with the blocking solution, membranes were incubated with α-mouse or α-rabbit (Bio-Rad Laboratories) or α-goat (Sigma Chemical Co.) or α-chicken (Jackson Immuno Research Laboratories, Inc.), horseradish-peroxidase-coniugated (HRP-conjugated) IgGs in the blocking solution for 1 hour at RT, washed twice with 0.1% Tween-20 in PBS and once with PBS.

Protein signals were detected by chemiluminescence with the Supersignal West Pico Substrate (PIERCE Biotechnology, Inc.) or the Supersignal West Fempto Maximum Sensitivity Substrate (PIERCE Biotechnology, Inc.) using a LAS-3000 Bioimaging System (Fuji) and quantified with the Image Gauge v3.45 software (Fuji). Protein gels images were arranged using Adobe Photoshop 7 and Adobe Illustrator CS softwares.

6.11 Expression of GST fusion proteins

Escherichia Coli cells, strain BL21, were transformed with the corresponding construct designed to express a GST fusion proteins. A single colony was used to inoculate 50 ml of LB medium (plus ampicillin 100 μg/ml) which was grown ON at 37 °C with shaking. The day after the culture was diluted to 1 l of LB medium plus ampicillin and grown at 37 °C with shaking until an OD_{600} of 0.75, as measured in the spectrophotometer. Induction of GST-fusion protein expression was achieved by adding 0.5 mM final concentration of isopropyl-β-D-thiogalactopyranoside (IPTG) (Sigma Chemical Co.) to the culture and incubating for 3 additional hours at 30 °C with shaking. The cells were sedimented by centrifugation at 4,400 rpm for 20 min at 4 °C in the Heraeus Multifuge centrifuge and then resuspended in 50 ml of PBS, containing 1% protease inhibitor cocktail. The cell suspenction was sonicated 5×20 sec with a 550 Sonic dismembrator (Fisher Scientific International, Inc.) and further homogenized with Triton X-100

(Sigma Chemical Co.) for 30 min at 4 °C. The lysates were spun at 12,000 rpm for 30 min at 4 °C in an Avanti^{TM} J20 (Beckman Coulter, Inc.) using a JA-25.50 rotor. The supernatant was incubated with 1 ml of 50 % Glutathione Sepharose 4B (Amersham Biosciences) slurry, pre-equilibrated with PBS, for 1.5 hours at 4 °C with rocking. Beads were sedimented by centrifugation at 500 × g for 6 min at 4 °C in the Heraeus Multifuge centrifuge and washed 3 times with 10 beads volume ice-cold 0.1% Triton X-100 in PBS. Bound proteins were eluted from the beads with 1.5 ml elution buffer (25 mM glutathione (Sigma Chemical Co.), 50 mM NaCl, 100 mM TRIS-HCl pH 8.0) (3 elution steps using 0.5 ml elution buffer, incubated for 15 min with the beads, followed by sedimentation of the beads and recovery of the supernatant). The protein solution was then dialyzed against PBS using Amicon Ultra centrifugal filter devices (Millipore Corp.) with the appropriate molecular weight cut off (MWCO) .

The purity of the GST fusion protein was assessed by staining SDS-polyacrilamide gels with Coomassie Brillant Blue R-250 (Bio-Rad Laboratories) (258).

6.12 GST pull down assay

75 μg of GST fusion protein (or GST) were used for each pull down assay. The GST fusion protein was incubated with 100 μl of 50 % Glutathione Sepharose 4B in PBS for 1.5 hours at 4 °C with shaking; beads were sedimented by centrifugation at 500 × g for 6 min at 4 °C in the centrifuge 5417R and washed once with 10 beads volume ice-cold 0.1% Triton X-100 in PBS. To determine the yield of the procedure, the bound GST fusion protein was eluted with SDS sample buffer containing dithiothreitol (DTT) (New England Biolabs, Inc.-NEB) (258). 1/20 of the eluted material was loaded on SDS-polyacrilamide gel and compared by Coomassie Brillant Blue staining of the gel with the GST fusion protein used to load the beads (1/20 of the amount of protein used to load the beads). The GST fusion protein immobilized with the beads was then loaded with GTPγS (or GDP), as described in (245). Briefly, the material was washed with 500 μl of nucleotide exchange buffer (NE buffer) containing 20 mM HEPES, 100 mM NaCl, 10 mM EDTA, 5 mM $MgCl_2$, 1 mM DTT, 10 μM GTPγS (Guanosine-5'-O-(3-thiotriphosphate)Tetralitium salt) (Sigma Chemical Co.) (or GDP (Guanosine-5'-diphosphate sodium salt) (Sigma Chemical Co.)), pH 7.5, and then incubated with 200 μl NE buffer containing 1 mM GTPγS (or GDP) for 30 min at RT under rotation. Afterwards, NE buffer was removed and the wash and incubation procedure described above was repeated once more. The material was then washed with 500 μl of nucleotide stabilization buffer (NS buffer) containing

20 mM HEPES, 100 mM NaCl, 5 mM $MgCl_2$, 1 mM DTT, 10 μM GTPγS (or GDP), pH 7.5, and further incubated with 100 μl NS buffer containing 1 mM GTPγS (or GDP) for 20 min at RT under rotation.

Triton X-100 soluble fractions of INS-1 cells were prepared as described above. The cell extract was then dialyzed against NS buffer in the absence of the nucleotide, precleared with 200 μl of 50 % Glutathione Sepharose 4B in PBS for 45 min at 4 °C with rocking, and then quantified as described above. 750 μg of total protein were used for each pull down.

GST fusion protein immobilized to the beads were incubated with the cell extracts for 10 hours at 4 °C with rocking in presence of 100 μM GTPγS (or GDP). The material was then washed with 500 μl of NS buffer containing 10 μM GTPγS (or GDP), 500 μl of NS buffer containing 250 mM NaCl final concentration and 10 μM GTPγS (or GDP), and then with 200 μl wash buffer 3 containing 20 mM HEPES, 250 mM NaCl, 1 mM DTT, pH 7.5. Beads were sedimented, bound material was eluted with SDS sample buffer (258) and loaded on SDS-polyacrilamide gel.

When GST alone was used for the pull down assay, the material was prepared exactly as described above, but neither GTPγS nor GDP were present in the buffers.

6.13 Production of an α-ICA69-RP antibody

RPantigen-GST was expressed in BL21 as described above and dialized against PBS. 3.3 mg of RPantigen were sent to Eurogentec (EGT Group) in order to immunize 2 rabbits, with 100 μg antigen per injection and per animal. The standard protocol offered by Eurogentec was applied; briefly: 1 ml volume per injection (500 μl antigen solution, 500 μl adjuvant); injections: days 0, 14, 28, $28 + n28$ (with n = 1, 2, 3 ...) (standard injection way: intradermic multisite); bleedings: days 0 (preimmune, 2 ml), 38 (2 ml), 53 (20 ml), $53 + n15$ (20 ml) ... day 320 final bleeding. The bleeds were tested by ICC and WB and purified by affinity chromatography. The chromatographic column was loaded with RPantigen, obtained from RPantigen-GST still loaded on the Glutathione Sepharose 4B (see above) after cleavage for 16 hours at RT with 100 units of Thrombin Protease (Amersham Biosciences). Thrombin was then removed using an HiTrap Benzamidine FF (high sub) column (Amersham Biosciences). The affinity chromatography was performed using an AminoLink® kit (PIERCE Biotechnology, Inc.) according to the manufacturer's recommendations. The fractions of interest, as assessed by reading their absorbance at 280 nm, were pooled and dialyzed against 0.02 % Na-azide in

PBS using a Slide-A-Lyzer® Dialysis Cassette (PIERCE Biotechnology, Inc.), 3.5 MWCO. The antibody was then aliquoted and stored at 4 °C.

6.14 Protein-lipid overlay assay

Phospolipid-spotted nitrocellulose membranes (PIP strips, Molecular Probes, Inc.) were blocked in 3% Albumin fraction V in 10 mM Tris-HCl pH 8.0, 150 mM NaCl, 0.1% Tween-20 (TBS-T). The membranes were incubated with 1 μg/ml GST, ICA69-GST or Amphyphisyn-GST in the blocking solution ON at 4 °C. The day after membranes were washed 3 times with the blocking solution. Thereafter the detection of bound proteins was performed by western blotting, as indicated above, using a rabbit α-GST (Molecular Probes, Inc.) (1:2,000).

6.15 Sequence alignment

Multiple sequence alignment and genealogical tree were produced with the program ClustalW (http://www.ebi.ac.uk/clustalw/); the alignments were manually refined manually.

Appendix A

ICA69 and ICA69-RP family: sequence alignment

Multiple sequence alignment (on the next page) of ICA69 protein family in humans, mice and rats, generated using ClustalW, a multiple sequence alignment program, at the European Bioinformatic institute (EBI). The BAR domain encompasses the region at the N-terminus, where the three helixes are positioned. The cyan rectangles (both at the C-terminus and at the N-terminus) indicate regions of high homology within the family members. Colors-code: red: small; blue: acidic; magenta: basic; green: Hydroxyl + Amine + Basic - Q. At the bottom of the sequence, "$\star$" indicates residues identical in all the sequences in the alignment; ":" indicates conserved substitution, according to the colors-code indicated above; "." indicates a semi-conserved substitution. Accession numbers (NCBI): *H.sapiens* ICA69: NP_071682.1; *M.musculus* ICA69: NP_034622.2; *R.norvegicus* ICA69: NP_110471.1; *H.sapiens* ICA69-RP: NP_612477.3; *M.musculus* ICA69-RP: NP_081683.2; *R.norvegicus* ICA69-RP.

Figure A.1: **ICA69 and ICA69-RP family: sequence alignment**

Appendix B

Antibodies

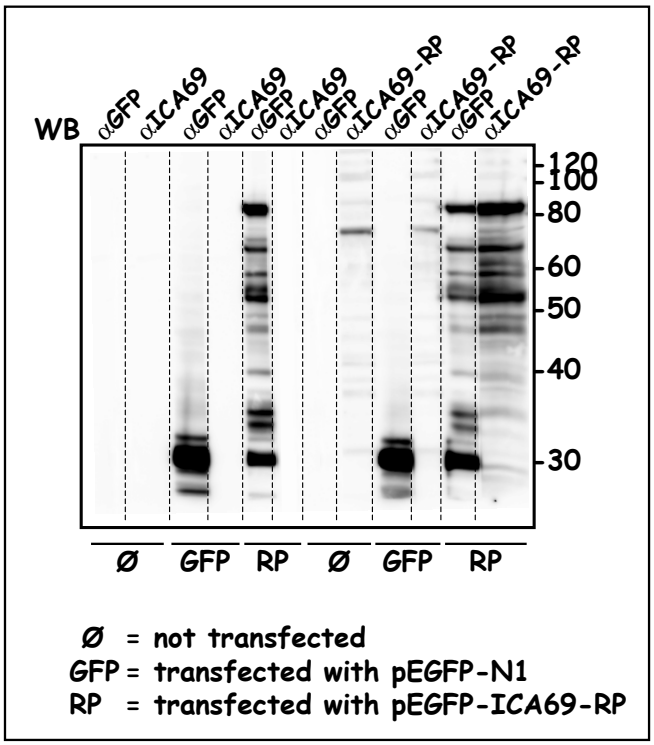

Figure B.1: **Specificity of the α-ICA69 antibody**

As a strong homology at the protein level exists between ICA69 and ICA69-RP, it was possible that the antibodies against ICA69 did crossreact with ICA69-RP. To test this hypothesis

Triton X-100 soluble fraction was prepared from HEK cells and HEK cells overexpressing GFP or ICA69-RP-GFP, followed by SDS/PAGE and western blotting with the antibodies indicated in Fig. B.1, on the top. The α-ICA69 antibody does not detect the endogenous ICA69 (Fig. B.1, lanes 2 and 4), as in this cell line the amount of the protein is negligible (215). The same antibody does not recognize ICA69-RP-GFP (Fig. B.1, lane 6), which is instead recognized by both the α-GFP and α-ICA69-RP antibodies (Fig. B.1, lanes 11 and 12). Therefore the polyclonal antibody against ICA69 does not crossreact with ICA69-RP. The figure is relative to the polyclonal α-ICA69, which was raised against residues 471-483 of human ICA69. Identical results were obtained with a monoclonal antibody, which recognize an epitope in the first 230 amino acids of human ICA69.

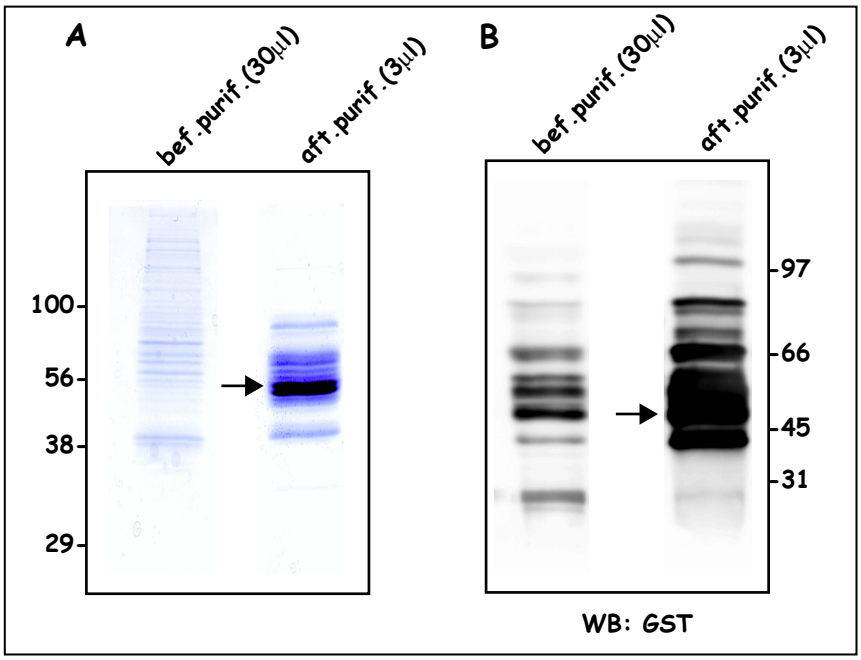

Figure B.2: **Purification of ICA69-RP-antigen in fusion with GST**

In order to obtain α-ICA69-RP specific antibodies a construct expressing a fusion protein between GST and the amino acids 266-402 of ICA69-RP (and termed ICA69-RP-antigen) was generated. The construct was expressed in bacteria and the corresponding GST-fusion protein purified. Fig. B.2 A shows a Comassie Brillant Blue-stained protein gel for bacterial extracts in which the expression of ICA69-RP-antigen has been induced (lane 1) and ICA69-RP-antigen after purification and dialysis (lane 2). Fig. B.2 B shows a western blotting, on an identical gel,

obtained with an α-GST antibody. The arrows point, in both cases, to the expected molecular weight of 45 kDa.

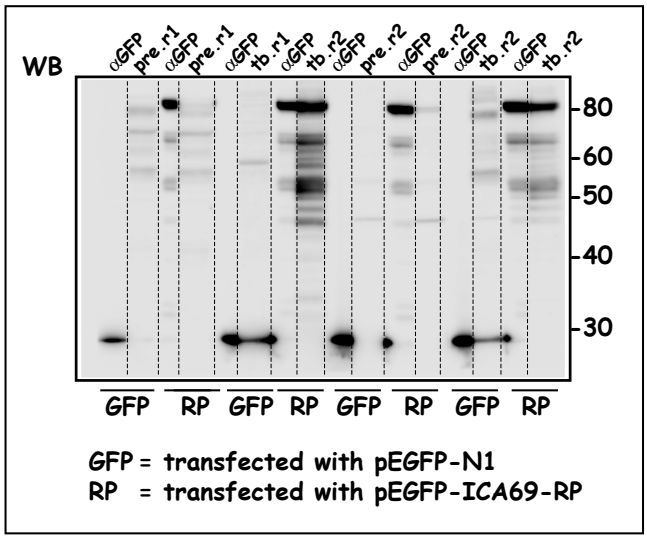

Figure B.3: **Specificity of sera for ICA69-RP**

In the production of α-ICA69-RP specific antibodies, the reactivity of the crude rabbit antisera was tested by evaluating its reactivity against a fusion protein between ICA69-RP and the green fluorescent protein (GFP). Fig. B.3 shows a western blotting on HEK cells Triton X-100 soluble fractions with an α-GFP antibody, with preimmune serum from two different rabbits (indicated as pre.r1 and pre.r2, respectively), or with serum from the same rabbits after immunization against the ICA69-RP-antigen; the cells were either transfected with pEGFP-N1, as a negative control, or with pEGFP-ICA69-RP. ICA69-RP-GFP is detected at the expected molecular weight of $\sim$80 kDa protein, with the α-GFP antibody and with the sera from the immunized rabbits, but not with the pre-immune sera from the same animals.

References

[1] G. Palade. Intracellular aspects of the process of protein synthesis. *Science*, 189(4200):347–58, 1975. 0036-8075 (Print) Journal Article Review. 1

[2] C. Duve. Exploring cells with a centrifuge. *Science*, 189(4198):186–94, 1975. 1

[3] P. Novick, S. Ferro, and R. Schekman. Order of events in the yeast secretory pathway. *Cell*, 25(2):461–9, 1981. 0092-8674 (Print) Journal Article. 1

[4] W. E. Balch, W. G. Dunphy, W. A. Braell, and J. E. Rothman. Reconstitution of the transport of protein between successive compartments of the golgi measured by the coupled incorporation of n-acetylglucosamine. *Cell*, 39(2 Pt 1):405–16, 1984. 0092-8674 (Print) Journal Article. 1

[5] J. S. Bonifacino and B. S. Glick. The mechanisms of vesicle budding and fusion. *Cell*, 116(2):153–66, 2004. 0092-8674 (Print) Comment Journal Article Review. 2, 3, 7

[6] J. E. Rothman and F. T. Wieland. Protein sorting by transport vesicles. *Science*, 272(5259):227–34, 1996. 0036-8075 (Print) Journal Article Review. 3

[7] R. Sannerud, J. Saraste, and B. Goud. Retrograde traffic in the biosynthetic-secretory route: pathways and machinery. *Curr Opin Cell Biol*, 15(4):438–45, 2003. 0955-0674 (Print) Journal Article Review. 3

[8] J. E. Rothman. Lasker basic medical research award. the machinery and principles of vesicle transport in the cell. *Nat Med*, 8(10):1059–62, 2002. 1078-8956 (Print) Biography Historical Article Journal Article. 3

[9] H. R. Pelham. Recycling of proteins between the endoplasmic reticulum and golgi complex. *Curr Opin Cell Biol*, 3(4):585–91, 1991. 0955-0674 (Print) Journal Article Review. 3

[10] J. S. Bonifacino and J. Lippincott-Schwartz. Coat proteins: shaping membrane transport. *Nat Rev Mol Cell Biol*, 4(5):409–14, 2003. 1471-0072 (Print) Journal Article Review. 2, 3, 6, 9, 14

[11] A. Luini, A. Ragnini-Wilson, R. S. Polishchuck, and M. A. De Matteis. Large pleiomorphic traffic intermediates in the secretory pathway. *Curr Opin Cell Biol*, 17(4):353–61, 2005. 0955-0674 (Print) Journal Article Review. 3

[12] J. C. Stinchcombe, H. Nomoto, D. F. Cutler, and C. R. Hopkins. Anterograde and retrograde traffic between the rough endoplasmic reticulum and the golgi complex. *J Cell Biol*, 131(6 Pt 1):1387–401, 1995. 0021-9525 (Print) Journal Article. 3

[13] K. Hirschberg, C. M. Miller, J. Ellenberg, J. F. Presley, E. D. Siggia, R. D. Phair, and J. Lippincott-Schwartz. Kinetic analysis of secretory protein traffic and characterization of golgi to plasma membrane transport intermediates in living cells. *J Cell Biol*, 143(6):1485–503, 1998. 0021-9525 (Print) Journal Article. 3

[14] J. Gruenberg and F. R. Maxfield. Membrane transport in the endocytic pathway. *Curr Opin Cell Biol*, 7(4):552–63, 1995. 0955-0674 (Print) Journal Article Review. 3

[15] A. E. Johnson and M. A. van Waes. The translocon: a dynamic gateway at the er membrane. *Annu Rev Cell Dev Biol*, 15:799–842, 1999. 1081-0706 (Print) Journal Article Review. 4

[16] T. A. Rapoport, B. Jungnickel, and U. Kutay. Protein transport across the eukaryotic endoplasmic reticulum and bacterial inner membranes. *Annu Rev Biochem*, 65:271–303, 1996. 0066-4154 (Print) Journal Article Review. 4

[17] N. Borgese, S. Brambillasca, P. Soffientini, M. Yabal, and M. Makarow. Biogenesis of tail-anchored proteins. *Biochem Soc Trans*, 31(Pt 6):1238–42, 2003. 0300-5127 (Print) Journal Article Review. 4

[18] C. Hammond and A. Helenius. Quality control in the secretory pathway. *Curr Opin Cell Biol*, 7(4):523–9, 1995. 0955-0674 (Print) Journal Article Review. 4

[19] R. Kornfeld and S. Kornfeld. Assembly of asparagine-linked oligosaccharides. *Annu Rev Biochem*, 54:631–64, 1985. 0066-4154 (Print) Journal Article Review. 4

[20] S. I. Bannykh, T. Rowe, and W. E. Balch. The organization of endoplasmic reticulum export complexes. *J Cell Biol*, 135(1):19–35, 1996. 0021-9525 (Print) Journal Article. 4

[21] J. Klumperman, A. Schweizer, H. Clausen, B. L. Tang, W. Hong, V. Oorschot, and H. P. Hauri. The recycling pathway of protein ergic-53 and dynamics of the er-golgi intermediate compartment. *J Cell Sci*, 111 (Pt 22):3411–25, 1998. 0021-9533 (Print) Journal Article. 4

[22] W. E. Balch, J. M. McCaffery, H. Plutner, and M. G. Farquhar. Vesicular stomatitis virus glycoprotein is sorted and concentrated during export from the endoplasmic reticulum. *Cell*, 76(5):841–52, 1994. 0092-8674 (Print) Journal Article. 4

[23] J. F. Presley, N. B. Cole, T. A. Schroer, K. Hirschberg, K. J. Zaal, and J. Lippincott-Schwartz. Er-to-golgi transport visualized in living cells. *Nature*, 389(6646):81–5, 1997. 0028-0836 (Print) Journal Article. 4

[24] A. Murshid and J. F. Presley. Er-to-golgi transport and cytoskeletal interactions in animal cells. *Cell Mol Life Sci*, 61(2):133–45, 2004. 1420-682X (Print) Journal Article Review. 4, 17

[25] A. Schweizer, K. Matter, C. M. Ketcham, and H. P. Hauri. The isolated er-golgi intermediate compartment exhibits properties that are different from er and cis-golgi. *J Cell Biol*, 113(1):45–54, 1991. 0021-9525 (Print) Journal Article. 4

[26] R. Sitia and J. Meldolesi. Endoplasmic reticulum: a dynamic patchwork of specialized subregions. *Mol Biol Cell*, 3(10):1067–72, 1992. 1059-1524 (Print) Journal Article Review. 4

[27] I. Mellman and K. Simons. The golgi complex: in vitro veritas? *Cell*, 68(5):829–40, 1992. 0092-8674 (Print) Journal Article Review. 4

[28] J. Lippincott-Schwartz. Bidirectional membrane traffic between the endoplasmic reticulum and golgi apparatus. *Trends Cell Biol*, 3(3):81–8, 1993. 0962-8924 (Print) Journal Article. 5

[29] H. R. Pelham. Control of protein exit from the endoplasmic reticulum. *Annu Rev Cell Biol*, 5:1–23, 1989. 0743-4634 (Print) Journal Article Review. 5

[30] C. Appenzeller-Herzog and H. P. Hauri. The er-golgi intermediate compartment (ergic): in search of its identity and function. *J Cell Sci*, 119(Pt 11):2173–83, 2006. 0021-9533 (Print) Journal Article. 5, 12, 17, 50, 86

[31] M. G. Farquhar and G. E. Palade. The golgi apparatus: 100 years of progress and controversy. *Trends Cell Biol*, 8(1):2–10, 1998. 0962-8924 (Print) Biography Historical Article Journal Article Review. 5

[32] N. B. Cole, N. Sciaky, A. Marotta, J. Song, and J. Lippincott-Schwartz. Golgi dispersal during microtubule disruption: regeneration of golgi stacks at peripheral endoplasmic reticulum exit sites. *Mol Biol Cell*, 7(4):631–50, 1996. 1059-1524 (Print) Journal Article. 5

[33] J. Seemann, E. Jokitalo, M. Pypaert, and G. Warren. Matrix proteins can generate the higher order architecture of the golgi apparatus. *Nature*, 407(6807):1022–6, 2000. 0028-0836 (Print) Journal Article. 5

[34] L. Orci, B. S. Glick, and J. E. Rothman. A new type of coated vesicular carrier that appears not to contain clathrin: its possible role in protein transport within the golgi stack. *Cell*, 46(2):171–84, 1986. 0092-8674 (Print) Journal Article. 5

[35] C. P. Leblond. Synthesis and secretion of collagen by cells of connective tissue, bone, and dentin. *Anat Rec*, 224(2):123–38, 1989. 0003-276X (Print) Journal Article Review. 5

[36] L. Bonfanti, Jr. Mironov, A. A., J. A. Martinez-Menarguez, O. Martella, A. Fusella, M. Baldassarre, R. Buccione, H. J. Geuze, A. A. Mironov, and A. Luini. Procollagen traverses the golgi stack without leaving the lumen of cisternae: evidence for cisternal maturation. *Cell*, 95(7):993–1003, 1998. 0092-8674 (Print) Journal Article. 5

[37] H. R. Pelham and J. E. Rothman. The debate about transport in the golgi–two sides of the same coin? *Cell*, 102(6):713–9, 2000. 0092-8674 (Print) Journal Article Review. 5

[38] G. Griffiths and K. Simons. The trans golgi network: sorting at the exit site of the golgi complex. *Science*, 234(4775):438–43, 1986. 0036-8075 (Print) Journal Article Review. 5

[39] H. J. Geuze, J. W. Slot, G. J. Strous, A. Hasilik, and K. von Figura. Possible pathways for lysosomal enzyme delivery. *J Cell Biol*, 101(6):2253–62, 1985. 0021-9525 (Print) Journal Article. 5

[40] L. M. Traub and S. Kornfeld. The trans-golgi network: a late secretory sorting station. *Curr Opin Cell Biol*, 9(4):527–33, 1997. 0955-0674 (Print) Journal Article Review. 6

[41] J. Lippincott-Schwartz, T. H. Roberts, and K. Hirschberg. Secretory protein trafficking and organelle dynamics in living cells. *Annu Rev Cell Dev Biol*, 16:557–89, 2000. 1081-0706 (Print) Journal Article Review. 6, 12

[42] B. M. Pearse. Coated vesicles from pig brain: purification and biochemical characterization. *J Mol Biol*, 97(1):93–8, 1975. 0022-2836 (Print) Journal Article. 7

[43] R. Schekman and L. Orci. Coat proteins and vesicle budding. *Science*, 271(5255):1526–33, 1996. 0036-8075 (Print) Journal Article Review. 7

[44] T. Kirchhausen. Three ways to make a vesicle. *Nat Rev Mol Cell Biol*, 1(3):187–98, 2000. 1471-0072 (Print) Journal Article Review. 7, 8, 11, 12, 13

[45] B. M. Pearse. Receptors compete for adaptors found in plasma membrane coated pits. *Embo J*, 7(11):3331–6, 1988. 0261-4189 (Print) Journal Article. 9

[46] J. L. Carpentier, J. P. Paccaud, P. Gorden, W. J. Rutter, and L. Orci. Insulin-induced surface redistribution regulates internalization of the insulin receptor and requires its autophosphorylation. *Proc Natl Acad Sci U S A*, 89(1):162–6, 1992. 0027-8424 (Print) Journal Article. 9

[47] P. Wigge, K. Kohler, Y. Vallis, C. A. Doyle, D. Owen, S. P. Hunt, and H. T. McMahon. Amphiphysin heterodimers: potential role in clathrin-mediated endocytosis. *Mol Biol Cell*, 8(10):2003–15, 1997. 1059-1524 (Print) Journal Article. 9

[48] B. J. Peter, H. M. Kent, I. G. Mills, Y. Vallis, P. J. Butler, P. R. Evans, and H. T. McMahon. Bar domains as sensors of membrane curvature: the amphiphysin bar structure. *Science*, 303(5657):495–9, 2004. 1095-9203 (Electronic) Journal Article. 9, 23, 24, 83, 85, 88, 89

[49] M. G. Ford, I. G. Mills, B. J. Peter, Y. Vallis, G. J. Praefcke, P. R. Evans, and H. T. McMahon. Curvature of clathrin-coated pits driven by epsin. *Nature*, 419(6905):361–6, 2002. 0028-0836 (Print) Journal Article. 9

[50] J. L. Gallop, C. C. Jao, H. M. Kent, P. J. Butler, P. R. Evans, R. Langen, and H. T. McMahon. Mechanism of endophilin n-bar domain-mediated membrane curvature. *Embo J*, 25(12):2898–910, 2006. 0261-4189 (Print) Journal Article. 9, 89

[51] O. Cremona, G. Di Paolo, M. R. Wenk, A. Luthi, W. T. Kim, K. Takei, L. Daniell, Y. Nemoto, S. B. Shears, R. A. Flavell, D. A. McCormick, and P. De Camilli. Essential role of phosphoinositide metabolism in synaptic vesicle recycling. *Cell*, 99(2):179–88, 1999. 0092-8674 (Print) Journal Article. 9

[52] S. M. Sweitzer and J. E. Hinshaw. Dynamin undergoes a gtp-dependent conformational change causing vesiculation. *Cell*, 93(6):1021–9, 1998. 0092-8674 (Print) Journal Article. 9

[53] T. Kirchhausen. Cell biology. boa constrictor or rattlesnake? *Nature*, 398(6727):470–1, 1999. 0028-0836 (Print) Comment News. 9

[54] A. Roux, K. Uyhazi, A. Frost, and P. De Camilli. Gtp-dependent twisting of dynamin implicates constriction and tension in membrane fission. *Nature*, 441(7092):528–31, 2006. 1476-4687 (Electronic) Journal Article. 9

[55] R. Puertollano, N. N. van der Wel, L. E. Greene, E. Eisenberg, P. J. Peters, and J. S. Bonifacino. Morphology and dynamics of clathrin/gga1-coated carriers budding from the trans-golgi network. *Mol Biol Cell*, 14(4):1545–57, 2003. 1059-1524 (Print) Journal Article. 9

[56] V. Malhotra, T. Serafini, L. Orci, J. C. Shepherd, and J. E. Rothman. Purification of a novel class of coated vesicles mediating biosynthetic protein transport through the golgi stack. *Cell*, 58(2):329–36, 1989. 0092-8674 (Print) Journal Article. 10

[57] R. Pepperkok, J. Scheel, H. Horstmann, H. P. Hauri, G. Griffiths, and T. E. Kreis. Beta-cop is essential for biosynthetic membrane transport from the endoplasmic reticulum to the golgi complex in vivo. *Cell*, 74(1):71–82, 1993. 0092-8674 (Print) Journal Article. 10

[58] A. Alberts, A. Johnson, J. Lewis, M. Raff, K. Roberts, and P. Walter. Molecular biology of the cell, fourth edition. *Book*, 2002. 10, 27, 31, 33

[59] W Nickel and B Brgger. Copi-mediated protein and lipid sorting in the early secretory pathway. *Protoplasma*, 207:115–24, 1999. 12

[60] R. Duden. Er-to-golgi transport: Cop i and cop ii function (review). *Mol Membr Biol*, 20(3):197–207, 2003. 0968-7688 (Print) Journal Article Review. 12, 14

[61] E. J. Tisdale, J. R. Bourne, R. Khosravi-Far, C. J. Der, and W. E. Balch. Gtp-binding mutants of rab1 and rab2 are potent inhibitors of vesicular transport from the endoplasmic reticulum to the golgi complex. *J Cell Biol*, 119(4):749–61, 1992. 0021-9525 (Print) Journal Article. 12, 53

[62] E. J. Tisdale and W. E. Balch. Rab2 is essential for the maturation of pre-golgi intermediates. *J Biol Chem*, 271(46):29372–9, 1996. 0021-9258 (Print) Journal Article. 12, 67, 86, 90

[63] E. J. Tisdale. Rab2 requires pkc iota/lambda to recruit beta-cop for vesicle formation. *Traffic*, 1(9):702–12, 2000. 1398-9219 (Print) Journal Article. 12, 20, 50, 55, 86, 88

[64] M. C. Lee, E. A. Miller, J. Goldberg, L. Orci, and R. Schekman. Bi-directional protein transport between the er and golgi. *Annu Rev Cell Dev Biol*, 20:87–123, 2004. 1081-0706 (Print) Journal Article Review. 12

[65] C. Kaiser. Thinking about p24 proteins and how transport vesicles select their cargo. *Proc Natl Acad Sci U S A*, 97(8):3783–5, 2000. 0027-8424 (Print) Comment Journal Article. 12

[66] J. Lanoix, J. Ouwendijk, A. Stark, E. Szafer, D. Cassel, K. Dejgaard, M. Weiss, and T. Nilsson. Sorting of golgi resident proteins into different subpopulations of copi vesicles: a role for arfgap1. *J Cell Biol*, 155(7):1199–212, 2001. 0021-9525 (Print) Journal Article. 12

[67] P. Novick, C. Field, and R. Schekman. Identification of 23 complementation groups required for post-translational events in the yeast secretory pathway. *Cell*, 21(1):205–15, 1980. 0092-8674 (Print) Journal Article. 12

[68] D. Baker, L. Hicke, M. Rexach, M. Schleyer, and R. Schekman. Reconstitution of sec gene product-dependent intercompartmental protein transport. *Cell*, 54(3):335–44, 1988. 0092-8674 (Print) Journal Article. 14

[69] C. Barlowe, L. Orci, T. Yeung, M. Hosobuchi, S. Hamamoto, N. Salama, M. F. Rexach, M. Ravazzola, M. Amherdt, and R. Schekman. Copii: a membrane coat formed by sec proteins that drive vesicle budding from the endoplasmic reticulum. *Cell*, 77(6):895–907, 1994. 0092-8674 (Print) Journal Article. 14, 90

[70] R. Peng, A. De Antoni, and D. Gallwitz. Evidence for overlapping and distinct functions in protein transport of coat protein sec24p family members. *J Biol Chem*, 275(15):11521–8, 2000. 0021-9258 (Print) Journal Article. 14

[71] T. Kirchhausen. Clathrin adaptors really adapt. *Cell*, 109(4):413–6, 2002. 0092-8674 (Print) Journal Article Review. 14

[72] W. M. Rohn, Y. Rouille, S. Waguri, and B. Hoflack. Bi-directional trafficking between the trans-golgi network and the endosomal/lysosomal system. *J Cell Sci*, 113 (Pt 12):2093–101, 2000. 0021-9533 (Print) Journal Article. 14

[73] J. Hirst, N. A. Bright, B. Rous, and M. S. Robinson. Characterization of a fourth adaptor-related protein complex. *Mol Biol Cell*, 10(8):2787–802, 1999. 1059-1524 (Print) Journal Article. 14

[74] A. L. Boman. Gga proteins: new players in the sorting game. *J Cell Sci*, 114(Pt 19):3413–8, 2001. 0021-9533 (Print) Journal Article Review. 14

[75] W. E. Miller and R. J. Lefkowitz. Expanding roles for beta-arrestins as scaffolds and adapters in gpcr signaling and trafficking. *Curr Opin Cell Biol*, 13(2):139–45, 2001. 0955-0674 (Print) Journal Article Review. 14

[76] M. Boehm and J. S. Bonifacino. Adaptins: the final recount. *Mol Biol Cell*, 12(10):2907–20, 2001. 1059-1524 (Print) Journal Article. 15

[77] R. N. Collins. Rab and arf gtpase regulation of exocytosis. *Mol Membr Biol*, 20(2):105–15, 2003. 0968-7688 (Print) Journal Article Review. 15, 19

[78] Z. Nie, D. S. Hirsch, and P. A. Randazzo. Arf and its many interactors. *Curr Opin Cell Biol*, 15(4):396–404, 2003. 0955-0674 (Print) Journal Article Review. 15

[79] C. D'Souza-Schorey and P. Chavrier. Arf proteins: roles in membrane traffic and beyond. *Nat Rev Mol Cell Biol*, 7(5):347–58, 2006. 1471-0072 (Print) Journal Article Review. 15

[80] O. Kuge, C. Dascher, L. Orci, T. Rowe, M. Amherdt, H. Plutner, M. Ravazzola, G. Tanigawa, J. E. Rothman, and W. E. Balch. Sar1 promotes vesicle budding from the endoplasmic reticulum but not golgi compartments. *J Cell Biol*, 125(1):51–65, 1994. 0021-9525 (Print) Journal Article. 15

[81] C. G. Burd, T. I. Strochlic, and S. R. Gangi Setty. Arf-like gtpases: not so arf-like after all. *Trends Cell Biol*, 14(12):687–94, 2004. 0962-8924 (Print) Journal Article Review. 15

[82] A. Kamal and L. S. Goldstein. Connecting vesicle transport to the cytoskeleton. *Curr Opin Cell Biol*, 12(4):503–8, 2000. 0955-0674 (Print) Journal Article Review. 15, 17

[83] J. Lippincott-Schwartz, N. B. Cole, A. Marotta, P. A. Conrad, and G. S. Bloom. Kinesin is the motor for microtubule-mediated golgi-to-er membrane traffic. *J Cell Biol*, 128(3):293–306, 1995. 0021-9525 (Print) Journal Article. 16, 17, 89

[84] N. Hirokawa, Y. Noda, and Y. Okada. Kinesin and dynein superfamily proteins in organelle transport and cell division. *Curr Opin Cell Biol*, 10(1):60–73, 1998. 0955-0674 (Print) Journal Article Review. 17

[85] A. A. Rogalski and S. J. Singer. Associations of elements of the golgi apparatus with microtubules. *J Cell Biol*, 99(3):1092–100, 1984. 0021-9525 (Print) Journal Article. 17

[86] R. L. Karcher, S. W. Deacon, and V. I. Gelfand. Motor-cargo interactions: the key to transport specificity. *Trends Cell Biol*, 12(1):21–7, 2002. 0962-8924 (Print) Journal Article Review. 17

[87] I. Jordens, M. Marsman, C. Kuijl, and J. Neefjes. Rab proteins, connecting transport and vesicle fusion. *Traffic*, 6(12):1070–7, 2005. 1398-9219 (Print) Journal Article Review. 17

[88] M. Zerial and H. McBride. Rab proteins as membrane organizers. *Nat Rev Mol Cell Biol*, 2(2):107–17, 2001. 1471-0072 (Print) Journal Article Review. 18, 19, 53, 90

[89] J. Somsel Rodman and A. Wandinger-Ness. Rab gtpases coordinate endocytosis. *J Cell Sci*, 113 Pt 2:183–92, 2000. 0021-9533 (Print) Journal Article Review. 19

[90] F. Schimmoller, I. Simon, and S. R. Pfeffer. Rab gtpases, directors of vesicle docking. *J Biol Chem*, 273(35):22161–4, 1998. 0021-9258 (Print) Journal Article Review. 19, 20

[91] D. R. TerBush, T. Maurice, D. Roth, and P. Novick. The exocyst is a multiprotein complex required for exocytosis in saccharomyces cerevisiae. *Embo J*, 15(23):6483–94, 1996. 0261-4189 (Print) Journal Article. 19

[92] Y. Kee, J. S. Yoo, C. D. Hazuka, K. E. Peterson, S. C. Hsu, and R. H. Scheller. Subunit structure of the mammalian exocyst complex. *Proc Natl Acad Sci U S A*, 94(26):14438–43, 1997. 0027-8424 (Print) Journal Article. 19

[93] H. Stenmark, G. Vitale, O. Ullrich, and M. Zerial. Rabaptin-5 is a direct effector of the small gtpase rab5 in endocytic membrane fusion. *Cell*, 83(3):423–32, 1995. 0092-8674 (Print) Journal Article. 19

[94] M. Sacher, Y. Jiang, J. Barrowman, A. Scarpa, J. Burston, L. Zhang, D. Schieltz, 3rd Yates, J. R., H. Abeliovich, and S. Ferro-Novick. Trapp, a highly conserved novel complex on the cis-golgi that mediates vesicle docking and fusion. *Embo J*, 17(9):2494–503, 1998. 0261-4189 (Print) Journal Article. 19

[95] C. Nuoffer, H. W. Davidson, J. Matteson, J. Meinkoth, and W. E. Balch. A gdp-bound of rab1 inhibits protein export from the endoplasmic reticulum and transport between golgi compartments. *J Cell Biol*, 125(2):225–37, 1994. 0021-9525 (Print) Journal Article. 20

[96] M. A. Riederer, T. Soldati, A. D. Shapiro, J. Lin, and S. R. Pfeffer. Lysosome biogenesis requires rab9 function and receptor recycling from endosomes to the trans-golgi network. *J Cell Biol*, 125(3):573–82, 1994. 0021-9525 (Print) Journal Article. 20

[97] H. McLauchlan, J. Newell, N. Morrice, A. Osborne, M. West, and E. Smythe. A novel role for rab5-gdi in ligand sequestration into clathrin-coated pits. *Curr Biol*, 8(1):34–45, 1998. 0960-9822 (Print) Journal Article. 20

[98] A. Echard, F. Jollivet, O. Martinez, J. J. Lacapere, A. Rousselet, I. Janoueix-Lerosey, and B. Goud. Interaction of a golgi-associated kinesin-like protein with rab6. *Science*, 279(5350):580–5, 1998. 0036-8075 (Print) Journal Article. 20

[99] C. C. Hoogenraad, P. Wulf, N. Schiefermeier, T. Stepanova, N. Galjart, J. V. Small, F. Grosveld, C. I. de Zeeuw, and A. Akhmanova. Bicaudal d induces selective dynein-mediated microtubule minus end-directed transport. *Embo J*, 22(22):6004–15, 2003. 0261-4189 (Print) Journal Article. 20

[100] T. Imamura, J. Huang, I. Usui, H. Satoh, J. Bever, and J. M. Olefsky. Insulin-induced glut4 translocation involves protein kinase c-lambda-mediated functional coupling between rab4 and the motor protein kinesin. *Mol Cell Biol*, 23(14):4892–900, 2003. 0270-7306 (Print) Journal Article. 20

[101] J. Huang, T. Imamura, and J. M. Olefsky. Insulin can regulate glut4 internalization by signaling to rab5 and the motor protein dynein. *Proc Natl Acad Sci U S A*, 98(23):13084–9, 2001. 0027-8424 (Print) Journal Article Research Support, Non-U.S. Gov't Research Support, U.S. Gov't, P.H.S. 20

[102] L. Pelkmans, E. Fava, H. Grabner, M. Hannus, B. Habermann, E. Krausz, and M. Zerial. Genome-wide analysis of human kinases in clathrin- and caveolae/raft-mediated endocytosis. *Nature*, 436(7047):78–86, 2005. 1476-4687 (Electronic) Journal Article. 20

[103] S. Hoepfner, F. Severin, A. Cabezas, B. Habermann, A. Runge, D. Gillooly, H. Stenmark, and M. Zerial. Modulation of receptor recycling and degradation by the endosomal kinesin kif16b. *Cell*, 121(3):437–50, 2005. 0092-8674 (Print) Journal Article. 20

[104] Y. A. Chen and R. H. Scheller. Snare-mediated membrane fusion. *Nat Rev Mol Cell Biol*, 2(2):98–106, 2001. 1471-0072 (Print) Journal Article Review. 20, 22, 32

[105] T. Sollner, S. W. Whiteheart, M. Brunner, H. Erdjument-Bromage, S. Geromanos, P. Tempst, and J. E. Rothman. Snap receptors implicated in vesicle targeting and fusion. *Nature*, 362(6418):318–24, 1993. 0028-0836 (Print) Journal Article. 20

[106] C. Walch-Solimena, R. Jahn, and T. C. Sudhof. Synaptic vesicle proteins in exocytosis: what do we know? *Curr Opin Neurobiol*, 3(3):329–36, 1993. 0959-4388 (Print) Journal Article Review. 20

[107] R. B. Sutton, D. Fasshauer, R. Jahn, and A. T. Brunger. Crystal structure of a snare complex involved in synaptic exocytosis at 2.4 a resolution. *Nature*, 395(6700):347–53, 1998. 0028-0836 (Print) Journal Article. 21

[108] D. Fasshauer, R. B. Sutton, A. T. Brunger, and R. Jahn. Conserved structural features of the synaptic fusion complex: Snare proteins reclassified as q- and r-snares. *Proc Natl Acad Sci U S A*, 95(26):15781–6, 1998. 0027-8424 (Print) Journal Article. 21

[109] J. E. Rothman. Mechanisms of intracellular protein transport. *Nature*, 372(6501):55–63, 1994. 0028-0836 (Print) Journal Article Review. 21

[110] R. Jahn, T. Lang, and T. C. Sudhof. Membrane fusion. *Cell*, 112(4):519–33, 2003. 0092-8674 (Print) Journal Article Review. 21

[111] R. F. Toonen and M. Verhage. Vesicle trafficking: pleasure and pain from sm genes. *Trends Cell Biol*, 13(4):177–86, 2003. 0962-8924 (Print) Journal Article Review. 21

[112] B. Short and F. A. Barr. Membrane fusion: caught in a trap. *Curr Biol*, 14(5):R187–9, 2004. 0960-9822 (Print) Journal Article Review. 21

[113] B. Habermann. The bar-domain family of proteins: a case of bending and binding? *EMBO Rep*, 5(3):250–5, 2004. 1469-221X (Print) Journal Article Review. 23, 24, 43, 89

[114] K. Takei, V. I. Slepnev, V. Haucke, and P. De Camilli. Functional partnership between amphiphysin and dynamin in clathrin-mediated endocytosis. *Nat Cell Biol*, 1(1):33–9, 1999. 1465-7392 (Print) Journal Article. 23

[115] E. Lee, M. Marcucci, L. Daniell, M. Pypaert, O. A. Weisz, G. C. Ochoa, K. Farsad, M. R. Wenk, and P. De Camilli. Amphiphysin 2 (bin1) and t-tubule biogenesis in muscle. *Science*, 297(5584):1193–6, 2002. 1095-9203 (Electronic) Journal Article. 23

[116] H. T. McMahon and J. L. Gallop. Membrane curvature and mechanisms of dynamic cell membrane remodelling. *Nature*, 438(7068):590–6, 2005. 1476-4687 (Electronic) Journal Article Review. 23

[117] J. L. Gallop and H. T. McMahon. Bar domains and membrane curvature: bringing your curves to the bar. *Biochem Soc Symp*, (72):223–31, 2005. 0067-8694 (Print) Journal Article Review. 23

[118] C. Tarricone, B. Xiao, N. Justin, P. A. Walker, K. Rittinger, S. J. Gamblin, and S. J. Smerdon. The structural basis of arfaptin-mediated cross-talk between rac and arf signalling pathways. *Nature*, 411(6834):215–9, 2001. 0028-0836 (Print) Journal Article. 24, 88, 89

[119] M. Miaczynska, S. Christoforidis, A. Giner, A. Shevchenko, S. Uttenweiler-Joseph, B. Habermann, M. Wilm, R. G. Parton, and M. Zerial. Appl proteins link rab5 to nuclear signal transduction via an endosomal compartment. *Cell*, 116(3):445–56, 2004. 0092-8674 (Print) Journal Article. 24, 89

[120] M. R. Wenk and P. De Camilli. Protein-lipid interactions and phosphoinositide metabolism in membrane traffic: insights from vesicle recycling in nerve terminals. *Proc Natl Acad Sci U S A*, 101(22):8262–9, 2004. 0027-8424 (Print) Journal Article Review. 24

[121] A. Simonsen, A. E. Wurmser, S. D. Emr, and H. Stenmark. The role of phosphoinositides in membrane transport. *Curr Opin Cell Biol*, 13(4):485–92, 2001. 0955-0674 (Print) Journal Article Review. 24, 25, 86

[122] A. Toker and L. C. Cantley. Signalling through the lipid products of phosphoinositide-3-oh kinase. *Nature*, 387(6634):673–6, 1997. 0028-0836 (Print) Journal Article Review. 24

[123] J. P. DiNitto, T. C. Cronin, and D. G. Lambright. Membrane recognition and targeting by lipid-binding domains. *Sci STKE*, 2003(213):re16, 2003. 1525-8882 (Electronic) Journal Article Review. 24

[124] O. Cremona and P. De Camilli. Phosphoinositides in membrane traffic at the synapse. *J Cell Sci*, 114(Pt 6):1041–52, 2001. 0021-9533 (Print) Journal Article Review. 25

[125] Y. J. Wang, J. Wang, H. Q. Sun, M. Martinez, Y. X. Sun, E. Macia, T. Kirchhausen, J. P. Albanesi, M. G. Roth, and H. L. Yin. Phosphatidylinositol 4 phosphate regulates targeting of clathrin adaptor ap-1 complexes to the golgi. *Cell*, 114(3):299–310, 2003. 0092-8674 (Print) Journal Article. 25

[126] T. L. Burgess and R. B. Kelly. Constitutive and regulated secretion of proteins. *Annu Rev Cell Biol*, 3:243–93, 1987. 0743-4634 (Print) Journal Article Review. 25, 26, 28, 32

[127] P. Keller and K. Simons. Post-golgi biosynthetic trafficking. *J Cell Sci*, 110 (Pt 24):3001–9, 1997. 0021-9533 (Print) Journal Article Review. 25, 26

[128] S. Ponnambalam and S. A. Baldwin. Constitutive protein secretion from the trans-golgi network to the plasma membrane. *Mol Membr Biol*, 20(2):129–39, 2003. 0968-7688 (Print) Journal Article Review. 26

[129] D. Toomre, P. Keller, J. White, J. C. Olivo, and K. Simons. Dual-color visualization of trans-golgi network to plasma membrane traffic along microtubules in living cells. *J Cell Sci*, 112 (Pt 1):21–33, 1999. 0021-9533 (Print) Journal Article. 26

[130] R. Bauerfeind and W. B. Huttner. Biogenesis of constitutive secretory vesicles, secretory granules and synaptic vesicles. *Curr Opin Cell Biol*, 5(4):628–35, 1993. 0955-0674 (Print) Journal Article Review. 26, 29

[131] R. B. Kelly. Pathways of protein secretion in eukaryotes. *Science*, 230(4721):25–32, 1985. 0036-8075 (Print) Journal Article. 26

[132] F. A. Barr, A. Leyte, S. Mollner, T. Pfeuffer, S. A. Tooze, and W. B. Huttner. Trimeric g-proteins of the trans-golgi network are involved in the formation of constitutive secretory vesicles and immature secretory granules. *FEBS Lett*, 294(3):239–43, 1991. 0014-5793 (Print) Journal Article. 26

[133] M. Liljedahl, Y. Maeda, A. Colanzi, I. Ayala, J. Van Lint, and V. Malhotra. Protein kinase d regulates the fission of cell surface destined transport carriers from the trans-golgi network. *Cell*, 104(3):409–20, 2001. 0092-8674 (Print) Journal Article. 26

[134] R. D. Burgoyne and A. Morgan. Secretory granule exocytosis. *Physil Rev*, 838:581–632, 2002. 28, 32

[135] A. Morgan and R. D. Burgoyne. Common mechanisms for regulated exocytosis in the chromaffin cell and the synapse. *Semin Cell Dev Biol*, 8(2):141–9, 1997. 1084-9521 (Print) Journal Article. 28, 33

[136] R. B. Kelly. Loading synaptic vesicles with neurotransmitter. *Curr Biol*, 3(1):59–61, 1993. 0960-9822 (Print) Journal Article. 28

[137] A. Thureson-Klein. Exocytosis from large and small dense cored vesicles in noradrenergic nerve terminals. *Neuroscience*, 10(2):245–59, 1983. 0306-4522 (Print) Journal Article. 28

[138] A. Reetz, M. Solimena, M. Matteoli, F. Folli, K. Takei, and P. De Camilli. Gaba and pancreatic beta-cells: colocalization of glutamic acid decarboxylase (gad) and gaba with synaptic-like microvesicles suggests their role in gaba storage and secretion. *Embo J*, 10(5):1275–84, 1991. 0261-4189 (Print) Journal Article. 28

[139] T. C. Sudhof. The synaptic vesicle cycle: a cascade of protein-protein interactions. *Nature*, 375(6533):645–53, 1995. 0028-0836 (Print) Journal Article Review. 28, 32, 33

[140] T. C. Sudhof. The synaptic vesicle cycle. *Annu Rev Neurosci*, 27:509–47, 2004. 0147-006X (Print) Journal Article Review. 29, 35, 36

[141] D. Elmqvist and D. M. Quastel. A quantitative study of end-plate potentials in isolated human muscle. *J Physiol*, 178(3):505–29, 1965. 0022-3751 (Print) Journal Article. 29

[142] J. B. Sorensen. Formation, stabilisation and fusion of the readily releasable pool of secretory vesicles. *Pflugers Arch*, 448(4):347–62, 2004. 0031-6768 (Print) Journal Article Review. 29

[143] F. Doussau and G. J. Augustine. The actin cytoskeleton and neurotransmitter release: an overview. *Biochimie*, 82(4):353–63, 2000. 0300-9084 (Print) Journal Article Review. 29

[144] S. A. Tooze. Biogenesis of secretory granules in the trans-golgi network of neuroendocrine and endocrine cells. *Biochim Biophys Acta*, 1404(1-2):231–44, 1998. 0006-3002 (Print) Journal Article Review. 29

[145] B. Borgonovo, J. Ouwendijk, and M. Solimena. Biogenesis of secretory granules. *Curr Opin Cell Biol*, 18(4):365–70, 2006. 0955-0674 (Print) Journal Article Review. 29

[146] S. A. Tooze, G. J. Martens, and W. B. Huttner. Secretory granule biogenesis: rafting to the snare. *Trends Cell Biol*, 11(3):116–22, 2001. 0962-8924 (Print) Journal Article Review. 29, 30, 31

[147] M. Molinete, J. C. Irminger, S. A. Tooze, and P. A. Halban. Trafficking/sorting and granule biogenesis in the beta-cell. *Semin Cell Dev Biol*, 11(4):243–51, 2000. 1084-9521 (Print) Journal Article Review. 29

[148] C. Thiele and W. B. Huttner. Protein and lipid sorting from the trans-golgi network to secretory granules-recent developments. *Semin Cell Dev Biol*, 9(5):511–6, 1998. 1084-9521 (Print) Journal Article Review. 29

[149] D. F. Steiner. The proprotein convertases. *Curr Opin Chem Biol*, 2(1):31–9, 1998. 1367-5931 (Print) Journal Article Review. 30

[150] G. Dodson and D. Steiner. The role of assembly in insulin's biosynthesis. *Curr Opin Struct Biol*, 8(2):189–94, 1998. 0959-440X (Print) Journal Article Review. 30

[151] E. Chanat, S. W. Pimplikar, J. C. Stinchcombe, and W. B. Huttner. What the granins tell us about the formation of secretory granules in neuroendocrine cells. *Cell Biophys*, 19(1-3):85–91, 1991. 0163-4992 (Print) Journal Article Review. 30

[152] L. Orci. Macro- and micro-domains in the endocrine pancreas. *Diabetes*, 31(6 Pt 1):538–65, 1982. 0012-1797 (Print) Journal Article Review. 30

[153] O. Kakhlon, P. Sakya, B. Larijani, R. Watson, and S. A. Tooze. Gga function is required for maturation of neuroendocrine secretory granules. *Embo J*, 25(8):1590–602, 2006. 0261-4189 (Print) Journal Article. 30

[154] B. A. Eaton, M. Haugwitz, D. Lau, and H. P. Moore. Biogenesis of regulated exocytotic carriers in neuroendocrine cells. *J Neurosci*, 20(19):7334–44, 2000. 1529-2401 (Electronic) Journal Article. 30

[155] R. R. Duncan, J. Greaves, U. K. Wiegand, I. Matskevich, G. Bodammer, D. K. Apps, M. J. Shipston, and R. H. Chow. Functional and spatial segregation of secretory vesicle pools according to vesicle age. *Nature*, 422(6928):176–80, 2003. 0028-0836 (Print) Journal Article. 30

[156] M. Solimena and H. H. Gerdes. Secretory granules: and the last shall be first. *Trends Cell Biol*, 13(8):399–402, 2003. 0962-8924 (Print) Comment Journal Article. 30

[157] S Schubert. The role of 2-syntrophin phosphorilation in secretory granule exocytosis (phd thesis). 2005. 30

[158] G. Schiavo, M. Matteoli, and C. Montecucco. Neurotoxins affecting neuroexocytosis. *Physiol Rev*, 80(2):717–66, 2000. 0031-9333 (Print) Journal Article Review. 32

[159] P. Novick and W. Guo. Ras family therapy: Rab, rho and ral talk to the exocyst. *Trends Cell Biol*, 12(6):247–9, 2002. 0962-8924 (Print) News. 32

[160] T. Coppola, C. Frantz, V. Perret-Menoud, S. Gattesco, H. Hirling, and R. Regazzi. Pancreatic beta-cell protein granuphilin binds rab3 and munc-18 and controls exocytosis. *Mol Biol Cell*, 13(6):1906–15, 2002. 1059-1524 (Print) Journal Article. 32

[161] Z. Yi, H. Yokota, S. Torii, T. Aoki, M. Hosaka, S. Zhao, K. Takata, T. Takeuchi, and T. Izumi. The rab27a/granuphilin complex regulates the exocytosis of insulin-containing dense-core granules. *Mol Cell Biol*, 22(6):1858–67, 2002. 0270-7306 (Print) Journal Article. 32

[162] A. Banerjee, V. A. Barry, B. R. DasGupta, and T. F. Martin. N-ethylmaleimide-sensitive factor acts at a prefusion atp-dependent step in ca2+-activated exocytosis. *J Biol Chem*, 271(34):20223–6, 1996. 0021-9258 (Print) Journal Article. 32

[163] V. A. Klenchin and T. F. Martin. Priming in exocytosis: attaining fusion-competence after vesicle docking. *Biochimie*, 82(5):399–407, 2000. 0300-9084 (Print) Journal Article Review. 32

[164] R. A. Easom. Beta-granule transport and exocytosis. *Semin Cell Dev Biol*, 11(4):253–66, 2000. 1084-9521 (Print) Journal Article Review. 32, 38

[165] C. Li, B. A. Davletov, and T. C. Sudhof. Distinct ca2+ and sr2+ binding properties of synaptotagmins. definition of candidate ca2+ sensors for the fast and slow components of neurotransmitter release. *J Biol Chem*, 270(42):24898–902, 1995. 0021-9258 (Print) Journal Article. 33

[166] E. R. Chapman. Synaptotagmin: a ca(2+) sensor that triggers exocytosis? *Nat Rev Mol Cell Biol*, 3(7):498–508, 2002. 1471-0072 (Print) Journal Article Review. 33

[167] M. Geppert, Y. Goda, R. E. Hammer, C. Li, T. W. Rosahl, C. F. Stevens, and T. C. Sudhof. Synaptotagmin i: a major ca2+ sensor for transmitter release at a central synapse. *Cell*, 79(4):717–27, 1994. 0092-8674 (Print) Journal Article. 33

[168] J. Lang, M. Fukuda, H. Zhang, K. Mikoshiba, and C. B. Wollheim. The first c2 domain of synaptotagmin is required for exocytosis of insulin from pancreatic beta-cells: action of synaptotagmin at low micromolar calcium. *Embo J*, 16(19):5837–46, 1997. 0261-4189 (Print) Journal Article. 34

[169] S. Barg. Mechanisms of exocytosis in insulin-secreting b-cells and glucagon-secreting a-cells. *Pharmacol Toxicol*, 92(1):3–13, 2003. 0901-9928 (Print) Journal Article Review. 34, 38

[170] K. Ann, J. A. Kowalchyk, K. M. Loyet, and T. F. Martin. Novel ca2+-binding protein (caps) related to unc-31 required for ca2+-activated exocytosis. *J Biol Chem*, 272(32):19637–40, 1997. 0021-9258 (Print) Journal Article. 34

[171] R. Jahn and T. C. Sudhof. Membrane fusion and exocytosis. *Annu Rev Biochem*, 68:863–911, 1999. 0066-4154 (Print) Journal Article Review. 34

[172] J. E. Heuser and T. S. Reese. Evidence for recycling of synaptic vesicle membrane during transmitter release at the frog neuromuscular junction. *J Cell Biol*, 57(2):315–44, 1973. 0021-9525 (Print) Journal Article. 34

[173] B. Ceccarelli, W. P. Hurlbut, and A. Mauro. Turnover of transmitter and synaptic vesicles at the frog neuromuscular junction. *J Cell Biol*, 57(2):499–524, 1973. 0021-9525 (Print) Journal Article. 34

[174] K. Takei and V. Haucke. Clathrin-mediated endocytosis: membrane factors pull the trigger. *Trends Cell Biol*, 11(9):385–91, 2001. 0962-8924 (Print) Journal Article Review. 34

[175] C. R. Artalejo, A. Elhamdani, and H. C. Palfrey. Secretion: dense-core vesicles can kiss-and-run too. *Curr Biol*, 8(2):R62–5, 1998. 0960-9822 (Print) Journal Article Review. 34

[176] P. Holroyd, T. Lang, D. Wenzel, P. De Camilli, and R. Jahn. Imaging direct, dynamin-dependent recapture of fusing secretory granules on plasma membrane lawns from pc12 cells. *Proc Natl Acad Sci U S A*, 99(26):16806–11, 2002. 0027-8424 (Print) Journal Article. 34

[177] J. W. Taraska, D. Perrais, M. Ohara-Imaizumi, S. Nagamatsu, and W. Almers. Secretory granules are recaptured largely intact after stimulated exocytosis in cultured endocrine cells. *Proc Natl Acad Sci U S A*, 100(4):2070–5, 2003. 0027-8424 (Print) Journal Article. 36

[178] E. Ales, L. Tabares, J. M. Poyato, V. Valero, M. Lindau, and G. Alvarez de Toledo. High calcium concentrations shift the mode of exocytosis to the kiss-and-run mechanism. *Nat Cell Biol*, 1(1):40–4, 1999. 1465-7392 (Print) Journal Article. 36

[179] F. Valtorta, J. Meldolesi, and R. Fesce. Synaptic vesicles: is kissing a matter of competence? *Trends Cell Biol*, 11(8):324–8, 2001. 0962-8924 (Print) Journal Article Review. 36

[180] L. Orci. The insulin factory: a tour of the plant surroundings and a visit to the assembly line. the minkowski lecture 1973 revisited. *Diabetologia*, 28(8):528–46, 1985. 0012-186X (Print) Journal Article. 36

[181] H Morrison. Contributions to the microscopic anatomy of the pancreas by paul langerhans (berlin, 1869). *Bullettin of the Institute of the History of Medicine*, (5):2259–97, 1937. 36

[182] B. Cheatham and C. R. Kahn. Insulin action and the insulin signaling network. *Endocr Rev*, 16(2):117–42, 1995. 0163-769X (Print) Journal Article Review. 36, 41

[183] K. Ohneda, H. Ee, and M. German. Regulation of insulin gene transcription. *Semin Cell Dev Biol*, 11(4):227–33, 2000. 1084-9521 (Print) Journal Article Review. 36

[184] M. Welsh, N. Scherberg, R. Gilmore, and D. F. Steiner. Translational control of insulin biosynthesis. evidence for regulation of elongation, initiation and signal-recognition-particle-mediated translational arrest by glucose. *Biochem J*, 235(2):459–67, 1986. 0264-6021 (Print) Journal Article. 36

[185] K. P. Knoch, H. Bergert, B. Borgonovo, H. D. Saeger, A. Altkruger, P. Verkade, and M. Solimena. Polypyrimidine tract-binding protein promotes insulin secretory granule biogenesis. *Nat Cell Biol*, 6(3):207–14, 2004. 1465-7392 (Print) Journal Article. 38, 92, 93

[186] J. T. Deeney, M. Prentki, and B. E. Corkey. Metabolic control of beta-cell function. *Semin Cell Dev Biol*, 11(4):267–75, 2000. 1084-9521 (Print) Journal Article Review. 38

[187] P. M. Dean. Ultrastructural morphometry of the pancreatic -cell. *Diabetologia*, 9(2):115–9, 1973. 0012-186X (Print) Journal Article. 38

[188] F. M. Ashcroft and P. Rorsman. Electrophysiology of the pancreatic beta-cell. *Prog Biophys Mol Biol*, 54(2):87–143, 1989. 0079-6107 (Print) Journal Article Review. 38

[189] P. Gilon, R. M. Shepherd, and J. C. Henquin. Oscillations of secretion driven by oscillations of cytoplasmic ca2+ as evidences in single pancreatic islets. *J Biol Chem*, 268(30):22265–8, 1993. 0021-9258 (Print) Journal Article. 38

[190] P. Bergsten, E. Grapengiesser, E. Gylfe, A. Tengholm, and B. Hellman. Synchronous oscillations of cytoplasmic ca2+ and insulin release in glucose-stimulated pancreatic islets. *J Biol Chem*, 269(12):8749–53, 1994. 0021-9258 (Print) Journal Article. 38

[191] P. Maechler, A. Gjinovci, and C. B. Wollheim. Implication of glutamate in the kinetics of insulin secretion in rat and mouse perfused pancreas. *Diabetes*, 51 Suppl 1:S99–102, 2002. 0012-1797 (Print) Journal Article. 38

[192] D. L. Curry, L. L. Bennett, and G. M. Grodsky. Dynamics of insulin secretion by the perfused rat pancreas. *Endocrinology*, 83(3):572–84, 1968. 0013-7227 (Print) Journal Article. 38

[193] L. Eliasson, E. Renstrom, W. G. Ding, P. Proks, and P. Rorsman. Rapid atp-dependent priming of secretory granules precedes ca(2+)-induced exocytosis in mouse pancreatic b-cells. *J Physiol*, 503 (Pt 2):399–412, 1997. 0022-3751 (Print) Journal Article. 38

[194] P. Rorsman and E. Renstrom. Insulin granule dynamics in pancreatic beta cells. *Diabetologia*, 46(8):1029–45, 2003. 0012-186X (Print) Journal Article Review. 38

[195] M. Trajkovski, H. Mziaut, A. Altkruger, J. Ouwendijk, K. P. Knoch, S. Muller, and M. Solimena. Nuclear translocation of an ica512 cytosolic fragment couples granule exocytosis and insulin expression in beta-cells. *J Cell Biol*, 167(6):1063–74, 2004. 0021-9525 (Print) Journal Article. 39

[196] H. Mziaut, M. Trajkovski, S. Kersting, A. Ehninger, A. Altkruger, R. P. Lemaitre, D. Schmidt, H. D. Saeger, M. S. Lee, D. N. Drechsel, S. Muller, and M. Solimena. Synergy of glucose and growth hormone signalling in islet cells through ica512 and stat5. *Nat Cell Biol*, 8(5):435–45, 2006. 1465-7392 (Print) Journal Article. 39

[197] C. R. Kahn, G. C. Weir, G. L. King, A. M. Jacobson, A. C. Moses, and R. J. Smith. Joslin's diabetes mellitus. 2005. 39

[198] A. K. Foulis, M. McGill, and M. A. Farquharson. Insulitis in type 1 (insulin-dependent) diabetes mellitus in man–macrophages, lymphocytes, and interferon-gamma containing cells. *J Pathol*, 165(2):97–103, 1991. 0022-3417 (Print) Journal Article. 39

[199] G. S. Eisenbarth. Type i diabetes mellitus. a chronic autoimmune disease. *N Engl J Med*, 314(21):1360–8, 1986. 0028-4793 (Print) Journal Article Review. 39

[200] D. T. Robles and G. S. Eisenbarth. Type 1a diabetes induced by infection and immunization. *J Autoimmun*, 16(3):355–62, 2001. 0896-8411 (Print) Journal Article Review. 39

[201] D. Daneman. Type 1 diabetes. *Lancet*, 367(9513):847–58, 2006. 1474-547X (Electronic) Journal Article Review. 39

[202] M. Solimena. Vesicular autoantigens of type 1 diabetes. *Diabetes Metab Rev*, 14(3):227–40, 1998. 0742-4221 (Print) Journal Article Review. 39, 41

[203] J. M. Barker, K. J. Barriga, L. Yu, D. Miao, H. A. Erlich, J. M. Norris, G. S. Eisenbarth, and M. Rewers. Prediction of autoantibody positivity and progression to type 1 diabetes: Diabetes autoimmunity study in the young (daisy). *J Clin Endocrinol Metab*, 89(8):3896–902, 2004. 0021-972X (Print) Journal Article. 39

[204] P. A. Silveira and S. T.w Grey. B cells in the spotlight: innocent bystanders or major players in the pathogenesis of type 1 diabetes. *Trends Endocrinol Metab*, 17(4):128–35, 2006. 1043-2760 (Print) Journal Article Review. 40

[205] R. J. DeHoratius, R. Pillarisetty, R. P. Messner, and N. Talal. Anti-nucleic acid antibodies in systemic lupus erythematosus patients and their families. incidence and correlation with lymphocytotoxic antibodies. *J Clin Invest*, 56(5):1149–54, 1975. 0021-9738 (Print) Journal Article. 40

[206] G.J. Mack, J. Rees, O. Sandblom, R. Balczon, M.J. Fritzler, and J.B. Rattner. Autoantibodies to a group of centrosomal proteins in human autoimmune sera reactive with thecentrosome. *Arthritis Rheum*, 41(3), 1998. 40

[207] J. L. Rodriguez, C. Gelpi, T. M. Thomson, F. J. Real, and J. Fernandez. Anti-golgi complex autoantibodies in a patient with sjogren syndrome and lymphoma. *Clin Exp Immunol*, 49(3):579–86, 1982. 0009-9104 (Print) Case Reports Journal Article. 40

[208] M. J. Fritzler. Autoantibodies in scleroderma. *J Dermatol*, 20(5):257–68, 1993. 0385-2407 (Print) Journal Article Review. 40

[209] M. J. Mamula. Epitope spreading: the role of self peptides and autoantigen processing by b lymphocytes. *Immunol Rev*, 164:231–9, 1998. 0105-2896 (Print) Journal Article Review. 41

[210] P. Froguel and G. Velho. Genetic determinants of type 2 diabetes. *Recent Prog Horm Res*, 56:91–105, 2001. 0079-9963 (Print) Journal Article Review. 41

[211] M. Trajkovski, H. Mziaut, P. E. Schwarz, and M. Solimena. Genes of type 2 diabetes in beta cells. *Endocrinol Metab Clin North Am*, 35(2):357–69, x, 2006. 0889-8529 (Print) Journal Article Review. 41

[212] J. L. Leahy. Pathogenesis of type 2 diabetes mellitus. *Arch Med Res*, 36(3):197–209, 2005. 0188-4409 (Print) Journal Article Review. 41

[213] M. T. Tusie Luna. Genes and type 2 diabetes mellitus. *Arch Med Res*, 36(3):210–22, 2005. 0188-4409 (Print) Journal Article Review. 41

[214] D. J. Pettitt, W. C. Knowler, H. R. Baird, and P. H. Bennett. Gestational diabetes: infant and maternal complications of pregnancy in relation to third-trimester glucose tolerance in the pima indians. *Diabetes Care*, 3(3):458–64, 1980. 0149-5992 (Print) Journal Article. 42

[215] M. Pietropaolo, L. Castano, S. Babu, R. Buelow, Y. L. Kuo, S. Martin, A. Martin, A. C. Powers, M. Prochazka, J. Naggert, and et al. Islet cell autoantigen 69 kd (ica69). molecular cloning and characterization of a novel diabetes-associated autoantigen. *J Clin Invest*, 92(1):359–71, 1993. 0021-9738 (Print) Journal Article. 42, 46, 92, 104, 113

[216] I. Miyazaki, R. Gaedigk, M. F. Hui, R. K. Cheung, J. Morkowski, R. V. Rajotte, and H. M. Dosch. Cloning of human and rat p69 cdna, a candidate autoimmune target in type 1 diabetes. *Biochim Biophys Acta*, 1227(1-2):101–4, 1994. 0006-3002 (Print) Journal Article. 42

[217] R. Gaedigk, W. Karges, M. F. Hui, S. W. Scherer, and H. M. Dosch. Genomic organization and transcript analysis of icap69, a target antigen in diabetic autoimmunity. *Genomics*, 38(3):382–91, 1996. 0888-7543 (Print) Journal Article. 42

[218] W. Karges, M. Pietropaolo, C. A. Ackerley, and H. M. Dosch. Gene expression of islet cell antigen p69 in human, mouse, and rat. *Diabetes*, 45(4):513–21, 1996. 0012-1797 (Print) Journal Article. 42, 92

[219] R. P. Friday, S. L. Pietropaolo, J. Profozich, M. Trucco, and M. Pietropaolo. Alternative core promoters regulate tissue-specific transcription from the autoimmune diabetes-related ica1 (ica69) gene locus. *J Biol Chem*, 278(2):853–63, 2003. 0021-9258 (Print) Journal Article. 42

[220] P. J. Bingley, E. Bonifacio, and P. W. Mueller. Diabetes antibody standardization program: first assay proficiency evaluation. *Diabetes*, 52(5):1128–36, 2003. 0012-1797 (Print) Journal Article. 42

[221] H. Dosch, R. K. Cheung, W. Karges, M. Pietropaolo, and D. J. Becker. Persistent t cell anergy in human type 1 diabetes. *J Immunol*, 163(12):6933–40, 1999. 0022-1767 (Print) Journal Article. 42

[222] W. Karges, D. Hammond-McKibben, R. Gaedigk, N. Shibuya, R. Cheung, and H. M. Dosch. Loss of self-tolerance to ica69 in nonobese diabetic mice. *Diabetes*, 46(10):1548–56, 1997. 0012-1797 (Print) Journal Article. 42

[223] S. Martin, J. Kardorf, B. Schulte, E. F. Lampeter, F. A. Gries, I. Melchers, R. Wagner, J. Bertrams, B. O. Roep, and A. Pfutzner. Autoantibodies to the islet antigen ica69 occur in iddm and in rheumatoid arthritis. *Diabetologia*, 38(3):351–5, 1995. 0012-186X (Print) Journal Article. 42

[224] S. Winer, I. Astsaturov, R. Cheung, H. Tsui, A. Song, R. Gaedigk, D. Winer, A. Sampson, C. McKerlie, A. Bookman, and H. M. Dosch. Primary sjogren's syndrome and deficiency of ica69. *Lancet*, 360(9339):1063–9, 2002. 0140-6736 (Print) Journal Article. 42

[225] M. Pilon, X. R. Peng, A. M. Spence, R. H. Plasterk, and H. M. Dosch. The diabetes autoantigen ica69 and its caenorhabditis elegans homologue, ric-19, are conserved regulators of neuroendocrine secretion. *Mol Biol Cell*, 11(10):3277–88, 2000. 1059-1524 (Print) Journal Article. 43, 46, 85, 92

[226] F. Spitzenberger, S. Pietropaolo, P. Verkade, B. Habermann, S. Lacas-Gervais, H. Mziaut, M. Pietropaolo, and M. Solimena. Islet cell autoantigen of 69 kda is an arfaptin-related protein associated with the golgi complex of insulinoma ins-1 cells. *J Biol Chem*, 278(28):26166–73, 2003. 0021-9258 (Print) Journal Article. 43, 46, 50, 58, 85, 86, 106

[227] K. G. Miller, A. Alfonso, M. Nguyen, J. A. Crowell, C. D. Johnson, and J. B. Rand. A genetic selection for caenorhabditis elegans synaptic transmission mutants. *Proc Natl Acad Sci U S A*, 93(22):12593–8, 1996. 0027-8424 (Print) Journal Article. 43

[228] S. Winer, I. Astsaturov, R. Gaedigk, D. Hammond-McKibben, M. Pilon, A. Song, V. Kubiak, W. Karges, E. Arpaia, C. McKerlie, P. Zucker, B. Singh, and H. M. Dosch. Ica69(null) nonobese diabetic mice develop diabetes, but resist disease acceleration by cyclophosphamide. *J Immunol*, 168(1):475–82, 2002. 0022-1767 (Print) Journal Article. 43, 92

[229] E. J. Tisdale and M. R. Jackson. Rab2 protein enhances coatomer recruitment to pre-golgi intermediates. *J Biol Chem*, 273(27):17269–77, 1998. 0021-9258 (Print) Journal Article. 50, 68, 86, 91

[230] B. Short, C. Preisinger, R. Korner, R. Kopajtich, O. Byron, and F. A. Barr. A grasp55-rab2 effector complex linking golgi structure to membrane traffic. *J Cell Biol*, 155(6):877–83, 2001. 0021-9525 (Print) Journal Article. 53, 87

[231] J. White, L. Johannes, F. Mallard, A. Girod, S. Grill, S. Reinsch, P. Keller, B. Tzschaschel, A. Echard, B. Goud, and E. H. Stelzer. Rab6 coordinates a novel golgi to er retrograde transport pathway in live cells. *J Cell Biol*, 147(4):743–60, 1999. 0021-9525 (Print) Journal Article. 53

[232] P. Chavrier, R. G. Parton, H. P. Hauri, K. Simons, and M. Zerial. Localization of low molecular weight gtp binding proteins to exocytic and endocytic compartments. *Cell*, 62(2):317–29, 1990. 0092-8674 (Print) Journal Article. 55, 86

[233] J. Saraste and K. Svensson. Distribution of the intermediate elements operating in er to golgi transport. *J Cell Sci*, 100 (Pt 3):415–30, 1991. 0021-9533 (Print) Journal Article. 61, 88, 104

[234] R. D. Klausner, J. G. Donaldson, and J. Lippincott-Schwartz. Brefeldin a: insights into the control of membrane traffic and organelle structure. *J Cell Biol*, 116(5):1071–80, 1992. 0021-9525 (Print) Journal Article Review. 63, 88

[235] T. Ort, S. Voronov, J. Guo, K. Zawalich, S. C. Froehner, W. Zawalich, and M. Solimena. Dephosphorylation of beta2-syntrophin and ca2+/mu-calpain-mediated cleavage of ica512

upon stimulation of insulin secretion. *Embo J*, 20(15):4013–23, 2001. 0261-4189 (Print) Journal Article. 65, 90, 94

[236] E. J. Tisdale. A rab2 mutant with impaired gtpase activity stimulates vesicle formation from pre-golgi intermediates. *Mol Biol Cell*, 10(6):1837–49, 1999. 1059-1524 (Print) Journal Article. 68, 90, 91, 98

[237] K. A. Goodge and J. C. Hutton. Translational regulation of proinsulin biosynthesis and proinsulin conversion in the pancreatic beta-cell. *Semin Cell Dev Biol*, 11(4):235–42, 2000. 1084-9521 (Print) Journal Article Review. 76

[238] N. Itoh and H. Okamoto. Translational control of proinsulin synthesis by glucose. *Nature*, 283(5742):100–2, 1980. 0028-0836 (Print) Journal Article. 76

[239] A. R. Ramjaun, J. Philie, E. de Heuvel, and P. S. McPherson. The n terminus of amphiphysin ii mediates dimerization and plasma membrane targeting. *J Biol Chem*, 274(28):19785–91, 1999. 0021-9258 (Print) Journal Article. 83, 88

[240] N. Richnau, A. Fransson, K. Farsad, and P. Aspenstrom. Rich-1 has a bin/amphiphysin/rvsp domain responsible for binding to membrane lipids and tubulation of liposomes. *Biochem Biophys Res Commun*, 320(3):1034–42, 2004. 0006-291X (Print) Journal Article. 86

[241] H. Plutner, A. D. Cox, S. Pind, R. Khosravi-Far, J. R. Bourne, R. Schwaninger, C. J. Der, and W. E. Balch. Rab1b regulates vesicular transport between the endoplasmic reticulum and successive golgi compartments. *J Cell Biol*, 115(1):31–43, 1991. 0021-9525 (Print) Journal Article. 86

[242] M. Aridor, S. I. Bannykh, T. Rowe, and W. E. Balch. Sequential coupling between copii and copi vesicle coats in endoplasmic reticulum to golgi transport. *J Cell Biol*, 131(4):875–93, 1995. 0021-9525 (Print) Journal Article. 86

[243] E. J. Tisdale, C. Kelly, and C. R. Artalejo. Glyceraldehyde-3-phosphate dehydrogenase interacts with rab2 and plays an essential role in endoplasmic reticulum to golgi transport exclusive of its glycolytic activity. *J Biol Chem*, 279(52):54046–52, 2004. 0021-9258 (Print) Journal Article. 86, 87

[244] B. Nagelkerken, E. Van Anken, M. Van Raak, L. Gerez, K. Mohrmann, N. Van Uden, J. Holthuizen, L. Pelkmans, and P. Van Der Sluijs. Rabaptin4, a novel effector of the small gtpase rab4a, is recruited to perinuclear recycling vesicles. *Biochem J*, 346 Pt 3:593–601, 2000. 0264-6021 (Print) Journal Article. 87

[245] S. Christoforidis and M. Zerial. Purification and identification of novel rab effectors using affinity chromatography. *Methods*, 20(4):403–10, 2000. 1046-2023 (Print) Journal Article. 87, 107

[246] A. Y. Cheung, C. Y. Chen, R. H. Glaven, B. H. de Graaf, L. Vidali, P. K. Hepler, and H. M. Wu. Rab2 gtpase regulates vesicle trafficking between the endoplasmic reticulum and the golgi bodies and is important to pollen tube growth. *Plant Cell*, 14(4):945–62, 2002. 1040-4651 (Print) Journal Article. 88

[247] P. Navarro, P. Durrens, and M. Aigle. Protein-protein interaction between the rvs161 and rvs167 gene products of saccharomyces cerevisiae. *Biochim Biophys Acta*, 1343(2):187–92, 1997. 0006-3002 (Print) Journal Article. 88

[248] C. A. Worby and J. E. Dixon. Sorting out the cellular functions of sorting nexins. *Nat Rev Mol Cell Biol*, 3(12):919–31, 2002. 1471-0072 (Print) Journal Article Review. 88

[249] W. Weissenhorn. Crystal structure of the endophilin-a1 bar domain. *J Mol Biol*, 351(3):653–61, 2005. 0022-2836 (Print) Journal Article. 89

[250] L. Lu, H. Horstmann, C. Ng, and W. Hong. Regulation of golgi structure and function by arf-like protein 1 (arl1). *J Cell Sci*, 114(Pt 24):4543–55, 2001. 0021-9533 (Print) Journal Article. 90

[251] J. Y. Zheng, T. Koda, T. Fujiwara, M. Kishi, Y. Ikehara, and M. Kakinuma. A novel rab gtpase, rab33b, is ubiquitously expressed and localized to the medial golgi cisternae. *J Cell Sci*, 111 (Pt 8):1061–9, 1998. 0021-9533 (Print) Journal Article. 90

[252] H. P. de Leeuw, P. M. Koster, J. Calafat, H. Janssen, A. J. van Zonneveld, J. A. van Mourik, and J. Voorberg. Small gtp-binding proteins in human endothelial cells. *Br J Haematol*, 103(1):15–9, 1998. 0007-1048 (Print) Journal Article. 90

[253] J. Guo, P. Zhu, C. Wu, L. Yu, S. Zhao, and X. Gu. In silico analysis indicates a similar gene expression pattern between human brain and testis. *Cytogenet Genome Res*, 103(1-2):58–62, 2003. 1424-859X (Electronic) Journal Article. 92

[254] M. Asfari, D. Janjic, P. Meda, G. Li, P. A. Halban, and C. B. Wollheim. Establishment of 2-mercaptoethanol-dependent differentiated insulin-secreting cell lines. *Endocrinology*, 130(1):167–78, 1992. 0013-7227 (Print) Journal Article. 94

[255] F. L. Graham, J. Smiley, W. C. Russell, and R. Nairn. Characteristics of a human cell line transformed by dna from human adenovirus type 5. *J Gen Virol*, 36(1):59–74, 1977. 0022-1317 (Print) Journal Article. 95

[256] Y. Gluzman. Sv40-transformed simian cells support the replication of early sv40 mutants. *Cell*, 23(1):175–82, 1981. 0092-8674 (Print) Journal Article. 95

[257] M. Gotoh, T. Maki, T. Kiyoizumi, S. Satomi, and A. P. Monaco. An improved method for isolation of mouse pancreatic islets. *Transplantation*, 40(4):437–8, 1985. 0041-1337 (Print) Journal Article. 96

[258] Sambrook J.E., Fristsch F., and Maniatis T. Molecular cloning: a laboratory manual, 2nd. edition. *Book*, 1989. 102, 105, 107, 108

[259] J. M. Hermel, Jr. Dirkx, R., and M. Solimena. Post-translational modifications of ica512, a receptor tyrosine phosphatase-like protein of secretory granules. *Eur J Neurosci*, 11(8):2609–20, 1999. 0953-816X (Print) Journal Article. 106